

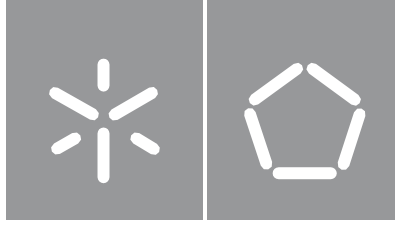


Cristiana Filipa Leite Oliveira

**Personalised hyaluronic acid
hydrogel for dermocosmetics**

Universidade do Minho
Escola de Engenharia





Universidade do Minho
Escola de Engenharia

Cristiana Filipa Leite Oliveira

**Personalised hyaluronic acid hydrogel for
dermocosmetics**

Master Thesis
Master in Biotechnology

Work developed under supervision of:
Doctor Cláudia Manuela Cunha Ferreira Botelho
Centre of Biological Engineering (CEB) – University of
Minho

Doctor Juan Luis Paris
Allergy Research Group – Instituto de Investigación
Biomédica de Málaga (IBIMA)

DIREITOS DE AUTOR E CONDIÇÕES DE UTILIZAÇÃO DO TRABALHO POR TERCEIROS

Este é um trabalho académico que pode ser utilizado por terceiros desde que respeitadas as regras e boas práticas internacionalmente aceites, no que concerne aos direitos de autor e direitos conexos.

Assim, o presente trabalho pode ser utilizado nos termos previstos na licença abaixo indicada.

Caso o utilizador necessite de permissão para poder fazer um uso do trabalho em condições não previstas no licenciamento indicado, deverá contactar o autor, através do RepositóriUM da Universidade do Minho.

Licença concedida aos utilizadores deste trabalho



Atribuição-NãoComercial-SemDerivações
CC BY-NC-ND

<https://creativecommons.org/licenses/by-nc-nd/4.0/>

Acknowledgments

First of all, I would like to thank my supervisors: Cláudia Botelho and Juan Paris, for their teachings, advice and encouragement, and also for their sympathy, availability, help and understanding during the development of this work. Without them I wouldn't have been able to overcome as many obstacles as much as I did. Thank you so much!

I would also like to thank Cristina Coelho and Javier Fidalgo for all the knowledge shared, availability, advices and help in the company Mesosystem S.A.

To Pedro and other colleagues from LTL, including Diana and Miguel, thank you for supporting and helping me in the lab.

I also need to thank Sara Amorim from the 3B's research group for all the sympathy, availability and help.

To my lovely friends: Catarina Cunha, Inês Mesquita Ferreira, Mariana Pereira, Inês Fonseca Ferreira and Filipa Silva for their friendship, attention, patience, help and energy given to me, and also for their advice, affection and unconditional support. The sincerest thank you for the strength, joy and craziness of every day.

Henrique Mendes, my love, so many times you had to deal with my stress and anxiety and so well you did! Thank you for all the support, attention, understanding, love, and strength you always gave me. For all our conversations, for always listening and advising me and, mainly, for always believing in me, even when I didn't, I am eternally grateful to you!

I want to thank to my family for always encouraging and supporting me throughout my life and for be always ready to celebrate with me and for sharing my happiness!

Now, I want to thank my parents, for the example of courage and constant struggle, in the face of adversity, for always believing in me and for all the love and unconditional support. A giant thank you for giving me this incredible experience, for the patience and strength that they transmitted to me and that was crucial to achieve my goals. Without them I wouldn't have made it.

Thank you everyone!

STATEMENT OF INTEGRITY

I hereby declare having conducted this academic work with integrity. I confirm that I have not used plagiarism or any form of undue use of information or falsification of results along the process leading to its elaboration.

I further declare that I have fully acknowledged the Code of Ethical Conduct of the University of Minho.

Hidrogel de Ácido Hialurónico Personalizado para Dermocosméticos

Resumo

A pele está sujeita ao processo de envelhecimento, que causa a degradação dos compostos extracelulares produzidos na derme, tais como o colagénio e a elastina, resultando numa pele mais fina, com menos elasticidade e conseqüente aparecimento de rugas. Tendo em conta que a pele é um indicador da própria saúde de uma pessoa e é tão importante que afeta o seu comportamento emocional e psicológico, torna-se essencial o desenvolvimento de procedimentos estéticos. Assim, este trabalho tem como principal objetivo o desenvolvimento de hidrogéis de ácido hialurónico personalizados, isto é, com propriedades facilmente moldáveis, que permitam um tratamento adequado às necessidades do cliente. Com o intuito de produzir hidrogéis com uma ótima composição de acordo com as características mecânicas e de degradação, procedeu-se a dois métodos diferentes (método I e II). Deste modo, foram preparados hidrogéis de ácido hialurónico modificado com tiramina, segundo o método I e o método II, que diferem no tipo de agentes de acoplamento utilizados. Os resultados obtidos pela análise dos hidrogéis preparados, revelaram que o método II apresenta uma maior eficiência na funcionalização do ácido hialurónico pela tiramina do que o método I. Além disso, foram preparados diferentes hidrogéis de ácido hialurónico silanizado através do método II, variando a concentração do agente de reticulação, ou seja, do alcóxido de silício. Os resultados obtidos, evidenciaram o sucesso das reações realizadas, pelo que se procedeu à caracterização físico-química dos hidrogéis de ácido hialurónico silanizado. Quanto à capacidade de reter água, verificou-se que o aumento da massa dos hidrogéis era menor, quanto maior fosse o grau de silanização. Relativamente às propriedades reológicas, de um modo geral, constatou-se que o valor do módulo elástico era maior, quanto maior fosse o grau de reticulação. Por fim, este projeto permitiu explorar diferentes estratégias para o desenvolvimento de hidrogéis de ácido hialurónico, revelando a possibilidade de modular a sua reticulação e, assim, obter hidrogéis com diferentes propriedades, que futuramente poderão conceder um tratamento personalizado aos clientes.

PALAVRAS-CHAVE: ÁCIDO HIALURÓNICO; ENVELHECIMENTO DA PELE; HIDROGÉIS; PROPRIEDADES MOLDÁVEIS; TRATAMENTO PERSONALIZADO

Personalised Hyaluronic Acid Hydrogel for Dermocosmetics

Abstract

The skin is subject to the ageing process, which causes the degradation of the extracellular compounds produced in the dermis, such as collagen and elastin, resulting in thinner skin, with less elasticity and the consequent appearance of wrinkles. Considering that skin indicates one's health and it is so important that affects a person emotional and psychological behaviour, the development of aesthetic procedures becomes essential. Thus, this work has as main goal the development of personalised hyaluronic acid hydrogels, i.e., with easily mouldable properties, which allow for a treatment suited to the client's needs. In order to produce hydrogels with an optimum composition according to the mechanical and degradation characteristics, two different methods (method I and II) were used. Thus, tyramine-modified hyaluronic acid hydrogels were prepared according to method I and method II, which differ in the type of coupling agents used. The results obtained by analysis of the prepared hydrogels, revealed that method II has higher efficiency in the functionalization of hyaluronic acid by tyramine than method I. Furthermore, different silanized hyaluronic acid hydrogels were prepared by method II, varying the concentration of the cross-linking agent, i.e., silicon alkoxide. The results obtained demonstrated the success of the reactions, so the physical-chemical characterization of the silanized hyaluronic acid hydrogels was performed. In terms of swelling, it was found that the swelling ratio was lower the higher the degree of silanization. Regarding the rheological properties, in general, the higher the degree of crosslinking, the higher was the value of the elastic modulus. Finally, this project allowed to explore different strategies for the development of hyaluronic acid hydrogels, revealing the possibility of modulating their crosslinking and thus obtaining hydrogels with different properties, which in the future may provide a personalized treatment to customers.

KEYWORDS: HYALURONIC ACID; HYDROGELS; MOULDABLE PROPERTIES; PERSONALISED TREATMENT; SKIN AGEING

Table of contents

DIREITOS DE AUTOR E CONDIÇÕES DE UTILIZAÇÃO DO TRABALHO POR TERCEIROS	ii
Acknowledgments.....	iii
STATEMENT OF INTEGRITY	iv
Resumo.....	v
Abstract.....	vi
Table of contents.....	vii
List of abbreviations.....	ix
List of figures.....	xi
List of tables.....	xiii
Scope of the thesis	xiv
Objectives of the thesis	xv
1. Introduction	1
1.1. Skin	1
1.1.1. Skin structure and functions.....	1
1.1.2. Human skin aging.....	3
1.2. Hyaluronic acid	4
1.2.1. Hyaluronic acid chemistry.....	4
1.2.2. Hyaluronic acid biosynthesis and degradation	5
1.2.3. Hyaluronic acid sources.....	5
1.2.4. Hyaluronic acid benefits.....	7
1.2.5. Hyaluronic acid cytotoxicity	7
1.2.6. Hyaluronic acid in Dermocosmetic	8
1.2.6.1. Hyaluronic acid as a topical application	8
1.2.6.2. Dermal filler.....	9
1.2.6.3. Hyaluronic acid as a filler	11

1.2.6.3.1.	Hyaluronic acid cross-linking.....	12
1.2.6.3.1.1.	Cross-linking methods.....	13
1.2.6.3.2.	Hyaluronic acid gel hardness and cohesivity.....	15
1.2.6.3.3.	Hyaluronic acid gel consistency	16
1.2.7.	Combination of hyaluronic acid with biocompatible polymers.....	17
1.2.8.	Hyaluronic acid grafted with silicon alkoxides.....	19
1.2.9.	Comparison of hyaluronic acid with collagen fillers	20
1.2.10.	Commercially available hyaluronic acid fillers	20
2.	Materials and methods.....	23
2.1.	Hydrogels preparation	23
2.1.1.	Method I – Preparation of the HA-Tyr hydrogel.....	23
2.1.2.	Method II – Preparation of the HA-Tyr hydrogel.....	25
2.1.3.	Method II – Preparation of the Si-HA hydrogel	25
2.2.	Hydrogels physical-chemical characterization.....	27
2.2.1.	ATR-FTIR	27
2.2.2.	NMR.....	27
2.2.3.	Swelling.....	27
2.2.4.	Rheology	28
3.	Results and discussion.....	28
3.1.	Preparation and characterization of the HA-Tyr hydrogel.....	28
3.2.	Preparation and characterization of the Si-HA hydrogel.....	36
4.	Conclusions and future perspectives.....	44
	References	47
	Appendix I - Characterization of the HA-Tyr hydrogel.....	63
	Appendix II - Characterization of the Si-HA hydrogel.....	72

List of abbreviations

AgNPs	Silver Nanoparticles
APTES	3-Aminopropyltriethoxysilane
ATR-FTIR	Attenuated Total Reflectance – Fourier Transform Infrared Spectroscopy
BDDE	1,4-Butanediol Diglycidyl Ether
CaHA	Calcium Hydroxylapatite
DEGMA	Diethylene Glycol Methacrylate
DMTMM	4-(4,6-Dimethoxy-1,3,5-Triazin-2-Yl)-4-Methyl-Morpholinium Chloride
DTT	Dithiothreitol
DVS	Divinyl Sulfone
EDC	Aminopropyl Dimethyl-Ethyl Carbodiimide Hydrochloride
EMA	European Medicines Agency
FDA	Food And Drug Administration
G'	Elastic Modulus
G''	Viscous Modulus
HA	Hyaluronic Acid
HA-AgNP	Hyaluronic Acid - Silver Nanoparticles Hydrogel
HA-PEG	Hyaluronic Acid - Polyethylene Glycol
HA-Tyr	Hyaluronic Acid - Tyramine
HABA	Hyaluronic Acid Bromoacetate
HAIA	Hyaluronic Acid Iodoacetate
HRP	Horseradish Peroxidase
HYAL	Hyaluronidases
MA-HA	Methacrylated Hyaluronic Acid
MES	2-(N-Morpholino)Ethanesulfonic Acid

NHS	Sulpho-Hydroxysuccinimide
NMR	Nuclear Magnetic Resonance
PBS	Phosphate Buffer Saline
PEG	Polyethylene Glycol
PEGDA	Polyethylene Glycol Diacrylate
PLLA	Poly-L-Lactic
PMMA	Polymethylmethacrylate
PNIPAA	Poly(N-Isopropylacrylamide)
Si-HA	Silanized Hyaluronic Acid
Tyr	Tyramine

List of figures

Figure 1 – Skin aging: causes and effects	4
Figure 2 – The structure of HA monomeric unit. One disaccharide unit consisting of the sodium salt of D-glucuronic acid (left) and N-acetyl-D-glucosamine (right) bound together by a glucuronicidic β (1 \rightarrow 3) bond. Figure taken from Tezel & Fredrickson, 2008	4
Figure 3 – Carbodiimide coupling reaction between the carboxyl groups of HA and the amine groups of Tyr through the addition of EDC and NHS. Figure taken from Hong and associates (2020).....	24
Figure 4 – Reaction for the silanization of HA, using DMTMM as the coupling agent and APTES as the aminoalkoxysilane. The synthesis is achieved in MES buffer at room temperature. Figure taken from Flegeau and collaborators (2020)	26
Figure 5 – NMR spectra obtained by NMR analysis for (a) Tyr and HA-Tyr reactions in (b) ultrapure H ₂ O and in (c) MES buffer (0.1 M, pH 6.0) after dialysis (D). The peaks marked in green correspond to the peaks of the Tyr spectrum.....	29
Figure 6 – Spectra obtained by ATR-FTIR analysis of the reaction of HA with Tyr in ultrapure H ₂ O before - HA-Tyr - and after purification with Amicon filters - HA-Tyr P	32
Figure 7 – Spectra obtained by ATR-FTIR analysis of the control consisting of HA alone and of the reaction of HA with Tyr in ultrapure H ₂ O after purification with Amicon filters - HA-Tyr P. The peaks represented at 1560 cm ⁻¹ and 3300-3500 cm ⁻¹ in the spectra of HA and HA-Tyr P corresponds to the amide bond bends and to the stretching vibration of -OH and -NH- groups, respectively.....	33
Figure 8 – (a) Spectra obtained by ATR-FTIR analysis of HA and Tyr controls and of the reaction of HA with Tyr in MES buffer (0.1 M, pH 6.0), using the DMTMM as a coupling agent, after purification with Amicon filters – HA-Tyr (with DMTMM) P. The red-highlighted peaks represented at (b) 826 cm ⁻¹ and (c) 1517 cm ⁻¹ in the spectrum of HA-Tyr (with DMTMM) P corresponds to the characteristic peaks of the Tyr spectrum. The peaks represented at (d) 1560 cm ⁻¹ and (e) 3300-3500 cm ⁻¹ in the spectra of HA and HA-Tyr (with DMTMM) P corresponds to the amide bond bends and to the stretching vibration of -OH and -NH- groups, respectively	35
Figure 9 – Preparation of the APTES modified HA hydrogels 1, 2, 3 and 4.....	37

Figure 10 – (a) Spectra obtained by ATR-FTIR analysis and **(b)** extended area between 900 cm⁻¹ and 1500 cm⁻¹ of the spectra of the APTES modified HA hydrogels 1, 2, 3 and 4 in MES buffer (0.1 M, pH 6.0). The peaks represented at 1004 cm⁻¹ in the spectra of Hydrogels 3 and 4 corresponds to the stretching vibration of Si-O-Si.....38

Figure 11 – Spectra obtained by ATR-FTIR analysis of the HA control and of the APTES modified HA hydrogels 1, 2, 3 and 4 in MES buffer (0.1 M, pH 6.0). The peaks represented at 1500-1600 cm⁻¹ in the spectra of all the formulations corresponds to the amide bond bends.....40

Figure 12 – Cross-linked APTES modified HA hydrogels 1, 2, 3 and 4, and the HA control after incubation at 37 °C for 24 h.....41

Figure 13 – Swelling behaviour of the APTES modified HA hydrogels 1, 2, 3 and 4 in ultrapure H₂O at 37 °C. The error bars represented in red correspond to the standard deviation42

Figure 14 – Rheological behaviour of the APTES modified HA hydrogels **(a)** 1, **(b)** 2, **(c)** 3 and **(d)** 4 at 37 °C varying frequency (0.1 to 10 Hz at a fixed strain of 0.1 %). The filled lines represent the elastic modulus (G') and the dashed lines represent the viscous modulus (G'')43

Figure 15 – Elastic modulus (G') of the APTES modified HA hydrogels 1, 2, 3 and 4 measured at 37 °C varying frequency (0.1 to 10 Hz at a fixed strain of 0.1 %). The error bars represented in red correspond to the standard deviation44

List of tables

Table 1 – Main characteristics of some of the FDA HA fillers	22
Table 2 – Conditions of the different tests performed for the preparation of HA-Tyr hydrogel	24
Table 3 – Reactions conditions for the preparation of tunable Si-HA hydrogels	26

Scope of the thesis

Skin is subject to the ageing process, which can be caused by intrinsic and extrinsic factors, such as hormonal changes and exposure to ultraviolet radiation, respectively. This ageing process causes the degradation of the extracellular compounds produced in the dermis, such as collagen and elastin, resulting in thinner skin with less elasticity and consequent appearance of wrinkles. Considering the impact of our appearance on our social behaviour and mental health, as well as the need to treat skin lesions such as scars, the development of aesthetic procedures becomes essential. In this context, it is worth noting the importance of developing personalised HA hydrogels with the advantage of providing treatment tailored to the customer's needs.

Objectives of the thesis

This project aimed to develop a series of hydrogels with tuneable characteristics for dermocosmetics purposes. Indeed, the production of hydrogels with easily mouldable properties can be an asset for the cosmetic industry, as it grants a personalised treatment to the customer. In other words, it was intended to produce fillers with different properties (degree of cross-linking, viscosity, degradability) according to the customer's needs, namely the type of wrinkles. For example, a person with deeper wrinkles needs a filler with higher viscosity, while a person with thinner wrinkles needs a filler with lower viscosity. Being the cosmetic industry a high value industry, this thesis is the result of a partnership with a national cosmetic company, Mesosystem S.A. This partnership will allow a quick translation of the developed fillers from the laboratory to the clinic.

1. Introduction

1.1. Skin

1.1.1. Skin structure and functions

Skin is the largest organ in the human body, comprising for 15 % of an adult total body weight with a surface area of approximately 2 m² and. Its main role is to protect the inner organs from the outside world (Marks & Miller, 2019). Skin complex structure can be divided into three layers. Describing from outside to inside, epidermis, which main role is to provide protection, dermis, that supplies support and nutrition for the dividing cells in the epidermis, and subcutaneous tissue (subcutis), which stores fat (Lai-Cheong & McGrath, 2009).

The outermost layer of the skin, epidermis, has a 0.1–0.2 mm in thickness and is tightly filled with cells like epidermal keratinocytes (95 % of cells), melanocytes, Langerhans cells and Merkel-Ranvier cells (the remaining 5 %) (Lai-Cheong & McGrath, 2009; Hirao, 2017). Depending on the state of keratinocyte differentiation, the epidermis can be divided into four layers, starting at the dermal junction with the basal cell layer, followed by stratum spinosum, stratum granulosum and finally stratum corneum (Campbell & Lichtensteiger, 2003). The basal layer is composed by undifferentiated, proliferating cells, such as skin stem cells, that are located in the interfollicular epidermis, giving rise to keratinocytes. On the other hand, the stratum spinosum lies above the basal layer and is constituted by keratinocytes, which differentiate from the basal cells. Keratinocytes are responsible for keratin production, which is a fibrous protein and the major component of the stratum corneum (Marks & Miller, 2019). In the stratum granulosum (granular cell layer), the differentiation process continues, and cells become more flattened, containing lamellar and keratohyalin granules within the cytosol. The cells in this layer are large, polyhedral, flat and plate-like envelopes filled with keratin, which makes the stratum corneum a semi-impenetrable layer that constitutes the major physical barrier of the skin (Marks & Miller, 2019). As previously mentioned, in addition to keratinocytes, the epidermis contains melanocytes, which are dendritic, pigment-producing cells located in the basal cell layer and that protects the skin from ultraviolet radiation. Langerhans cells are also present in the epidermis and are considered immune system sentinels (Clayton *et al.*, 2017). In a normal physiological condition these cells are responsible for a continuous state of immune tolerance (Clayton *et al.*, 2017). On the other hand, if there is any sign of infection or skin trauma, Langerhans cells are able to signal T lymphocytes so that the adaptive immune system can respond to the threat (Clayton *et al.*, 2017). Therefore,

these cells are an important component of skin immunologic barrier. Merkel cells are connected to keratinocytes by desmosomes which are located at the basal cell layer. These cells act as mechanoreceptors, transmitting sensory information from the skin to sensory nerves (Lai-Cheong & McGrath, 2009; Marks & Miller, 2019).

The dermis is a tough, but elastic, support structure. It is composed by blood vessels, nerves, and cutaneous appendages. This layer has 1–4 mm thickness, being much thicker than the epidermis, and its role is to provide structural integrity, as well as to interact and regulate cell functions like tissue regeneration (Marks & Miller, 2019). The dermal matrix is composed mainly by collagen and elastic fibres, as well as ground substance (extrafibrillar matrix). The ground substance is synthesized by dermal fibroblasts, that derived from the mesenchyme and are the predominant cell type in the dermis. Collagens accounts for 70 % of skin dry weight and the predominant types are types I and III (Lai-Cheong & McGrath, 2009; Hirao, 2017). Collagen fibres are fine and loosely arranged in the uppermost part of the dermis (papillary dermis), however, in the remainder of the dermis (reticular dermis), the fibres are thick and densely packed (Marks & Miller, 2019). These fibrous proteins form a triple-helical structure with three collagen molecules intermolecularly cross-linked, leading to hierarchical architecture of collagen matrices (Hirao, 2017). Elastic fibres are less tough than collagen fibres but impart extensible properties to the skin. They account for about 5 % of dermis dry weight and consist of elastin and elastic microfibrils, like fibrillin (Lai-Cheong & McGrath, 2009). Elastic fibres are located predominantly in the reticular dermis, where they are thinner and more loosely arranged than collagen fibres (Marks & Miller, 2019). These fibres, together with collagen fibres, construct a network in the dermis, which is responsible for the recovery upon skin deformation (Hirao, 2017). Additionally, the extrafibrillar matrix, that fills the interspaces among these protein structures, is a non-fibrous material made up of several different mucopolysaccharide molecules, such as hyaluronic acid (HA), chondroitin sulphate, and heparan sulphate, which can retain large amounts of water, facilitating the movement of fluids, molecules, and inflammatory cells (Hirao, 2017; Marks & Miller, 2019). The components turnover determined by production and degradation in the dermis are very slow when compared with the epidermal components turnover. Indeed, epidermal components are renewed within several weeks, while renewal of dermal components requires more time, i.e., several months, or sometimes years. The synthesis of extracellular components gradually declines with age, leading to thinning of the skin, elasticity loss, and further alteration, as sagging accompanies the declining

performance of muscles (Brincaat, 2000; Makrantonakia & Zouboulis, 2009; Hirao, 2017; McCabe *et al.*, 2020).

The interface between the epidermis and dermis is called the basement membrane and it is composed of a network of macromolecules that link keratin intermediate filaments of basal keratinocytes with collagen fibres in the superficial dermis. The proteins and glycoproteins that constitute the basement membrane zone are responsible for providing adhesion between the two layers (Lai-Cheong & McGrath, 2009).

The subcutis, the innermost layer of the skin, is composed of lipocytes, that are arranged into fat lobules, which in turn are separated from one another by fibrous septae. Bundles of fibres originating from the dermis into the subcutis strengthen the connection between these two compartments (Lai-Cheong & McGrath, 2009).

1.1.2. Human skin aging

Skin aging is a complex biological process consisting of two distinct and independent mechanisms – intrinsic and extrinsic (Papakonstantinou *et al.*, 2012) (Figure 1). The first affects the skin in the same pattern as it affects all internal organs and it is influenced by hormonal changes that occur with age (Makrantonaki *et al.*, 2006), such as the gradual decrease of sex hormones production starting at the midtwenties; estrogens and progesterone diminution associated with menopause. It is known that the deficit in estrogens and androgens causes collagen degradation, dryness, loss of elasticity, epidermal atrophy and skin wrinkling (Brincaat, 2000; Makrantonakia & Zouboulis, 2009). On the other hand, extrinsic aging results from exposure to external factors, primarily ultraviolet irradiation (Ralf Paus *et al.*, 2008). The ultraviolet irradiation induces the overexpression of enzymes such as matrix metalloproteinases, which degrades collagen in the dermis. This irradiation induces denaturation and aggregation of elastic fibers leading to a less elastic dermis causing wrinkles (Hirao, 2017). Skin aging is also associated with loss of skin moisture in which HA is the key molecule involved, given its capacity to bind and retain water molecules (Papakonstantinou *et al.*, 2012). Furthermore, HA prevents cellular damage from free radicals, which have an important role in skin aging. (Presti & Scott, 1994). HA can mediate various physiologic functions by binding proteins and cell surface receptors, such as CD44 (Banerji

et al., 1999; Laugier *et al.*, 2000; Knudson *et al.*, 2002) in the epidermis, suggesting that this molecule may be involved in different cell functions (Isacke, 2002; Keen, 2017).

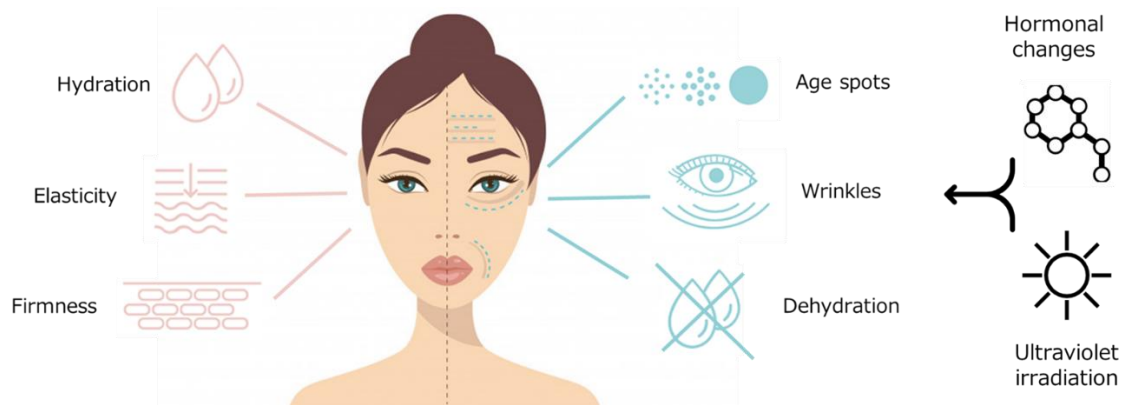


Figure 1 – Skin aging: causes and effects.

1.2. Hyaluronic acid

1.2.1. Hyaluronic acid chemistry

HA is a non-sulphated glycosaminoglycan composed of repeating polymeric disaccharides of D-glucuronic acid and N-acetyl-D-glucosamine linked by a glucuronicidic β (1 \rightarrow 3) bond (Weissmann *et al.*, 1954). It is a high molecular weight negatively charged polysaccharide. Usually, the carboxyl group (-COOH) of D-glucuronic acid is converted into its sodium salt, leading to the disaccharide structure shown in Figure 2. The disaccharide monomers that constitute HA polymer are linked together into a linear chain through β (1 \rightarrow 4) glycosidic bonds (Tezel & Fredrickson, 2008). HA also has a β -sheet tertiary structure due to molecular aggregation and it is stabilized by the presence of intermolecular hydrogen bonds (John E. Scott & Heatley, 1999). It is one of the main constituents of the extracellular matrix and it is indispensable for the cellular framework (Fraser *et al.*, 1997; Keen, 2017).

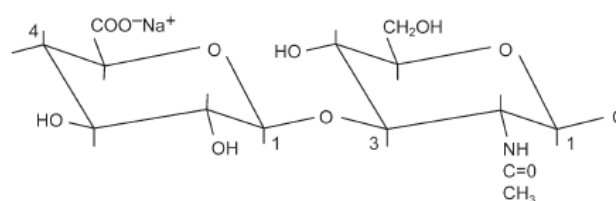


Figure 2 – The structure of HA monomeric unit. One disaccharide unit consisting of the sodium salt of D-glucuronic acid (left) and N-acetyl-D-glucosamine (right) bound together by a glucuronicidic β (1 \rightarrow 3) bond. Figure taken from Tezel & Fredrickson, 2008.

1.2.2. Hyaluronic acid biosynthesis and degradation

HA is synthesized by membrane-bound enzymes called HA synthases, which synthesize HA on the inner surface of the plasma membrane (McKee *et al.*, 1997). HA is then extruded through pore-like structures into the extracellular space (Prehm, 1990; Keen, 2017). The synthesis of HA increases during tissue injury and wound healing (Weigel *et al.*, 1986; Slevin *et al.*, 2002). This substance regulates several aspects of tissue repair, including inflammatory cell activation to enhance immune response (McKee *et al.*, 1996; Horton *et al.*, 1998; Teriete *et al.*, 2004), mediate fibroblasts (Itano *et al.*, 2002; Bai *et al.*, 2005) and epithelial cells response (Zoltan-Jones *et al.*, 2003; Jameson *et al.*, 2005; Jiang *et al.*, 2005; Jiang *et al.*, 2006) to the injury. HA half-life is variable, ranging from 3 to 5 min in the blood stream, less than a day in the skin, and 1 to 3 weeks in the cartilage (Fraser *et al.*, 1981; Reed *et al.*, 1990; Laurent *et al.*, 1991). HA is degraded into fragments of varying sizes by hyaluronidases (HYAL). Enzymes can hydrolyse the hexosaminidic β (1–4) link between N-acetyl-D-glucosamine and D-glucuronic acid residues in HA (Papakonstantinou *et al.*, 2012). HA can also be degraded nonenzymatically by free-radical mechanism in the presence of reducing agents such as ascorbic acid or thiols, ferrous, or cuprous ions (Lapcik *et al.*, 1991; Keen, 2017).

1.2.3. Hyaluronic acid sources

In terms of distribution, HA is present in both eukaryotic (Prehm, 1990) and prokaryotic cells (Lowther & Rogers, 1955; MacLennan, 1956). HA can be extracted from eukaryotic cells, mainly from bovine vitreous, umbilical cords and rooster combs (Laurent & Fraser, 1992; Gunasekaran *et al.*, 2020). HA is extracted from these tissues by using mixtures of chloroform and water, later replaced by mixtures of water and ethanol or acetone. After the extraction, solutions containing HA are subjected to treatments, involving bacterial removal and further separation of protein chains linked to HA structure by using bactericides and proteolytic enzymes, respectively (Cavalcanti *et al.*, 2020). However, the fact that protein chains are linked directly to the molecule, with large quantities of nucleic acids and viral contamination risks can lead to undesired effects in the form of immune responses and allergy (Boeriu *et al.*, 2013; Cavalcanti *et al.*, 2020). Thus, given the risk of viral infection, as well as, the limited tissue sources, this approach is progressively being replaced by microbial fermentation. Indeed, the microbial production presents several advantages

over animal-derived products. The fermentation parameters can be controlled leading to reproducibility, easy to manipulate, biocompatible, and with low toxicity (Pan *et al.*, 2021). The use of cheaper substrates, like residues and agroindustrial byproducts as fermentation substrate decreases HA production cost (Amado *et al.*, 2017; Pan *et al.*, 2017; Pan *et al.*, 2021). HA can also be produced by prokaryotic cells, such as *Pasteurella* sp. and *Streptococcus* sp., of which *Streptococcus zooepidemicus* is the most commonly used bacteria for microbial fermentation (Rangaswamy & Jain, 2008; Choi *et al.*, 2014; Gunasekaran *et al.*, 2020). On the other hand, HA may be obtained through recombinant strains by using metabolic engineering (Pan *et al.*, 2021). For example, recombinant *Bacillus subtilis* and *Escherichia coli* strains were created for the HA production (Yu & Stephanopoulos, 2008; Mao *et al.*, 2009; Jia *et al.*, 2013; Westbrook *et al.*, 2018). This compound has also been produced by a large variety of heterologous host as *Lactococcus lactis* (Chahuki *et al.*, 2019), *Pichia pastoris* (Jeong *et al.*, 2014; Westbrook *et al.*, 2018), *Agrobacterium*, *Corynebacterium glutamicum* (Cheng *et al.*, 2016), and *Pasteurella* (Chu *et al.*, 2016). Microbial HA is chemically identical to mammalian polysaccharide and therefore ensures its non-immunogenicity (Chong & Nielsen, 2003; Pan *et al.*, 2021). Indeed, the basic unit of HA, that is, the monomeric unit that composes HA polymer chains, is identical regardless of its origin. However, the length, that corresponds to the degree of polymerization, or molecular weight, of the final polymer chain is the principal difference between animal-based and bacterial-based HA. Polymer chains from bacterial-based HA are usually shorter, comprising approximately 4000-6000 monomeric units per chain that correspond to an average molecular weight of approximately 1.5-2.5 MDa, while animal-based HA chains have about 10000-15000 monomeric units per chain that correspond to an average molecular weight of approximately 4-6 MDa (Tezel & Fredrickson, 2008).

In humans, HA is most abundant in the skin (Tammi *et al.*, 1988; Armstrong & Bell, 2002; Tzellos *et al.*, 2009; Tzellos *et al.*, 2011), accounting for 50 % of the total quantity of HA present in the human body (Reed *et al.*, 1988). Even though, HA is also present in the eye vitreous (Meyer & Palmer, 1934), the umbilical cord (Weissmann & Meyer, 1954), and synovial fluid (Ragan & Meyer, 1949; Hamerman & Schuster, 1958), skeletal tissues (Armstrong & Bell, 2002), heart valves (Toole, 2004), lung (Papakonstantinou *et al.*, 1995; Papakonstantinou *et al.*, 2002; Papakonstantinou *et al.*, 2008; Klagas *et al.*, 2009; Papakonstantinou & Karakiulakis, 2009), the aorta (Papakonstantinou *et al.*, 1998), the prostate (Goulas *et al.*, 2000), tunica albuginea, corpora cavernosa and corpus spongiosum of the penis (Goulas *et al.*, 2000; Papakonstantinou *et al.*, 2012).

1.2.4. Hyaluronic acid benefits

HA derived from either bacterial or animal sources has a diversity of physicochemical properties and encompasses a large volume of water, providing high viscosity, even at low concentrations (Turino & Cantor, 2003). HA water solubility is mainly due to the presence of four hydroxyl (-OH) groups and one $-\text{COO}^- \text{Na}^+$ salt group per disaccharide repeat unit. The hydroxyl groups can participate in hydrogen bonding with water, which stabilizes the solvated state. In addition, the salt group dissociates in water with a favourable release of free energy that derives from the solvation energy of the $-\text{COO}^-$ and Na^+ ions and the gain in entropy due to sodium ion (Na^+) released. The net effect is that HA polymer dissolves readily in water (Tezel & Fredrickson, 2008).

The water-binding capacity of HA allows skin hydration and increasing its moisture content (Keen, 2017). Furthermore, it is well established that HA plays an important role in exchange between cells and blood, in cellular migration and in increasing cellular differentiation as well as cellular motility, thus promoting wound healing (Nehls & Hayen, 2000).

1.2.5. Hyaluronic acid cytotoxicity

As previously mentioned, HA is abundantly present in the skin and has many receptors on cells, such as CD44. It is a biocompatible molecule that has been extensively applied on the development of new materials due to its positive effects on cells (Zhu *et al.*, 2020). Indeed, its non-cytotoxicity has been revealed when used as a support polymer in the production of various formulations, such as hydrogels, which were tested through cytotoxicity assay and whose results showed a high cell viability (Kwarta *et al.*, 2017; Flegeau *et al.*, 2020). Furthermore, a study reported in the literature highlighted the ability of HA to reduce the cytotoxicity induced by surfactants on different human cell types (Sauerová *et al.*, 2017).

1.2.6. Hyaluronic acid in Dermocosmetic

1.2.6.1. Hyaluronic acid as a topical application

Topical formulations may consist of a hydrogel, that comprises a group of polymeric materials, whose hydrophilic structure holds water in the three-dimensional networks (Zhu *et al.*, 2020). Hydrogels can be produced by various methods, including physical interaction of the polymers (electrostatics, crystallite formation, and entanglements), the linkage between polymer chains via chemical reaction, and the linkage between polymer chains via ionizing radiation which generates main-chain free radicals to form cross-link junctions (Ahmed, 2015).

Giving the distinctive ability of HA to bind and retain water (Papakonstantinou *et al.*, 2012), as well as its capacity to form highly viscoelastic gels in the aqueous solution (Lázaro *et al.*, 2018), HA is primarily used as the gelling agent in hydrogels. Moreover, HA has several characteristics, including its role in skin hydration, exchange nutrients, cellular differentiation and motility, as well as its biosafety and high compatibility with various tissue types, that make it suitable to be used in topical formulations (Zhu *et al.*, 2020). HA, as a topical formulation, allows the delivery of medication to the skin, that is, enables the drug to penetrate the outer skin barrier and insert it within the stratum, restricting its general absorption. This can be advantageous specially for the delivery of cytotoxic agents in the treatment of cancer (Brown & Jones, 2005; Vasvani *et al.*, 2020).

The delivery efficacy of HA hydrogels depends on several factors, such as molecular weight and concentration. Indeed, studies on HA topical formulations revealed a significant improvement in skin hydration and elasticity, as well as a significant reduction of wrinkle depth, particularly with the use of low molecular weight HA formulations. This is an indication that low molecular weight has better penetration abilities than HA with high molecular weight (Pavicic *et al.*, 2011). HA can also be chemically modified to alter and optimize the hydrophobicity and biological activity through its active functional groups, including carboxylic acid, N-acetyl groups, glucuronic acid, and hydroxyl groups (Burdick & Prestwich, 2011).

Furthermore, HA topical formulations are frequently associated with nanoparticles, such as silver nanoparticles (AgNPs), as bioactive agents in order to enhance its antibacterial properties. The application of the HA-AgNP cream to damaged skin results in the improvement of skin tissue homeostasis (Abou-Okeil *et al.*, 2018; Vasvani *et al.*, 2020). Rusu *et al.* has confirmed the benefits of embedding synthetic/natural hybrid nanogels in a HA-based hydrogels as a concept of

protection, stability in physiological conditions and control over rapid release of antimicrobial drugs. This study also showed that Amox-loaded nanogels were well dispersed in the hydrogel matrix demonstrating a gradual drug release under physiological conditions, being a potential wound dressing material (Rusu *et al.*, 2022). On the other hand, Khan *et al.* showed an alternative for the treatment and prevention of acne that consists in the production of cubosomes loaded with erythromycin, constituting an effective manner for topical drug delivery. This study demonstrated that cubosomes easily penetrate into the skin and enhance drug retention for a long period of time (Khan *et al.*, 2018). It should be noted that the incorporation of molecules in nanocarriers, such as hydrogels or cubosomes, has allowed a significant increase in the effectiveness of the products (Oliveira *et al.*, 2022).

1.2.6.2. Dermal filler

A dermal filler is a substance that is injected into or under the skin and has the function of restoring lost volumes and correcting various facial imperfections, such as scars or wrinkles (Fallacara *et al.*, 2017). In fact, a dermal filler stimulates the dermis leading to an improved cell turnover with increased elastin and collagen production. These molecules will fill the depressed areas (Johl & Burgett, 2006). An ideal dermal filler should be safe, effective, nonimmunogenic, biocompatible, easy to distribute and store, and it should not induce an allergic response. It should be low cost, persist in the injected area for the required amount of time and easy to remove if necessary (Fallacara *et al.*, 2017).

Dermal fillers can be classified into three main classes according to their longevity in the tissues, which depends on its structure and composition. Thus, fillers can be temporary, lasting less than 18 months, semipermanent, lasting greater than 18 months, and permanent, lasting longer than 24 months (Vedamurthy, 2018). Furthermore, temporary fillers typically consist of HA, semipermanent fillers involve poly-L-lactic acid (PLLA) or calcium hydroxylapatite (CaHA), and permanent fillers comprise polymethylmethacrylate (PMMA) microspheres and highly purified silicone (Liu *et al.*, 2019).

PLLA is a biocompatible, biodegradable, synthetic polymer which does not induce immediate correction unlike typical fillers. Indeed, if there are immediate post injection contour changes, these are due to water volume that will be resorbed in the following days (Liu *et al.*, 2019). Instead, PLLA

provides soft tissue augmentation through fibroblast activation with subsequent new collagen formation (Funt & Pavicic, 2013; Liu *et al.*, 2019). This is due to the slowly metabolization of microparticles of PLLA that results in the production of carbon dioxide and water over the course of weeks to months. Moreover, it is invoked a host tissue response by these degrading microparticles, causing the ingrowth of type I collagen, connective tissue, and inflammatory cells, and eventually the collagen deposition around this foreign body reaction (Liu *et al.*, 2019; Vleggaar & Bauer, 2004). It should be noted that this foreign body reaction is still biocompatible as shown in histological studies (Lemperle *et al.*, 2003; Liu *et al.*, 2019). Each injection session with PLLA produces a gradual treatment effect and limited correction. Thus, three injection sessions are usually needed, but once the final correction is accomplished, results last up to 2 years (Funt & Pavicic, 2013).

CaHA can be natural, as a constituent of human bone and teeth, or synthetic, as a material biocompatible and biodegradable that has been widely used for medical application (Liu *et al.*, 2019). Fillers of CaHA consists of a carrier gel with synthetic CaHA microspheres suspended and its injection provides instant visual improvement (Funt & Pavicic, 2013). This visual improvement results from long-term deposition of new collagen surrounding the microspheres, which allows an average duration of effect of around 15 months (Bass *et al.*, 2010; Funt & Pavicic, 2013). Radiesse (Merz Pharma) is an example of a filler that comprises both immediate mechanical filling upon injection through the gel and long-term neocollagenesis through the CaHA microspheres (Liu *et al.*, 2019). Furthermore, this filler has a long effect duration of typically 1 to 2 years, which may be due to the slow enzymatic metabolism and phagocytosis of the CaHA microspheres as they act as a scaffold for the ingrowth of fibroblasts and collagen (Jacovella, 2008). These deposited particles have the ability of mimic the host environment and support fibroblastic growth without calcification. In addition, the microspheres are eventually completely degraded and they are renally eliminated as calcium and phosphate ions (Jones, 2009; Liu *et al.*, 2019).

Given the biocompatibility of PMMA, this polymer has been safely used in medical implants such as orthopaedic bone cement and craniectomy plates for many years (Lemperle *et al.*, 2010; Liu *et al.*, 2019). PMMA microspheres can be combined with bovine collagen resulting in a filler comprising 20 % PMMA microspheres suspended in 80 % bovine collagen gel (Funt & Pavicic, 2013; Liu *et al.*, 2019). Bovine collagen offers only a temporary effect, rarely lasting many years, so its combination with PMMA microspheres significantly increases the duration of the filler's effect, given the permanence of the microspheres (Liu *et al.*, 2019). Indeed, the collagen vehicle is

degraded within 1-3 months, leaving the microspheres encapsulated by a fine fibrous capsule (Funt & Pavicic, 2013). The permanence of the PMMA microspheres is due to the fact that they are not metabolized and therefore can be considered a “living implant” providing tissue augmentation through fibroplasia (Liu *et al.*, 2019).

Silicone refers to a heterogeneous group of polymers based on the element silicon and can take several forms such as solid, liquid, and gel (Liu *et al.*, 2019; Rohrich & Potter, 2004). A highly purified silicone-based filler can stimulate the body to form collagen around the silicone particles, like the other permanent fillers. However, the permanent nature of the nonbiodegradable fillers can make their complications more long-lasting and difficult to treat (Funt & Pavicic, 2013).

1.2.6.3. Hyaluronic acid as a filler

Given its excellent biodegradability, versatility, biocompatibility and viscoelastic properties, HA has been extensively used in cosmetology (Manuskiatti & Maibach, 1996; Keen, 2017). Its immunologic reaction and implant rejection is negligible, as its structure is similar across all species, which make HA a suitable material to be used as a dermal filler (Matarasso *et al.*, 2006; Tezel & Fredrickson, 2008). In addition, HA, when in aqueous medium, forms an extended hydrogen-bonded system, intramolecularly and intermolecularly (Scott & Heatley, 1999; Fallacara *et al.*, 2017). As a result of these H-bonds, but also of hydrophobic interactions that arise from HA hydrophobic patches, the polymer can self-aggregate (Scott, 2007; Fallacara *et al.*, 2017). These intra- and interchain interactions are weak and lead to the formation of a temporary network structure, which can be reversible (Scott, 2007; Fallacara *et al.*, 2017). This feature is the basis of the gel shear-thinning and self-healing properties, that is, the gel undergoes a reversible deconstruction, upon a shear, of the transient polymer network. Upon cessation of the shear, the hydrogel can autonomously reassemble and recover its initial network (Lapcik *et al.*, 1998; Scott, 2007; Fallacara *et al.*, 2017). Therefore, HA rheologic properties make it ideal for cosmetic uses. (Fallacara *et al.*, 2017).

1.2.6.3.1. Hyaluronic acid cross-linking

The main limitation of HA, when used as it is (free chains, i.e., uncross-linked chains), is its poor durability (about 1-2 d), especially due to the rapid enzyme degradation by hyaluronidase and free radicals, which are naturally present in the skin. Uncross-linked HA solutions do not provide the persistence required for a dermal filler, they must be viscoelastic to deform when subjected to a stress and recover to its original shape upon the disappearing of the stress, ensuring facial enhancement once implanted. Hence, HA is often subjected to chemical cross-linking in order to increase its polymer network rigidity (i.e., the gel viscoelasticity), extend its permanence in the site of application and reduce its susceptibility to enzymatic degradation (Fallacara *et al.*, 2017). Normally, HA cross-linkers are difunctional molecules of synthetic origin, for example divinyl sulfone (DVS) and 1,4-butanediol diglycidyl ether (BDDE) (Tomihata & Ikada, 1997; Ramamurthi & Vesely, 2002), which binds HA polymer chains to each other, creating a polymer 'network' and transforming the viscous liquid into a gel. The resulting HA gel acts as a single unit, imposing a physical and chemical barrier to enzymatic and free radical breakdown. Indeed, because of the gel network is multiply connected, enzymes and free radicals can break down the chains, but in smaller portions compared to uncross-linked chains. Moreover, due to large size of enzymes, they can have difficulty penetrating the gel network, contributing to a slower degradation. Consequently, the HA gel has a longer persistence in the skin to be used as a dermal filler (Tezel & Fredrickson, 2008).

Moreover, the two main variables in HA cross-linked fillers are represented by the amount of HA cross-linked chains and the cross-linking degree, that corresponds to the percent of cross-linker, that is, number of cross-linker molecules for every 100 disaccharide monomeric units of HA (Fallacara *et al.*, 2017).

Various HA dermal fillers are composed by cross-linked and uncross-linked fractions. Cross-linked is relevant to maintain the volume of the filler implanted into the skin, while the uncross-linked HA will aid extrusion and flow being cleared from the body in a matter of days (Tezel & Fredrickson, 2008). A high cross-linking degree means longer persistence of the filler in the skin, but if the cross-linking degree is too high, it might reduce the hydrophilicity of the HA polymer chains and, therefore, the lifting capacity of the implanted gel. The biocompatibility of the product may also be compromised and induce an immune reaction. Rather than metabolize the gel, the body might reject it, initiating undesired reactions such as encapsulation of the gel implant and formation of a granule or sterile abscess. Hence, it is important to achieve a balance between

cross-linking HA polymer chains to achieve extended persistence, but avoiding any undesired complications, such as rejection (Tezel & Fredrickson, 2008).

On the other hand, cross-linking HA chains can result in the presence of unreacted, or residual, cross-linker in the finished product. These residual cross-linker molecules are artifacts of the manufacturing process and can be toxic at high concentrations when unbound to other molecules. So, it is important to eliminate any residual cross-linking agent from the finished product (Tezel & Fredrickson, 2008).

1.2.6.3.1.1. Cross-linking methods

HA can be modified and cross-linked by various methods, such as amide modification with gelatine, thiol modification, enzymatic methods through use of reactive oxygen species, bromoacetic anhydride reaction and cross-linking with methacrylates (Dovedytis *et al.*, 2020). It is noteworthy that the goal of a cross-linking agent is to change some HA properties, in order to improve its mechanical properties and increase its permanence at the application site, while retaining its biocompatibility (Burdick & Prestwich, 2011).

The method concerning amide modification with gelatine consists in chemical modification by targeting the carboxylate group, which can easily be achieved by using reagents that usually form amide or ester bonds. The reaction product is reactive, permitting it to be targeted by a secondary reaction from a desired polymer, such as gelatine, creating a cross-link. In order to create reactive species, Schiff base reactions are commonly used, as it allows the incorporation of many different ligands to HA via amide bonds (Khunmanee *et al.*, 2017; Dovedytis *et al.*, 2020).

The thiol method involves the addition of thiol groups, which allows the formation of disulphide bonds via oxidation. Hydrogels formed by thiolated HA are smart hydrogels that have the ability to gel in air (Khunmanee *et al.*, 2017; Dovedytis *et al.*, 2020). A thiol group can be incorporated in various ways, most of which target the carboxylate functional group in HA. One method consists in using aminopropyl dimethyl-ethyl carbodiimide hydrochloride (EDC) as a reagent to form an amide bond with an intermediate, that is replaced through a reaction with sulpho-hydroxysuccinimide (NHS), introducing the thiol group (Khunmanee *et al.*, 2017; Dovedytis *et al.*, 2020). Another method involves the attachment to the carboxylate group with a hydrazide reagent linked with a thiol group (Vanderhooft *et al.*, 2007; Dovedytis *et al.*, 2020). Moreover, the

thiol group can also form disulphide bonds or be bound to a polyethylene glycol diacrylate (PEGDA) (Vanderhooft *et al.*, 2007; Dovedytis *et al.*, 2020). The formation of the cross-link between the modified HA and PEGDA results in an injectable hydrogel.

The cross-linking for hydrogel formation can also be induced by an enzymatic method using reactive oxygen species, like hydrogen peroxide and horseradish peroxidase (HRP). These reagents are used in an enzymatic reaction, whose target is HA-tyramine (HA-Tyr) (Loebel *et al.*, 2015; Loebel *et al.*, 2017; Dovedytis *et al.*, 2020). Initially, HA-Tyr is formed by the reaction of HA with EDC/NHS, in which occurs the amidation of the carboxylic group on HA and of the amine group on Tyr to link the two together. Another method for the production of HA-Tyr consists in the use of 4-(4,6-dimethoxy-1,3,5-triazin-2-yl)-4-methyl-morpholinium chloride (DMTMM), that has the advantage of providing a reaction with a pH suitable for Tyr, unlike in the EDC/NHS reaction (Loebel *et al.*, 2015; Dovedytis *et al.*, 2020). When reactive oxygen species attack Tyr, there is the formation of singlet oxygen mediated cross-linking. The Tyr amino acids form a di-Tyr bond cross-linking the HA (Loebel *et al.*, 2017; Dovedytis *et al.*, 2020). This reaction with reactive oxygen species is nontoxic (Loebel *et al.*, 2015; Dovedytis *et al.*, 2020). In addition, HA-Tyr can be used to cross-link with aqueous silk by a substitution reaction using hydrogen peroxide and HRP to link silk and HA. The resulting product reveals better mechanical properties than native HA (Khunmanee *et al.*, 2017; Dovedytis *et al.*, 2020).

Another method for HA cross-linking to produce a biocompatible hydrogel is a substitution reaction with bromoacetic anhydride. The C(6) of the N-acetyl-D-glucosamine is the group targeted for substitution, forming HA bromoacetate (HABA), which can undergo a Finkelstein reaction with sodium iodide to form HA iodoacetate (HAIA). Either HABA or HAIA are electrophilic and slightly cytotoxic due to the thiol group, however, they do not reveal cytotoxicity when exposed to a nucleophile, which can donate electrons to the electrophilic polymer. In this case, HABA and HAIA favour the proliferation of fibroblast cells (Serban & Prestwich, 2007; Dovedytis *et al.*, 2020). Thiolated gelatine can be used as a nucleophile, forming a hydrogel without a cross-linker like PEGDA when bound to HABA or HAIA (Burdick & Prestwich, 2011; Dovedytis *et al.*, 2020).

Moreover, a methacrylated HA (MA-HA) hydrogel can be formed by HA cross-linking with methacrylates. Firstly, MA-HA must be formed in solution, using sodium hyaluronate and methacrylic anhydride in a basic solution ($\text{pH} \geq 8$) that drives the reaction forward (Marklein & Burdick, 2010; Dovedytis *et al.*, 2020). The hydroxyl group of HA backbone is modified in

consequence of the addition of methacrylic anhydride, resulting in MA-HA. Subsequently, the hydrogel can be formed through one or two-step cross-linking process, like Michael-type addition cross-linking, which consists in introducing dithiothreitol (DTT) into a solution of MA-HA (Khetan *et al.*, 2013; Dovedytis *et al.*, 2020). These reactions are thermodynamically controlled and involve the interaction of electron donors, like methylenes with donors as α , β -unsaturated carbonyl compounds. The methacrylates are consumed by DTT resulting in the formation of a gel-like network. Then the remaining unconsumed methacrylates can be cross-linking when gels are exposed to ultraviolet light and to a photoinitiator (Khetan *et al.*, 2013; Dovedytis *et al.*, 2020). Free radical photopolymerization produces radicals that propagate through the vinyl groups of MA-HA and form kinetic chains which will be enzymatically cleaved into the HA backbone (Burdick *et al.*, 2005; Dovedytis *et al.*, 2020).

Most of these methods are based on covalent cross-linking of HA to polymers producing hydrogels that are mechanistically stronger. In addition to these methods HA can be cross-linked by other methods like ionic cross-linking, thermoresponsive cross-linking, and photo-cross-linking (Khunmanee *et al.*, 2017; Dovedytis *et al.*, 2020). For each cross-linking method there are various mechanisms, for example, photo-cross-linking can also performed with HA-Tyr. Indeed, the di-Tyr bonds, which forms HA-Tyr hydrogel, can be formed by singlet oxygen mediated oxidation, that in turn can be triggered by light (Loebel *et al.*, 2017; Dovedytis *et al.*, 2020). On the other hand, thermoresponsive cross-linking properties can be given to HA by incorporating polymers with these properties, such as dopamine with thiolated pluronic F127 copolymer, diethylene glycol methacrylate (DEGMA), among others (Khunmanee *et al.*, 2017; Dovedytis *et al.*, 2020).

1.2.6.3.2. Hyaluronic acid gel hardness and cohesivity

Other properties of HA fillers are gel hardness and cohesivity, which are its resistance to be deformed and its tendency to stick together and hold its form or shape under stress, respectively. These parameters are higher the lower is the amount of free polymer chains, at a given HA concentration. In fact, cohesivity increases with HA concentration, but also with cross-linking degree (Tezel & Fredrickson, 2008; Pierre *et al.*, 2015; Fallacara *et al.*, 2017).

As previously mentioned, injectable fillers need to have specific mechanical properties namely, viscoelasticity and elasticity. These properties are very important as the filler must be

viscous enough to be easily extruded through a needle or cannula and elastic enough to retain their shape once implanted in the face and subjected to the mechanical stresses of facial animation and/or other external forces (Caton *et al.*, 2007; Greene & Sidle, 2015; Pierre *et al.*, 2015). In this way, parameters like elastic modulus (G'), which is a measure of a material hardness, cross-linking degree and cohesivity affect the dermal filler characteristics of extrusion as the gel is subjected to forces of injection through a fine needle (Fallacara *et al.*, 2017). Generally, the increasing amount of HA cross-linked chains leads to a high G' , resulting in a gel with high hardness. A gel with these characteristics will be impossible to inject through a fine needle. Thus, it is necessary to incorporate into the dermal filler a small amount of uncross-linked HA chains to lubricate and fluidize the gel. This also causes a decrease in the cohesivity of the dermal fillers (Tezel & Fredrickson, 2008; Borrell *et al.*, 2011; Fallacara *et al.*, 2017). Yet, as previously mentioned, a dermal filler requires a cohesivity enough high to resist to compression forces that could potentially provoke its migration, after its injection into the skin (Pierre *et al.*, 2015; Fallacara *et al.*, 2017). Therefore, it is necessary to balance these two characteristics in order to obtain a filler with the required properties.

1.2.6.3.3. Hyaluronic acid gel consistency

Consistency or gel particle size is another parameter that affects a dermal filler injection as well as its rheologic properties. After the cross-linking step, the dermal filler should be sized to allow injection into the skin. In this way, the gel could be extruded through a series of screens or sieves, to confer a HA filler a high G' value and particles of a well-defined average size (Fallacara *et al.*, 2017). Alternatively, the gel particle could be sized by homogenization, which produces a dermal filler that shows a lower G' value and a smooth consistency, probably due to a much broader distribution of molecule sizes in comparison to a product obtained by sieving (Tezel & Fredrickson, 2008; Fallacara *et al.*, 2017). The consistency also influences the degradation rate of HA since bigger HA chains offer limited total surface area for enzymes to degrade it, while smaller HA molecules offer more total surface area for enzymes to break it down more readily (Tezel & Fredrickson, 2008; Fallacara *et al.*, 2017).

1.2.7. Combination of hyaluronic acid with biocompatible polymers

HA is often combined with biocompatible polymers to improve its characteristics properties as an injectable hydrogel. Thus, HA can be combined, for example, with polyethylene glycol (PEG), chitosan and polyacrylates (Tripodo *et al.*, 2015).

PEG is a linear branched polyether that is synthesized by the ethylene oxide ring opening polymerization, which could be initiated by different anions in order to obtain PEGs with different terminal groups, such as the methoxyl, hydroxyl, thiol, carboxyl or the amine one (Roberts *et al.*, 2002). PEG has a wide range of applications in the biomedical field, but it has also been studied for the covalent modification of biological macromolecules and surfaces for various pharmaceutical and biotechnical applications (Roberts *et al.*, 2002; Zerbinati *et al.*, 2020). This polymer is only biodegradable, when it has a lower molecular weight (less than 400 Da), which enables its degradation *in vivo* by alcohol dehydrogenase, resulting toxicity (Tripodo *et al.*, 2015). Furthermore, PEG is considered highly biocompatible in a wide range of molecular weights (Roberts *et al.*, 2002; Tripodo *et al.*, 2015) and it has been often conjugated with HA to form hydrogels, because of its ability to escape the mononuclear phagocyte system in the bloodstream (Tripodo *et al.*, 2015). Thus, PEG can be used as a cross-linker for HA hydrogels stems because of its low toxicity and good rheological properties (Martina *et al.*, 2019; Zerbinati *et al.*, 2020). Studies of HA-PEG cross-linking hydrogels reveal a high cohesivity and, simultaneously, the maintenance of the correct viscoelasticity properties (Zerbinati *et al.*, 2020). This elevated cohesivity enables a better resistance to mechanical degradation and prevents gel migration, leading to an extended duration in the skin and maintenance of the initial shape of the gel. Moreover, the results of the cytotoxicity assay in a study of a hydrogel made from HA and PEG by using enzymatic cross-linking HRP, reveal a cell viability of 90 %, which demonstrates that this hydrogel is not toxic. On the other hand, PEG protects HA from enzymatic degradation (Kwarta *et al.*, 2017).

Chitosan is a linear polysaccharide with a cationic nature, that consists in a versatile biomaterial because of its diverse bioactivities, non-toxicity, low-allergenicity, biocompatibility and biodegradability (Cheung *et al.*, 2015; Dash *et al.*, 2011; Tripodo *et al.*, 2015). In addition, it has excellent physical properties, such as high surface area, tensile strength, porosity and conductivity. Chitosan is easily moulded into different shapes, such as films, sponges, fibres, beads, gel and solutions (Cheung *et al.*, 2015; Shukla *et al.*, 2013). Chitosan is advantageous for wound healing, due to its ability to activate polymorphonuclear leukocytes, macrophages and fibroblasts that

enhance granulation, as well, as the organization of the repaired tissues (Ueno *et al.*, 2001; Cheung *et al.*, 2015). Its slowly degradation into N-acetyl- β -D-glucosamine stimulates fibroblast proliferation, aids regular collagen deposition and stimulates HA synthesis at the wound site, accelerating the healing process and preventing scar formation (Muzzarelli *et al.*, 1999; Cheung *et al.*, 2015). Chitosan is commonly used in formulations for trans-mucosal administration, since it has mucoadhesive and permeation-enhancing properties (Garcia-Fuentes & Alonso, 2012; Trapani *et al.*, 2014; Tripodo *et al.*, 2015). In fact, chitosan reveals longer residence times at the application site because of the electrostatically interaction between its positive charges and the opposite charges in the mucus constituents, like sialic acids. Furthermore, as in HA, the performance of chitosan formulations depends on molecular weight, degree of deacetylation and preparation method. Moreover, chitosan may electrostatically interact with the polyanion HA giving rise to polyelectrolyte complexes which have showed a great potential in various biomedical applications, such as drug and gene delivery and cancer therapy (Choi *et al.*, 2012; Tripodo *et al.*, 2015). In literature it is reported the development of a HA hydrogel cross-linked with glycol chitosan that can be easily formulated into an injectable gel, membrane, film and sponge for soft-tissue augmentation, drug delivery, visco-supplementation, wound dressing and as tissue-engineering scaffold. This hydrogel showed a soft and viscoelastic structure, excellent water adsorption properties and biostability (W. Wang, 2006).

HA can be conjugated with polyacrylates, that belong to a class of polymers obtained from a wide range of acrylate monomers (Sehlinger *et al.*, 2013). They have good mechanical properties and easily functionalized, being often applied in the biomedical field (Tripodo *et al.*, 2015). Most of HA polyacrylates conjugates consists in graft co-polymers obtained by radical polymerization approach, however it was been demonstrated that they also can be obtained by atom transfer radical polymerization process (Fiorica *et al.*, 2013). One example of a polyacrylate is poly(N-isopropylacrylamide) (PNIPAA), which is a thermosensitive polymer and with a low critical solution temperature at around 32 °C, which is close to human body physiological temperature (Tripodo *et al.*, 2015). Thus, PNIPAA is frequently used to obtain *in-situ* forming gels for drug delivery applications, like the production of HA grafted with PNIPAA in order to obtain a thermoresponsive system for ocular topical delivery of cyclosporine A (Wu *et al.*, 2013).

1.2.8. Hyaluronic acid grafted with silicon alkoxides

Hydrogels can be cross-linked by organic or inorganic molecules, resulting respectively in organic and inorganic networks. Since organic hydrogels are not always obtained under biocompatible conditions, due to toxicity that may arise from reagents, by-products, catalysts or reaction conditions, hybrid hydrogels synthesized by inorganic sol-gel polymerization have been emerged as an alternative to organic hydrogels (Montheil *et al.*, 2018). A hybrid hydrogel consists in the coexistence of organic and inorganic moieties, namely metal oxides which can be grafted onto polymer backbones. Among the different metal oxides that can be used, silicon alkoxides ($\text{Si}(\text{OR})_n$), are especially suited for the design of *in situ* forming hydrogels, leveraging the reversible self-condensation of silanol moieties ($\text{Si}=\text{OH}$) into siloxanes ($\text{Si}=\text{O}=\text{Si}$) at neutral pH (Bourges *et al.*, 2002). The hydrogel is only formed upon pH neutralization prior to injection, to avoid any detrimental influence on living tissues (Trojani *et al.*, 2006). Furthermore, three covalent bonds are formed due to the tetravalence of the silicon atom, thus the network stability is reinforced through the formation of cross-linking nodes (Montheil *et al.*, 2018). Flegeau and collaborators (2020) successfully designed for the first time *in situ* forming Si-HA (silanized HA) hydrogels using the hybrid inorganic-organic silanization chemistry. This study showed that single-polymer gels can be produced under physiological conditions of pH and temperature with tuneable gelation time and stiffness. The resulting gel was placed in contact with different cell line demonstrating its cytocompatibility. In addition, Si-HA hydrogel degradation profile was tuned to achieve degradation from days to weeks *in vivo* (Flegeau *et al.*, 2020). The chemically bound inorganic compounds, such as silica, and polysaccharides restrict the gel swelling degree, due to their natural hydrophilicity (reduced number of hydrophilic molecules) (Heinemann *et al.*, 2013; Sánchez-Téllez *et al.*, 2020). In literature it was reported the development of hybrid hydrogels, using polysaccharides such as HA modified with aminosilane molecules and inorganically cross-linked by a three-dimensional siloxane organic-inorganic matrix via sol-gel method. This study revealed the strength of HA matrix provided by inorganic cross-linking, through decreasing its natural hydrophilicity, increasing thermal degradation temperatures and improving rheological properties (Sánchez-Téllez *et al.*, 2020).

1.2.9. Comparison of hyaluronic acid with collagen fillers

Collagen and HA are macromolecules naturally present in the human body and can be used for aesthetic treatments, but they differ in terms of manufacturing and clinical applicability. The first type of heterologous collagen used for aesthetic purposes was bovine collagen, being the Zyderm (Allergan) the first commercial filler of bovine collagen. However, the degradation rate of this product was very high, only lasted implanted for three months, leading to the formulation of a new collagen filler named Zyplast (Collagen Corporation). This new filler has a prolonged aesthetic effect (Baumann, 2004; Fallacara *et al.*, 2017). In addition, CosmoDerm and CosmoPlast (Inamed Corporation) were approved in 2003 by the Food and Drug Administration (FDA) and consists in allogeneic purified human collagen, from fibroblast cell culture. These fillers have the advantage of not requiring allergy tests before the treatment, in contrast with the collagen fillers previously mentioned (Sapijaszko, 2007; Fallacara *et al.*, 2017). Despite the improvement of collagen fillers, HA fillers have a longer longevity and do not require skin testing before use (Klein & Fagien, 2007; Greene & Sidle, 2015). Furthermore, HA is nonimmunogenic, since has an identical chemical structure across species. On the other hand, collagen may induce an allergic or immune response, probably due to the fact that it can vary between species (Richter *et al.*, 1979; Baumann, 2004; Greene & Sidle, 2015; Kim *et al.*, 2015). Although, HA fillers are increasingly emerging on the market, collagen products will continue to be important in soft tissue augmentation, since high type I collagen levels have a strong correlation with skin rejuvenation (Baumann, 2004). On the other hand, HA fillers have the same capacity to provide structural support as human bioengineered dermal fillers, unlike CosmoDerm and CosmoPlast, that cannot provide the same volume as the HA fillers (Baumann, 2004). Nevertheless, these collagen fillers have less side effects, namely, swelling and bruising as compared with the HA products. Thus, HA fillers used in combination with collagen fillers may result in less bruising and swelling than normally seen with HA fillers alone because of the effects of lidocaine included in the collagen products and the platelet aggregating effects of collagen fibrils (Okada *et al.*, 1998; Perret *et al.*, 2003; Baumann, 2004).

1.2.10. Commercially available hyaluronic acid fillers

For cosmetic products, such as HA fillers to be commercially available, they must be approved by FDA, which is responsible for protecting the public health by ensuring the safety,

efficacy and security of human and veterinary drugs, biological products, and medical devices in the United States. In the Europe the similar body is EMA – European Medicines Agency.

Commercially available HA fillers include Hylaform (Genzyme Biosurgery), which was approved in 2004 by FDA and it is derived from an avian source (rooster comb). Hylaform has a HA concentration of 4.5 to 6 mg/mL, a degree of cross-linking of 20 % and its cross-linker is DVS. This HA-based dermal filler is indicated for the treatment of moderate to severe facial wrinkles and folds, such as nasolabial folds. Its main disadvantage is longevity, as benefits generally last 3 to 4 months. Hylaform was withdrawn from the U.S. market (Fallacara *et al.*, 2017).

Captique (Genzyme Biosurgery) is an FDA-approved (2004) HA filler produced through a patented non-animal stabilized HA technology. It is the gram-positive bacterium derived equivalent of Hylaform, so its origin prevents the risk of immunologic issues related to HA animal source and, consequently, skin testing is not required prior to its injection. Captique contains 4.5 to 6 mg/mL HA, and it is characterized by a 20 % cross-linking degree (the cross-linker is DVS). This dermal filler is indicated for the correction of fine lines and moderate to severe wrinkles of the face, like nasolabial folds, and this effect duration is from 3 to 6 months (Gold, 2007; Bogdan Allemann & Baumann, 2008; Fallacara *et al.*, 2017).

Eleveess (Anika Therapeutics) was the first FDA-approved dermal filler (2006) to incorporate the anesthetic lidocaine hydrochloride (0.3 %) for enhanced patient comfort. It has a HA concentration of 28 mg/mL and HA is cross-linked with p-phenylene bis-ethyl carbodiimide. This product is recommended for injection into the mid to deep dermis for the correction of moderate to severe facial wrinkles and folds (Brandt & Cazzaniga, 2008; Fallacara *et al.*, 2017).

In 2020 the FDA approved Juvéderm Voluma XC (Allergan) (Juvéderm® Volumatm XC – P110033/S047 | FDA), Restylane Kysse (Q-med AB) (Restylane® Kysse - P140029/S021 | FDA) and Revanesse Lips+ (Prollenium Medical Technologies, Inc.) (Revanesse® Lips+ – P160042/S010 | FDA). These fillers consist of cross-linked HA (the cross-linker is BDDE) made by the *Streptococcus* species of bacteria, formulated to a concentration of 20 mg/mL (Juvéderm and Restylane) and 22–28 mg/mL (Revanesse) with 0.3 % (Juvéderm) and 3 mg/mL (Restylane and Revanesse) of the drug lidocaine as a numbing agent. Juvéderm Voluma XC (Krause-S, 2020) is indicated for injection into facial tissue to temporarily restore volume and fullness to the areas of the mid-face and chin region while Restylane Kysse (Krause-S, 2020) and Revanesse Lips+ (Chang-S, 2020) are used for injection into the lips. The company responsible for Juvéderm Voluma

XC states that 56 % of subjects had an improvement in their chin profile for 6 months. Restylane Kysse and Revanesse Lips+ can have side effects, such as bruising, itching, lump formation, pain, redness and swelling.

Recently, in 2021, the FDA approved Restylane Defyne (Q-med AB) (Restylane Defyne – P140029/S027 | FDA), that has the same HA and lidocaine concentration and cross-linker as Restylane Kysse. This product was previously approved for injection into facial tissue to improve the appearance of smile or laugh lines. This approval expands its use for injection into the chin region to improve the chin profile appearance. Nevertheless, Restylane Defyne treatment can have the side effects mentioned above (Chang-S, 2021). Other FDA approved HA fillers are shown in Table 1.

Table 1 – Main characteristics of some of the FDA HA fillers

HA Filler	Restylane	Juvéderm Ultra	Juvéderm Ultra Plus	Belotero Balance
Manufacturer	Q-med AB	Allergan	Allergan	Merz Pharmaceuticals
FDA approval	2003	2006	2006	2011
HA (mg/mL)	20	24	24	22.5
Cross-linker	BDDE (1 %)	BDDE (9 %)	BDDE (11 %)	BDDE
Specific uses	Correction of moderate to severe facial wrinkles and folds	Deep wrinkles and defects	Deeper furrows (nasolabial folds)	Smooth moderate and severe wrinkles and folds (nasolabial folds)
Duration	6 to 12 months	6 to 12 months	6 to 12 months	6 months

As can be seen by the HA fillers described above, HA can be cross-linked with multiple types of polyfunctional reagents, including BDDE and DVS. Nevertheless, cross-linkers have several functional groups and invariable characteristics that can lead to cytotoxicity and adverse effects in local tissues, especially if a large volume of filler is injected (Liang *et al.*, 2004; Choi *et al.*, 2015). Indeed, it was reported that a gel composed by HA cross-linked with BDDE induce alterations in cell morphology and decreased cell viability in mouse fibroblasts at a concentration of 0.5 mg/mL (Xue *et al.*, 2020). Cells treated with BDDE reveals high cytotoxicity, reactive oxygen species production, and inflammatory responses than cells in the presence of other cross-linker (Jeong *et al.*, 2021). Likewise, the use of DVS in HA cross-linking revealed a decrease of cell viability and an

increase of inflammatory cytokines expression in retinal pigment epithelial cells (Lai, 2014). Furthermore, the commercial fillers described do not have a very long duration, as a result of enzymatic degradation.

2. Materials and methods

2.1. Hydrogels preparation

In order to develop a filler with excellent characteristics it was necessary to chemically alter HA. One way is to use cross-linking agents in order to increase the viscoelasticity of the gel, as well as its permanence at the application site by decreasing susceptibility to enzymatic degradation. In this way, to obtain a filler with an optimal composition according to mechanical and degradation characteristics, two distinct filler production methods that are well described in the literature (Kwarta *et al.*, 2017; Flegeau *et al.*, 2020) were tested. Thus, the method for the preparation of a HA-Tyr hydrogel was tested (method I), as well as the cross-linking with the HRP. This method uses EDC/NHS chemistry for the coupling between HA and Tyr. On the other hand, method II, which consists in the use of DMTMM as coupling agent was also applied in the preparation of HA-Tyr hydrogels and in the production of hydrogels with different characteristics based on Si-HA for cosmetic purposes. In the production of Si-HA hydrogels, it was used a silicon alkoxide as cross-linker which has the advantage of having biologic properties and, therefore, does not present cytotoxicity.

2.1.1. Method I – Preparation of the HA-Tyr hydrogel

The HA-Tyr hydrogel was prepared according to the reaction described by Kwarta and associates (2017), which consists in HA carboxyl groups activation by EDC and NHS (Figure 3). Indeed, HA carboxyl group is the most suitable for chemical modification, allowing not only the functionalisation of HA, but also the maintenance of its biological properties. Thus, the activation of these groups with EDC/NHS allowed the binding of amines to HA and consequent formation of amides (Hong *et al.*, 2020). Firstly, EDC acted as a condensing agent and activated HA, forming a reactive O-acylisourea intermediate, which rapidly undergoes a rearrangement to stable N-acylurea, which is not reactive to amines (Darr & Calabro, 2009). This quenching of the active intermediate

can be avoided using NHS, which forms an active ester that is more resistant to hydrolysis, reactive and non-rearrangeable, thus increasing the coupling efficiency of primary amines to HA. The amide bond that covalently links Tyr to the HA molecule is formed by the nucleophilic attack of the electron-rich amine group of Tyr on the carbonyl carbon of HA, which due to activation by EDC is electron deficient (Darr & Calabro, 2009).

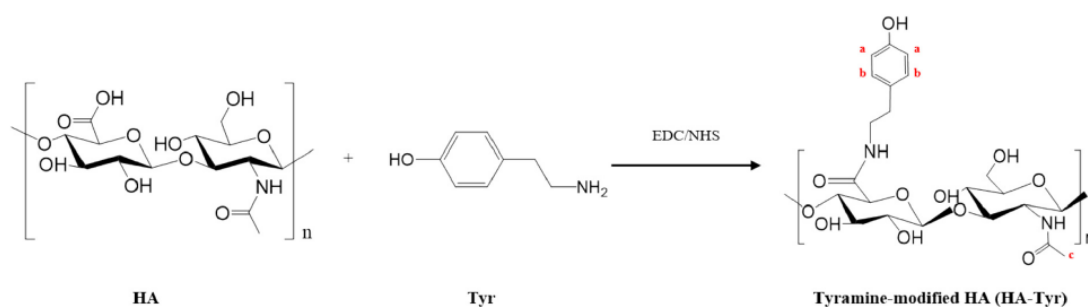


Figure 3 – Carbodiimide coupling reaction between the carboxyl groups of HA and the amine groups of Tyr through the addition of EDC and NHS. Figure taken from Hong and associates (2020).

In general, the reaction performed consisted on dissolving HA (500 kDa) in ultrapure H₂O/MES (2-(N-Morpholino)ethanesulfonic acid) buffer (0.1 M, pH 6.0), in order to prepare a polymeric solution with a concentration of 0.1 % (w/V). After HA was completely dissolved, EDC and NHS were added to the HA solution. After a while, Tyr was also added to the solution and the reaction remained stirring overnight at room temperature. Moreover, with the aim of optimise the described method, several tests were performed at different times, and some steps of the experimental methodology were changed according to the results that were obtained. In this way, table 2 describes the conditions of the main tests performed.

Table 2 – Conditions of the different tests performed for the preparation of HA-Tyr hydrogel

Assay	m (HA) (g)	m (EDC) (g)	m (NHS) (g)	m (Tyr) (g)	Δt NHS – Tyr addition (min)	Solvent	V (Solvent) (mL)	HA repeating monomer:EDC:NHS:Tyr (Mole Ratio)
1	0.01	0.011	0.016	0.013	60	MES Buffer (0.1 M, pH 6.0)	10	1:3:3:3
2	0.1	0.011	0.016	0.013	60	Ultrapure H ₂ O	10	1:3:3:3
3	0.1	0.011	0.016	0.013	15	Ultrapure H ₂ O	10	1:3:3:3
4	0.1	0.011	0.016	0.021	60	Ultrapure H ₂ O	10	1:3:3:5

Subsequently, the hydrogels were purified using Amicon filters (30 kDa), which allowed the “washing out” of impurities by adding more ultrapure H₂O and concentrating it by centrifugation (8000 rpm, 10 min). Upon purification, the samples were lyophilized. Finally, the cross-linking reaction with HRP was performed by dissolving 5 mg of the lyophilized product in 1 mL of PBS (Phosphate-buffered saline) (0.1 M). Then, 72.54 μ L of this solution were added to 2.6 mg of HRP (279 U/mg). Ultimately, 2.9 μ L of H₂O₂ (0.25 %) was added and incubated at 37 °C for 2 h. The H₂O₂ was the gelation agent. Indeed, the resting ferric state of HRP [Fe (III)] is oxidized by H₂O₂ to form a high oxidation-state intermediate with a cation radical. In the presence of Tyr phenol as a reducing substrate, this intermediate is converted to another compound after the first one-electron reduction, followed by an additional one-electron reduction step that returns HRP to its resting state. Therefore, the generated phenol radicals enable covalent bridge formation between the aromatic rings of Tyr bound to HA (Bae *et al.*, 2015; Lee *et al.*, 2008). Moreover, the cross-linking degree can be controlled by varying the concentrations of both H₂O₂ and phenol (Bae *et al.*, 2015; Kurisawa *et al.*, 2005).

2.1.2. Method II – Preparation of the HA-Tyr hydrogel

Contrary to method I, method II consists in developing HA-Tyr hydrogels by using DMTMM as coupling agent. Thus, HA (0.1 g, 2.5×10^{-4} mol) was dissolved in 10 mL of MES buffer (0.1 M, pH 6.0) and after complete dissolution the DMTMM reagent (0.069 g) was added for 1 h. Thereafter, Tyr (0.043 g) was added, and the reaction mixture was kept under vigorous stirring overnight at room temperature.

2.1.3. Method II – Preparation of the Si-HA hydrogel

Si-HA hydrogel was prepared by the reaction described by Flegeau and collaborators (2020), shown in figure 4. In this reaction, the silicon alkoxide, 3-aminopropyltriethoxysilane (APTES), had the function of amidating the carboxyl group of HA in a reaction mediated by DMTMM. DMTMM-mediated amidation of HA occurred via an aromatic substitution, forming an s-triazine ester intermediate of HA reactive to amines. Furthermore, the silicon alkoxide modulated hydrogels mechanical properties by providing the formation of cross-linking nodes. Additionally, the incorporation of silicon ions into the hydrogels structure allowed the improvement of their biological

properties (Botelho, 2005; Botelho *et al.*, 2006; Botelho *et al.*, 2006). With the aim to develop a dermal filler with an optimal composition according to mechanical and degradation characteristics, different formulations were evaluated.

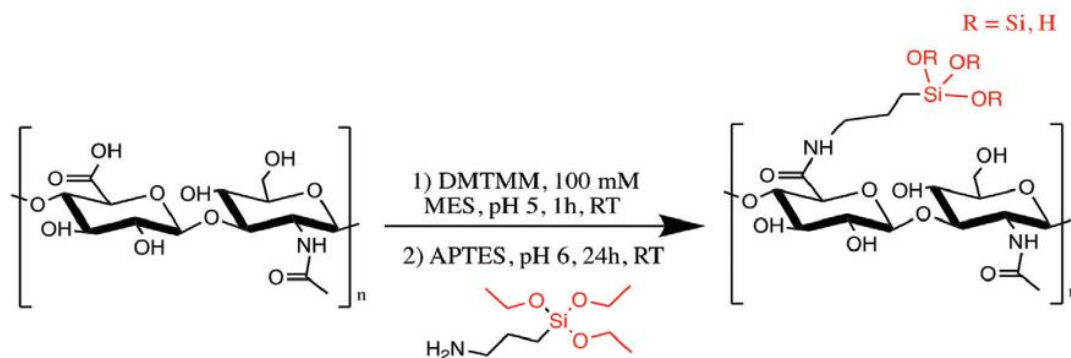


Figure 4 – Reaction for the silanization of HA, using DMTMM as the coupling agent and APTES as the aminoalkoxysilane. The synthesis is achieved in MES buffer at room temperature. Figure taken from Flegeau and collaborators (2020).

This reaction was performed by dissolving HA (500 kDa) in MES buffer (0.1 M, pH 6.0), in order to prepare a polymeric solution with a concentration of 1 % (w/V). After HA was completely dissolved, DMTMM (1 eq) were added to the HA solution. After 1 h, APTES was also added to the solution and the reaction remained stirred overnight at room temperature. Several reactions were performed with different APTES ratios, as described in Table 3.

Table 3 – Reactions conditions for the preparation of tunable Si-HA hydrogels

Hydrogel	m (HA) (g)	m (DMTMM) (g)	m (APTES) (g)	V (MES Buffer) (mL)	HA repeating monomer:DMTMM:APTES (Mole Ratio)
1	0.1	0.069	0.028	10	1:1:1/2
2	0.1	0.069	0.055	10	1:1:1
3	0.1	0.069	0.111	10	1:1:2
4	0.1	0.069	0.553	10	1:1:10

After performing the reactions, the samples were purified using Amicon filters (30 kDa), through several centrifugations (8000 rpm, 10 min) and subsequent addition of ultrapure H₂O. Finally, cross-linking was performed, incubating the different samples at 37 °C for 24 h.

2.2. Hydrogels physical-chemical characterization

The resulting hydrogels were fully characterized. The most important features that were characterized are: chemical structure, swelling and viscosity.

2.2.1. ATR-FTIR

Structural characterization of the HA hydrogels was performed by an Attenuated Total Reflectance – Fourier Transform Infrared Spectroscopy (ATR-FTIR), which provides information related to the presence or absence of specific functional groups, as well as the chemical structure of polymer materials. To perform the ATR-FTIR spectroscopy, the samples obtained by the reactions described above were freeze-dried. The spectra were obtained at room temperature and recorded in absorbance mode.

2.2.2. NMR

Nuclear magnetic resonance (NMR) allows the study of the physical, chemical and biological properties of the sample, allowing the identification of its molecular structure. To perform the NMR spectroscopy, the samples obtained were freeze-dried and 2 mg of lyophilized product was dissolved in 1 mL of deuterated H₂O.

2.2.3. Swelling

The swelling of Si-HA hydrogels was analysed by monitoring the mass of the hydrogels immersed in ultrapure H₂O over time at 37 °C. The swelling was carried out using 6-well transwell chambers. Si-HA hydrogels (1.5 mL) were formed *in situ* in the transwell inserts and the swelling was examined by placing the transwell in the bottom wells containing 2.0 mL of ultrapure H₂O and adding 1.0 mL of ultrapure H₂O inside the transwell inserts. The ultrapure H₂O was removed, and the inserts weighed after, 1, 2, 4, 7, 24, 48 and 120 h. The ultrapure H₂O was replenished after each weighing. Thus, the swelling was determined as the ratio of a hydrogel mass at a given time point divided by its initial mass.

2.2.4. Rheology

The viscosity profiles of the hydrogels were evaluated under 37 °C by performing multiwave frequency sweeps on a stress-controlled rheometer. The viscoelastic limit was determined by a shear strain sweep and then, G' and viscous modulus (G'') were measured at 37 °C varying frequency (0.1 to 10 Hz at a fixed strain of 0.1 %). Both strain and frequency sweeps were measured in triplicate.

3. Results and discussion

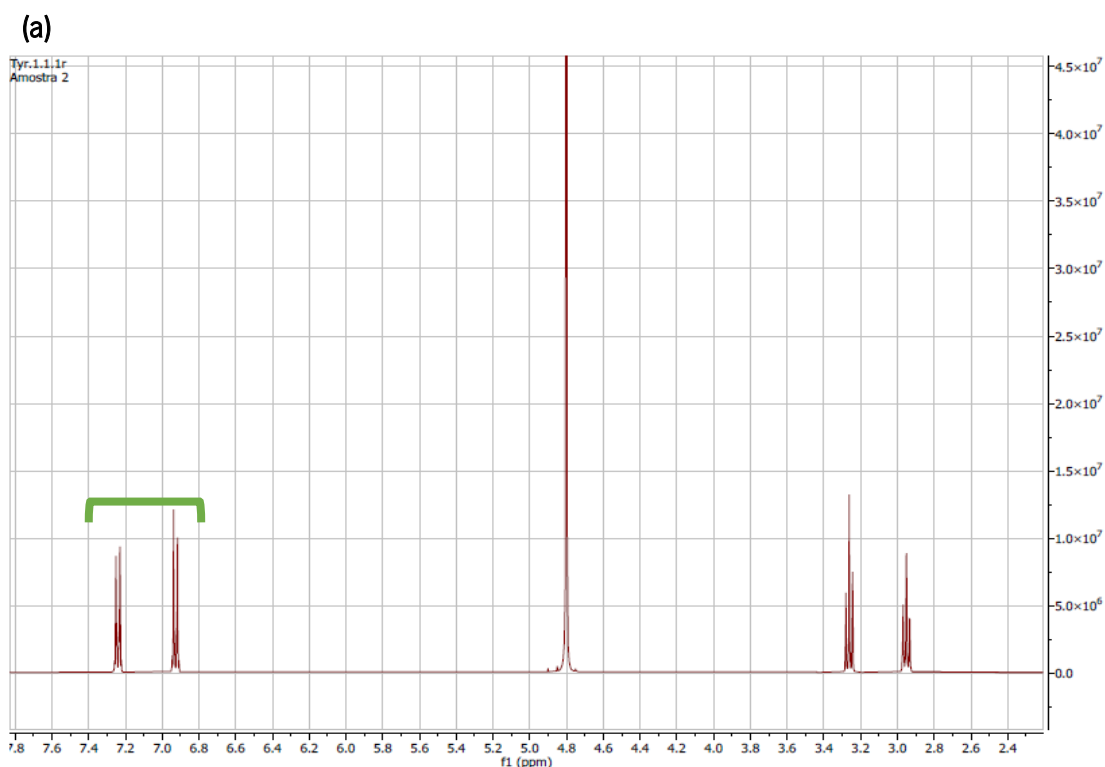
Skin gives an indication of one's health. It is so important that affects a person emotional and psychological behaviour (Barankin & DeKoven, 2002; Humphrey *et al.*, 2021). These facts propelled the cosmetic industry development. Indeed, the development of aesthetic procedures becomes essential for the treatment of skin lesions, as well as wrinkles. The ageing process is responsible for the degradation of the extracellular compounds produced in the dermis, such as collagen and elastin, resulting in thinner skin with less elasticity (Hirao, 2017), but it can be treated by dermal fillers, which consist of low-viscosity hydrogels that are injected into the skin. HA is one of the most commonly used materials in the development of fillers, given its excellent properties (Keen, 2017; Manuskiatti & Maibach, 1996). However, HA shows a high rate of degradation, not granting the necessary persistence to exert a positive effect on skin cells (Fallacara *et al.*, 2017). Therefore, it is necessary to chemically modify it. Through a cross-linking method it is possible to increase the viscoelasticity of the gel, as well as, its permanence at the application site, decreasing susceptibility to enzymatic degradation (Fallacara *et al.*, 2017). Furthermore, the cross-linking with the silicon alkoxide allows modulation of the properties of hydrogels (Flegeau *et al.*, 2020). Thus, in this work different methods/cross-linkers to produce HA hydrogels were used.

3.1. Preparation and characterization of the HA-Tyr hydrogel

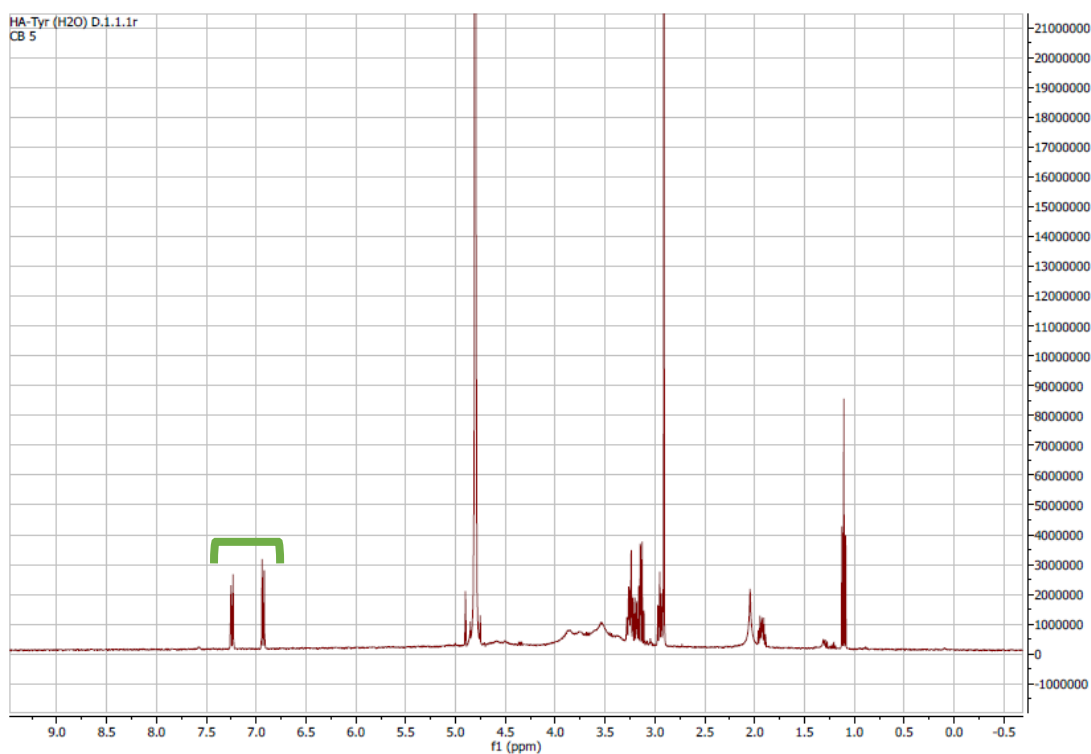
Several trials were performed in order to optimise the preparation of HA-Tyr hydrogels according to the described method. Firstly, two reactions were performed under the conditions described in assays 1 and 2 of table 2. Initially, the products obtained were purified by dialysis in ultrapure H₂O for 1 d using 8 kDa dialysis membranes. In fact, dialysis was the preferred

purification method since it is simpler and more economical to be performed at industrial scale. The obtained samples were then freeze-dried and analysed by ATR-FTIR and NMR. The ATR-FTIR spectra were plotted through the Microsoft Excel tool and the NMR spectra were obtained through the software MestReNova v14.2.1-27684.

The ATR-FTIR results obtained for assays 1 and 2 (Table 2) revealed apparently "clean" spectra after dialysis (Figure A1, Appendix I), but the NMR results showed the presence of EDC (Figure A2, Appendix I), which indicates the inefficiency of dialysis. On the other hand, NMR results revealed an apparent functionalization of HA by Tyr (Figure 5). Indeed, new peaks were found to be present in the HA-Tyr spectrum compared to the HA spectrum, these peaks corresponding to phenol groups ($\approx 6.7-7.1$ ppm) (Wang *et al.*, 2020). These results are also in line with the results presented in other scientific papers, which highlight the presence of distinct signals in the HA-Tyr spectrum corresponding to both proton pairs of the aromatic ring (≈ 6.8 and 7.2 ppm) (Hong *et al.*, 2019; Kim *et al.*, 2011; Wang *et al.*, 2020).



(b)



(c)

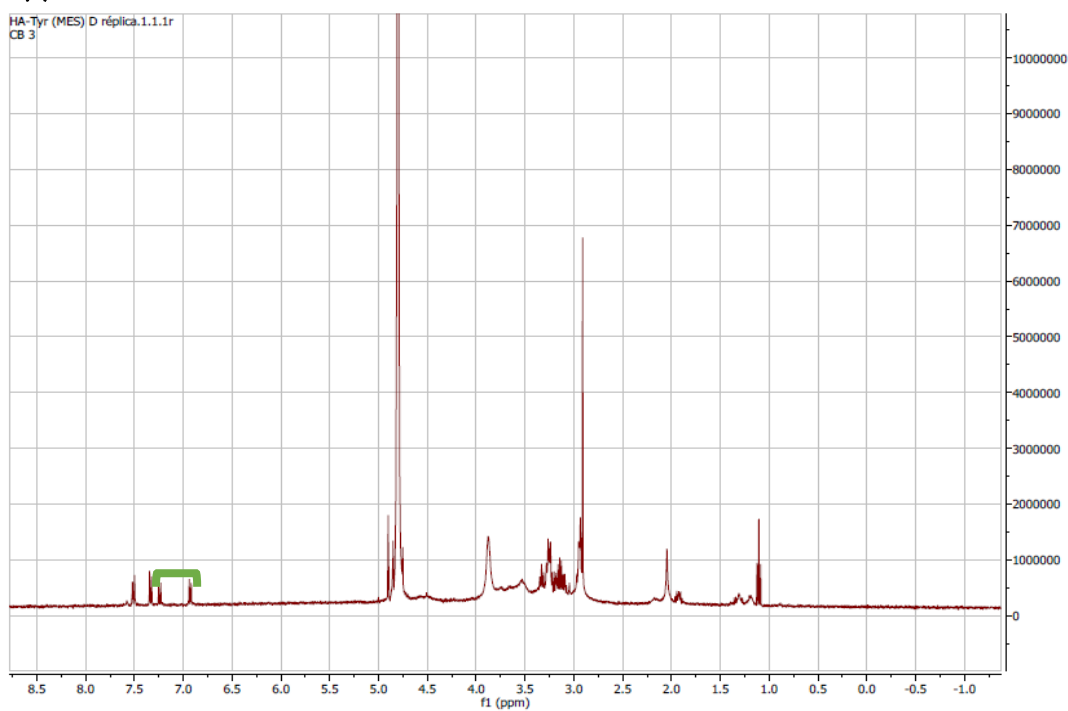


Figure 5 – NMR spectra obtained by NMR analysis for (a) Tyr and HA-Tyr reactions in (b) ultrapure H₂O and in (c) MES buffer (0.1 M, pH 6.0) after dialysis (D). The peaks marked in green correspond to the peaks of the Tyr spectrum.

However, as the spectra are not completely "clean" it is not possible to confirm the success of the reaction. In fact, it cannot be stated that the peaks that the product (HA-Tyr) presents,

corresponding to the peaks of Tyr, concern the Tyr that reacted, since the dialysis was not efficient and, therefore, the sample could contain Tyr that did not react. Thus, in order to optimise the dialysis and verify the efficiency of the reaction, new trials were performed, in which the reactions were carried out again under the same conditions, but the purification was altered, so that the dialysis had a duration of 3 d. However, signals from unreacted small molecules (such as EDC and NHS) were still visible after dialysis, as well as an apparent functionalisation of HA in the reactions with Tyr. Another trial was performed in which only the HA-Tyr reaction in ultrapure H₂O was carried out, under the same conditions, since it appeared to be the most promising. In this assay, the dialysis volume was increased to 1 L in order to optimise the purification process. After lyophilization, ATR-FTIR and NMR analyses were performed again. However, it was again verified by the NMR results the presence of peaks characteristic of the EDC spectrum in the spectrum relating to the HA-Tyr sample obtained after dialysis (Figure A3, Appendix I). Thus, the purification was not efficient, so it is not possible to confirm the functionalisation of HA, and the doubt remains whether the Tyr present corresponds to unreacted Tyr or to reacted Tyr. On the other hand, it was found from the NMR spectra that the characteristic peaks of HA are not well evidenced in the spectrum of the dialysed HA-Tyr sample, since the product did not completely dissolve in deuterated H₂O when preparing the samples for NMR analysis. Alternatively, it was attempted to dissolve the product in DMSO for NMR analysis, but without success, so the analysis of the hydrogels structure was now performed only by ATR-FTIR.

Since dialysis did not allow the efficiency of the reaction to be evaluated, the cross-linking reaction was performed with HRP. Thus, if gelation occurred after the cross-linking reaction, it would mean that the functionalisation of HA had in fact occurred. However, gelation did not occur, which may have been due to the fact that part of the enzyme remained on the walls of the vial in which the reaction occurred, as well as the fact that they were very small quantities, and there may have been losses. This may have contributed to the inefficiency of the cross-linking reaction, making it impossible to assess the efficiency of the HA-Tyr reaction.

Furthermore, given the inefficiency of dialysis in purifying the formulations, the purification method was changed to centrifugation with Amicon filters. The sample that was not purified and the sample obtained after purification were analysed by ATR-FTIR. Comparison of the resulting ATR-FTIR spectra highlights the efficiency of the purification process, as the spectrum of the purified

sample lacks the characteristic bands of the non-reacted small molecules in the reaction medium (such as EDC, NHS and Tyr) (Figure 6).

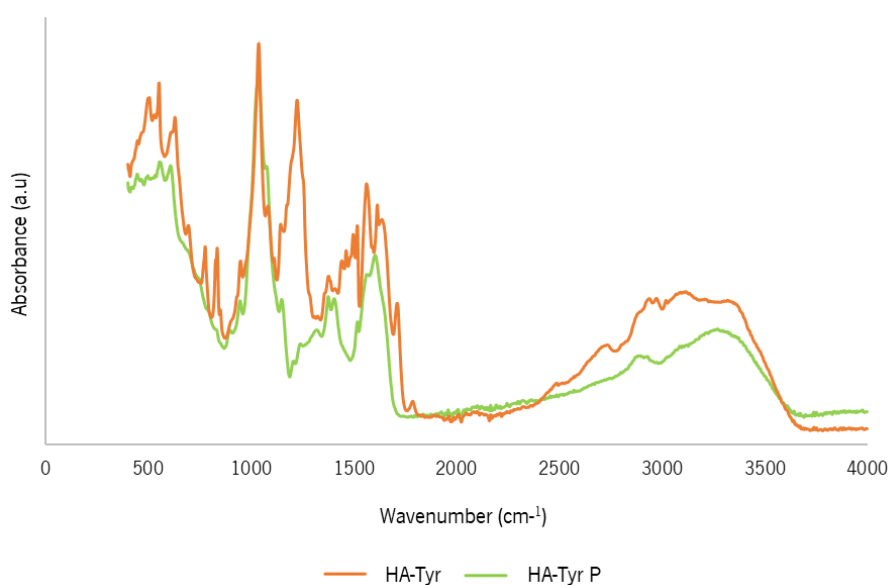


Figure 6 – Spectra obtained by ATR-FTIR analysis of the reaction of HA with Tyr in ultrapure H₂O before - HA-Tyr - and after purification with Amicon filters - HA-Tyr P.

In addition, it can be seen that some of the characteristic Tyr peaks (1216 cm⁻¹ and 1492 cm⁻¹) disappeared from the spectrum of the sample after purification, which implies that part of the Tyr present corresponds to unreacted Tyr (Figure A4, Appendix I). However, it is worth noting the presence of two small peaks associated with Tyr (826 cm⁻¹ and 1517 cm⁻¹) in the spectrum of the pure HA-Tyr sample, which suggests that a small part of the Tyr might have reacted with HA (Figure A5, Appendix I). Furthermore, it should be noted that the peaks represented at 1550-1680 cm⁻¹ (1560 cm⁻¹) and 3300-3500 cm⁻¹ in the spectra of HA and the pure HA-Tyr sample corresponds to the amide bond bends and to the stretching vibration of -OH and -NH- groups, respectively (Figure 7). According to Wang and collaborators, if the functionalisation of HA was successful, these absorption peaks of pure HA-Tyr sample would be significantly stronger than that of HA (Wang *et al.*, 2020). Indeed, if the Tyr conjugation to HA via amide bond was accomplished well, the peaks of amide bond between HA and Tyr would overlap with that of amide bond on HA backbone, i.e., if there were more amide groups, the stronger the corresponding peaks would be. As this is not the case, it can be stated that a large part of Tyr was not successfully grafted onto HA.

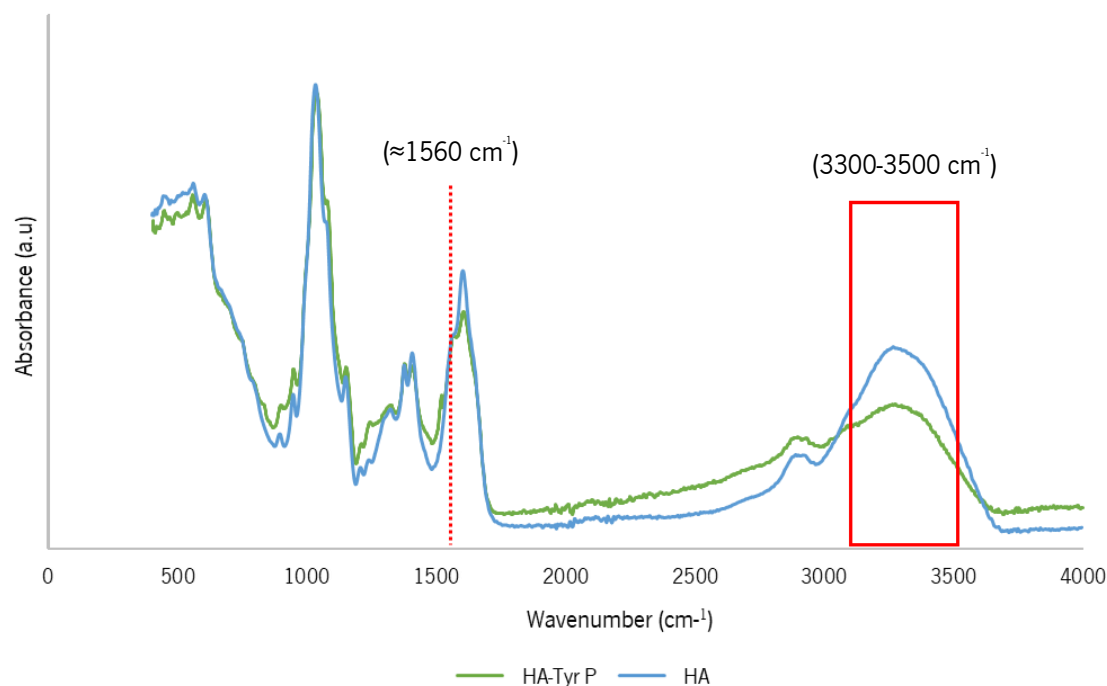


Figure 7 – Spectra obtained by ATR-FTIR analysis of the control consisting of HA alone and of the reaction of HA with Tyr in ultrapure H₂O after purification with Amicon filters - HA-Tyr P. The peaks represented at 1560 cm⁻¹ and 3300-3500 cm⁻¹ in the spectra of HA and HA-Tyr P corresponds to the amide bond bends and to the stretching vibration of -OH and -NH- groups, respectively.

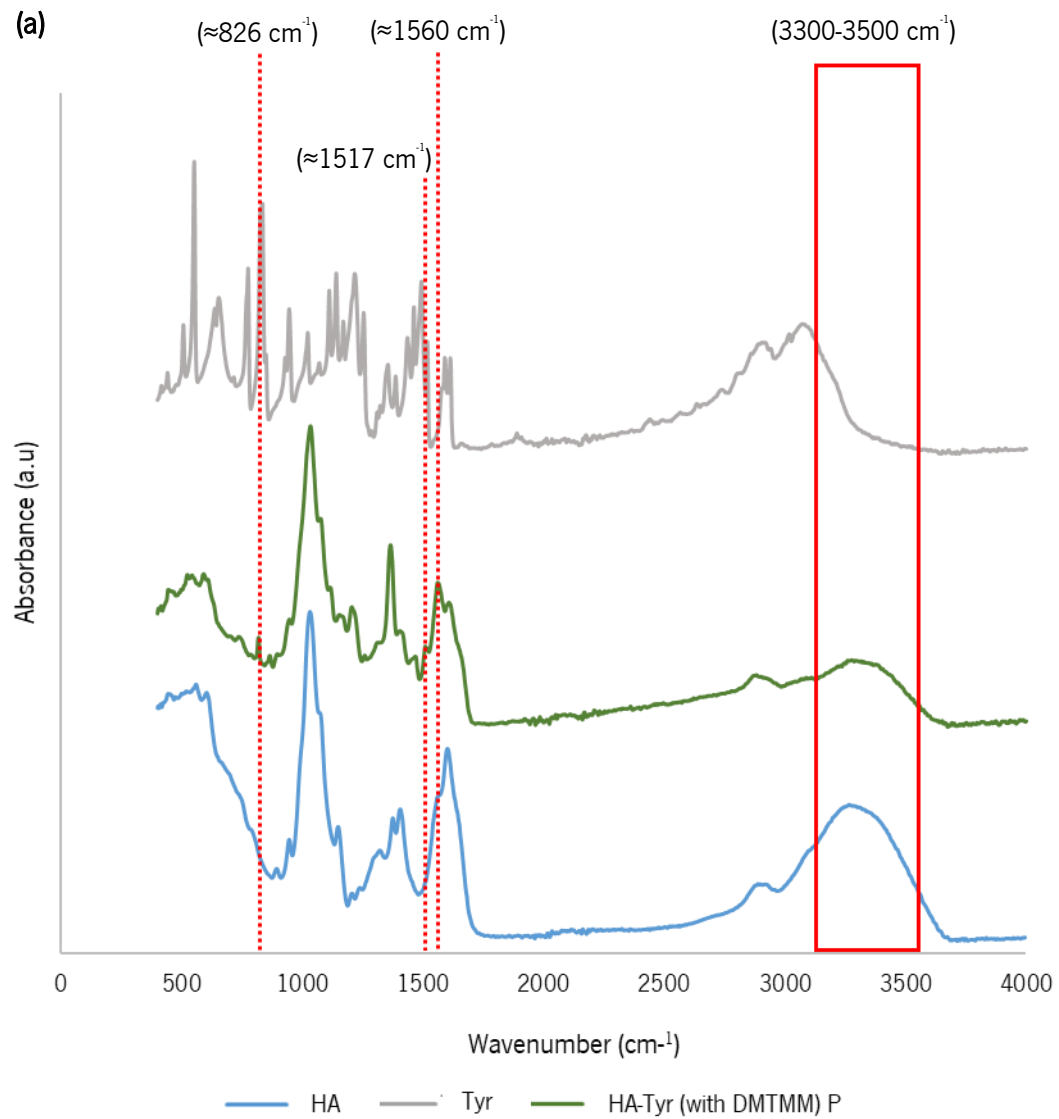
It should be noted that after freeze-drying the samples, the cross-linking reaction was attempted again, but this was not possible as the pure HA-Tyr sample did not dissolve in PBS (0.1 M). This suggests that some modification occurred in the HA, i.e., part of the added Tyr may have reacted with the polymer. However, the reaction was not very efficient which may be due to the possible occurrence of side reactions that generate adducts, that do not participate in the subsequent cross-linking reaction, and are therefore regarded as unproductive and undesirable (Aslam & Dent, 1998; Darr & Calabro, 2009). These adducts can occur as a result of two different side reactions. The first side reaction consists in the intramolecular rearrangement of the reactive O-acylisourea intermediate to form N-acylurea adducts on HA. Given the asymmetric nature of the EDC molecule, it is possible the formation of two distinct adducts. The second side reaction involves molecules containing a hydroxyphenyl group like Tyr. In this case, the EDC reacts directly with the hydroxyphenyl group on Tyr, whether free in solution or already covalently bound to HA through its amine group, forming Tyr-O-EDC adducts on HA. Also, in this reaction two distinct adducts can be formed due to the asymmetric nature of the EDC molecule (Darr & Calabro, 2009).

With the aim of minimizing the occurrence of these side reactions and at the same time optimize the functionalisation of the HA by Tyr, a new test was performed (Assay 3, Table 2), reducing the time interval between the addition of NHS and Tyr, which instead of 60 min became

15 min. The resulting ATR-FTIR spectra also showed the characteristic peaks of Tyr at 826 cm^{-1} and 1517 cm^{-1} , and it was again found that the peaks at 1560 cm^{-1} and $3300\text{-}3500\text{ cm}^{-1}$ are not more prominent than those of HA (Figure A6, Appendix I). Indeed, there was no difference in the ATR-FTIR analysis between the sample prepared with a time interval of 60 min between the addition of NHS and Tyr and the sample prepared with a time interval of only 15 min. Therefore, another assay was performed (Assay 4, Table 2), keeping the time interval of 60 min between the addition of NHS and Tyr, but the ratio of Tyr was increased to 5x. After the ATR-FTIR analysis, it was found that the spectrum related to the new assay presents the same peaks as the spectra related to the previous assays (Assays 2 and 3, Table 2) (Figure A6, Appendix I). Thus, it is possible to assess that the functionalization of HA by Tyr through EDC/NHS chemistry was not efficient, since a large part of the added Tyr does not react with HA, regardless of the changes made to the experimental procedure in order to optimize the reaction.

As it was found that the reaction between HA and Tyr through EDC/NHS chemistry was not very efficient, a new assay was performed using the methodology of the preparation of Si-HA hydrogels for the functionalisation of HA by Tyr. Indeed, given the limitations of the EDC/NHS chemistry, such as the possibility of side reactions, there are studies in the literature that demonstrate the applicability of DMTMM as an alternative coupling agent to synthesize HA-Tyr conjugates (Fu *et al.*, 2021; Loebel *et al.*, 2015; Ziadlou *et al.*, 2021). Thus, instead of EDC and NHS, DMTMM was used as coupling agent and the HA-Tyr reaction was performed according to method II. After purification with Amicon filters and subsequent freeze-drying of the samples, the spectra for ATR-FTIR analysis were obtained (Figure 8). By observation of figure 8, the spectrum of the pure HA-Tyr sample, prepared with the coupling agent DMTMM, presents peaks characteristic of Tyr at 827 cm^{-1} and 1517 cm^{-1} well defined. Moreover, it is found that the peak at 1560 cm^{-1} , which corresponds to the amide bond bends (Haxaire *et al.*, 2003), is stronger in the spectrum of the pure HA-Tyr sample than in the HA spectrum, contrary to what was found in the spectra corresponding to the previous experiments. Thus, it can be stated that the HA-Tyr reaction using DMTMM as coupling reagent is more efficient than the HA-Tyr reaction via EDC/NHS chemistry. Indeed, the presence of a more prominent peak at 1560 cm^{-1} indicates the presence of more amide bonds and, therefore, a greater Tyr conjugation to HA via amide bond (Wang *et al.*, 2020). On the other hand, the peak at $3300\text{-}3500\text{ cm}^{-1}$ of the spectrum of the pure HA-Tyr sample is not stronger than that of the HA spectrum, but since this peak corresponds to the stretching vibration of -OH

group, the presence of H₂O influences, so the HA sample could contain more H₂O and therefore have a stronger peak.



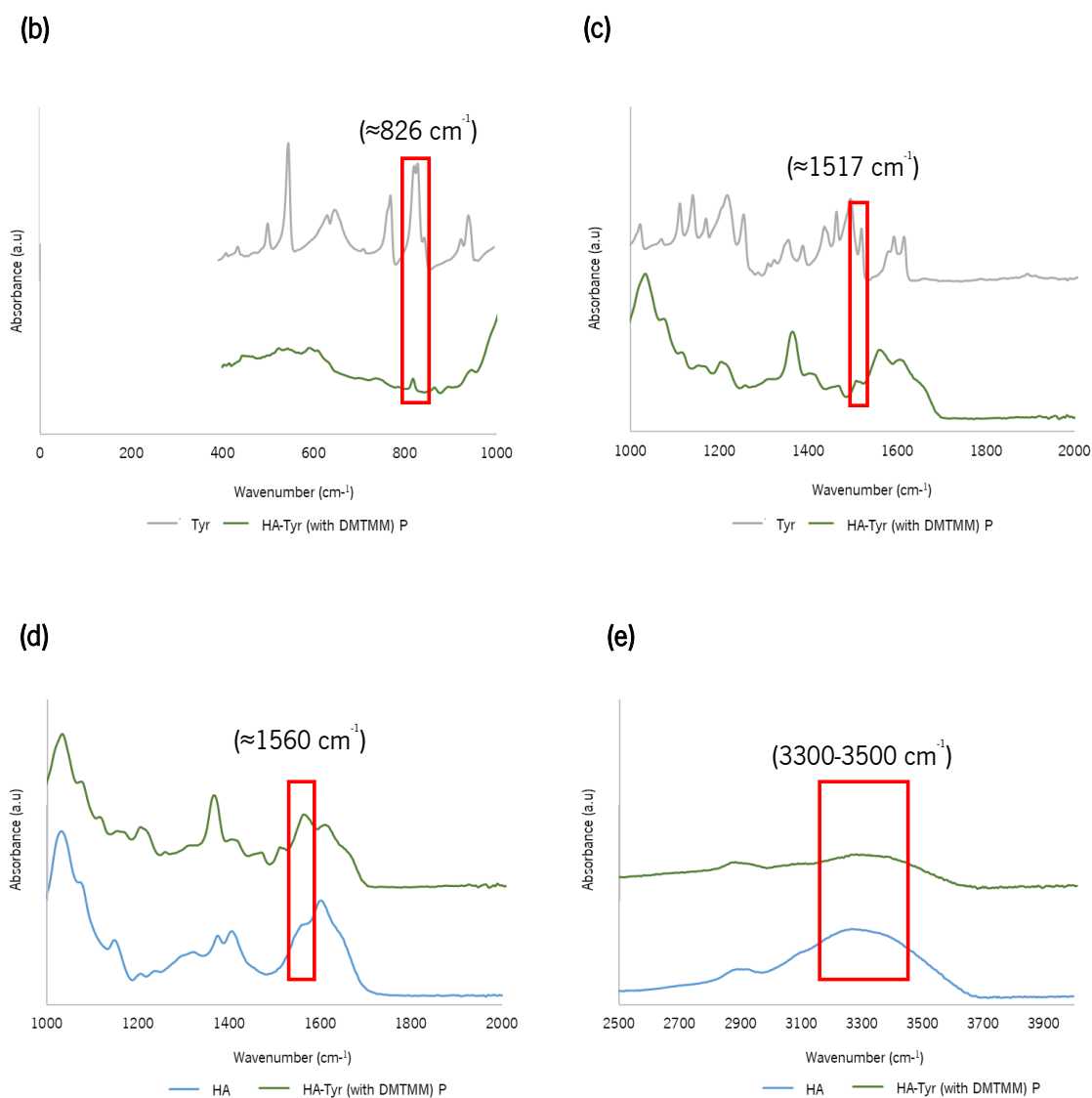


Figure 8 – (a) Spectra obtained by ATR-FTIR analysis of HA and Tyr controls and of the reaction of HA with Tyr in MES buffer (0.1 M, pH 6.0), using the DMTMM as a coupling agent, after purification with Amicon filters – HA-Tyr (with DMTMM) P. The red-highlighted peaks represented at **(b)** 826 cm^{-1} and **(c)** 1517 cm^{-1} in the spectrum of HA-Tyr (with DMTMM) P corresponds to the characteristic peaks of the Tyr spectrum. The peaks represented at **(d)** 1560 cm^{-1} and **(e)** 3300-3500 cm^{-1} in the spectra of HA and HA-Tyr (with DMTMM) P corresponds to the amide bond bends and to the stretching vibration of -OH and -NH- groups, respectively.

3.2. Preparation and characterization of the Si-HA hydrogel

Several reactions were performed with different APTES ratios (Table 3), in order to highlight the possibility of shaping the properties of hydrogels through cross-linking, allowing personalized hydrogels to be obtained according to customer needs. After preparation of the hydrogels, the hydrogel 4 was found to be turbid compared to the other formulations (Figure 9). This may be due to the condensation of the APTES, i.e., APTES does not fully react with HA, so some of the APTES molecules may react with each other, causing the turbidity. This phenomenon only happens in the

formulation with a higher amount of cross-linker, which means that the rapid addition of a large quantity of APTES may not grant the necessary time for the APTES to react with the polymer, hence the cross-linker molecules react with each other. Therefore, in order to optimize this reaction and increase the degree of substitution, APTES was added fractionally at 1 h intervals.

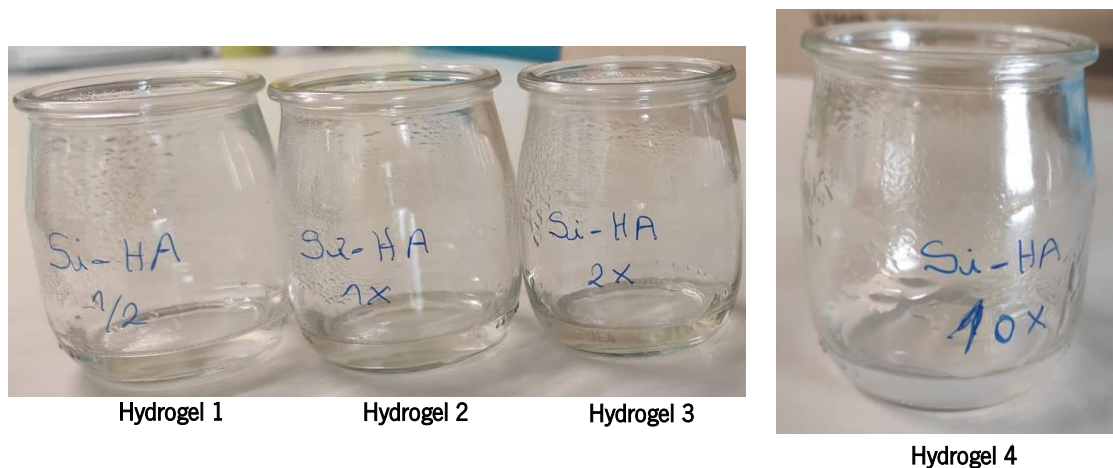
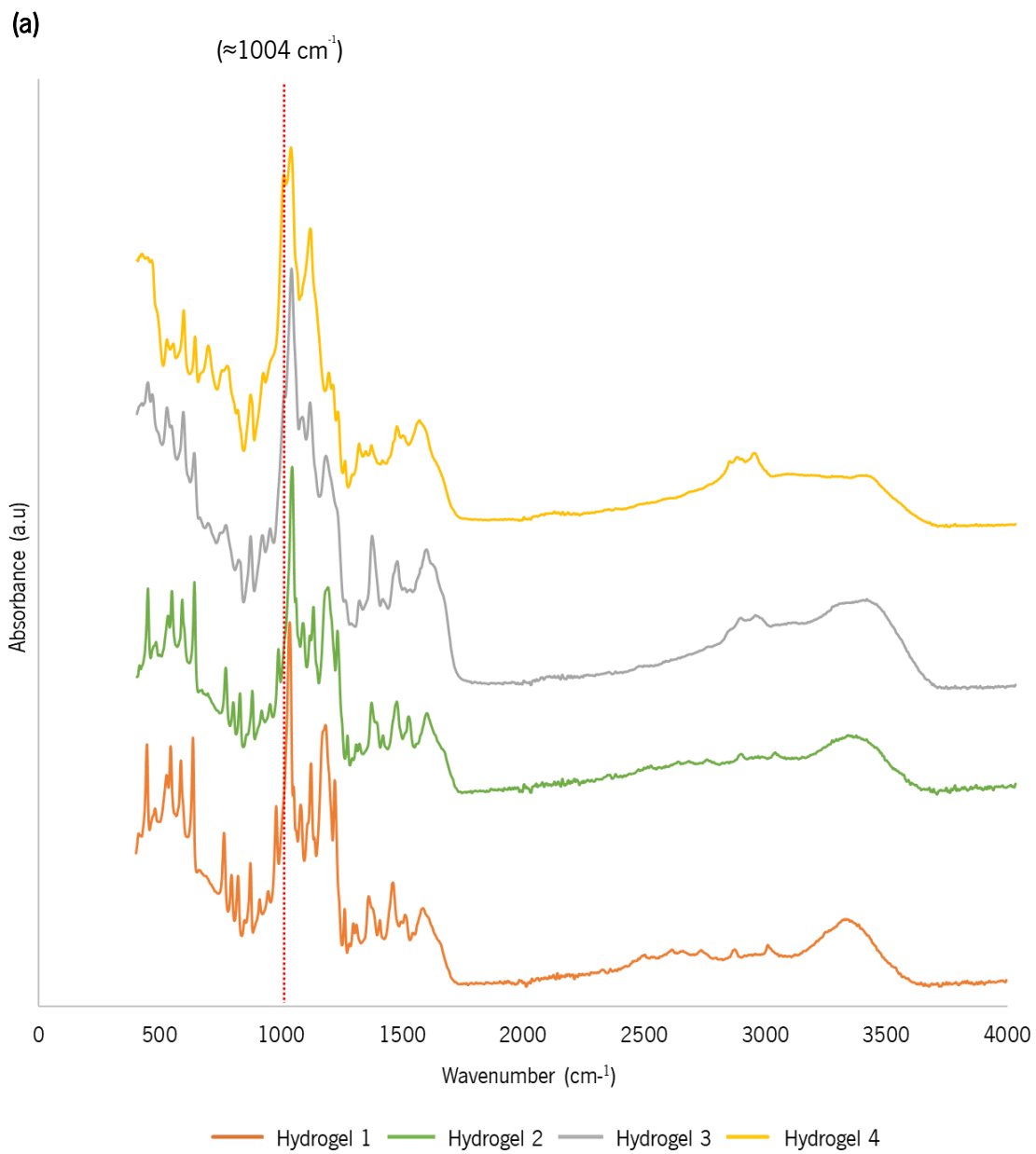


Figure 9 – Preparation of the APTES modified HA hydrogels 1, 2, 3 and 4.

After preparation of the hydrogel 4 by fractional addition of APTES, there was a slight decrease in turbidity. Once again, it was observed the quantity of APTES added, even fractionally, was too high, preventing a high degree of substitution. The formulations obtained were subsequently freeze-dried and analysed by ATR-FTIR, without further purification (Figure 10). The ATR-FTIR spectra of hydrogels 3 and 4 confirmed the condensation of the APTES molecules, due to the presence of a peak at 1004 cm^{-1} , which corresponds to the Si-O-Si stretching vibration (Eslahi *et al.*, 2016; Feifel & Lisdat, 2011). It should be noted that although hydrogel 3 shows this peak, the APTES condensation in this hydrogel was insignificant when compared to that occurring in hydrogel 4, which is clearly seen by the turbidity that the hydrogel presents. On the other hand, hydrogels 1 and 2 did not present this peak, meaning that the addition of smaller amounts of APTES allows a higher degree of substitution.



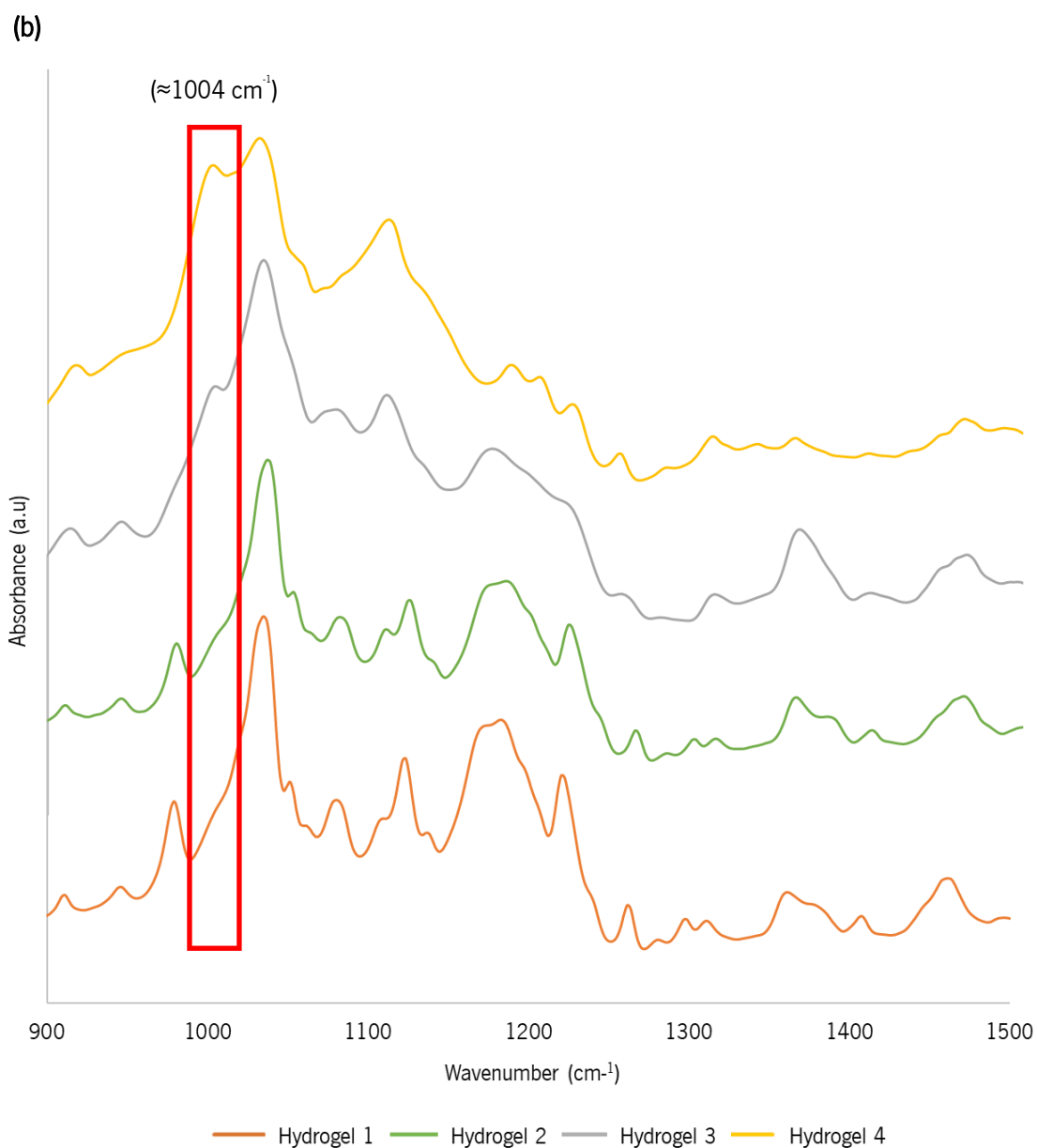


Figure 10 – (a) Spectra obtained by ATR-FTIR analysis and **(b)** extended area between 900 cm⁻¹ and 1500 cm⁻¹ of the spectra of the APTES modified HA hydrogels 1, 2, 3 and 4 in MES buffer (0.1 M, pH 6.0). The peaks represented at 1004 cm⁻¹ in the spectra of Hydrogels 3 and 4 corresponds to the stretching vibration of Si-O-Si.

Additionally, the comparison between HA, hydrogels 1, 2, 3 and 4 spectra show that the reaction was successfully carried out. The peak present in the interval 1500-1600 cm⁻¹ is more prominent in the spectra of the hydrogels than in the HA spectrum (Figure 11). This peak represents the formation of the amide II bonding between the carboxyl COO⁻ group in HA and the amine group in APTES (Hu *et al.*, 2011; Sánchez-Téllez *et al.*, 2020).

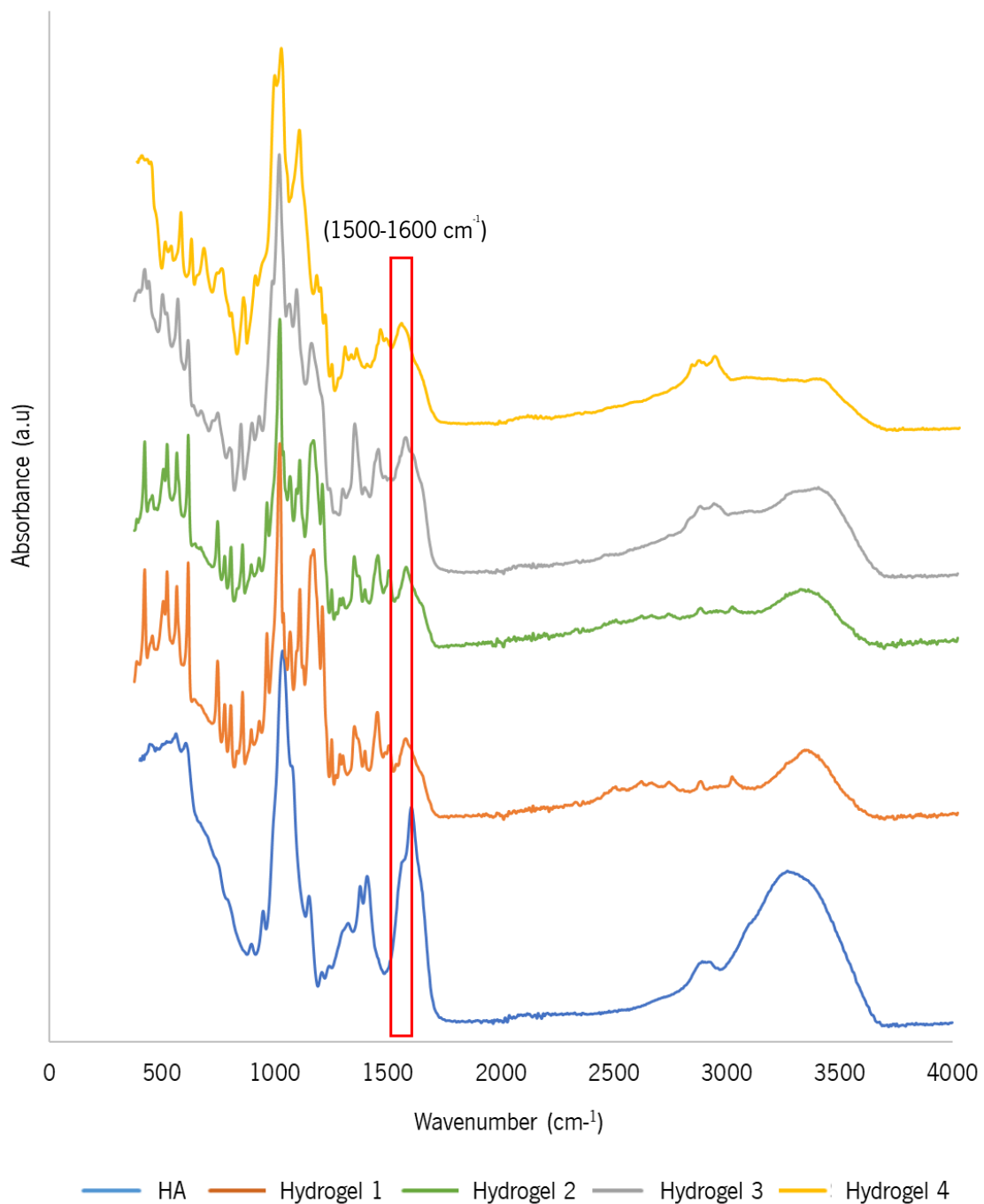


Figure 11 – Spectra obtained by ATR-FTIR analysis of the HA control and of the APTES modified HA hydrogels 1, 2, 3 and 4 in MES buffer (0.1 M, pH 6.0). The peaks represented at 1500-1600 cm^{-1} in the spectra of all the formulations corresponds to the amide bond bends.

After having verified the efficiency of the reactions between HA and APTES by ATR-FTIR analysis, the cross-linking was performed. Thus, the formulations were incubated at 37 °C in eppendorffs for 24 h, and it was verified that the hydrogels cross-linked. In fact, the hydrogels did not move along the eppendorff when it was inverted, remaining at the bottom of the eppendorff

unlike the HA control (Figure 12). Thus, it can be stated that the reaction between HA and APTES, as well as the crosslinking was successful.

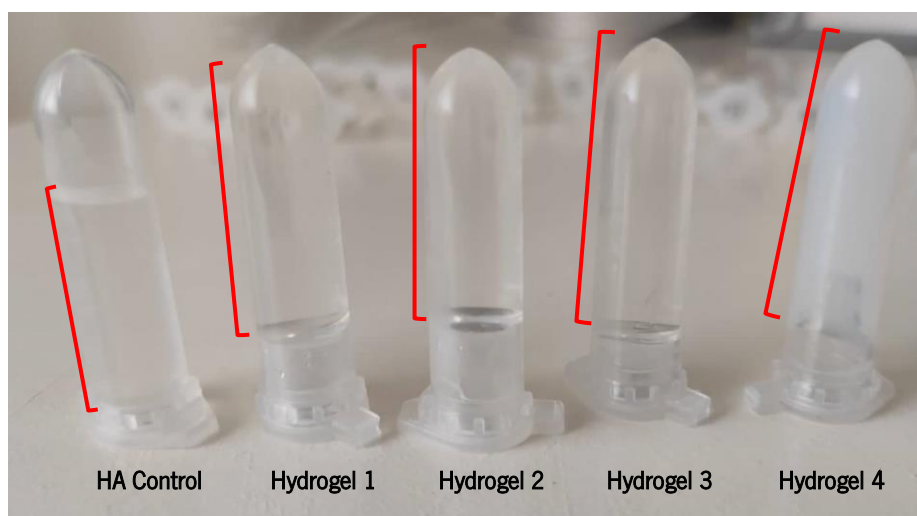


Figure 12 – Cross-linked APTES modified HA hydrogels 1, 2, 3 and 4, and the HA control after incubation at 37 °C for 24 h.

In addition, new formulations were prepared which were purified with Amicon filters and were subsequently lyophilised. Analysis of the spectra obtained by ATR-FTIR of a sample that was purified, and the respective impure sample showed the efficiency of the purification process (Figure A1, Appendix II). In fact, some peaks disappeared from the spectrum of the purified sample, including the peak at 1004 cm^{-1} , which suggested the condensation of the APTES molecules, i.e., APTES that had not reacted with HA. Thus, considering the success of the reactions, as well as the efficiency of the purification process, the hydrogels were further characterised in terms of swelling and rheology.

The swelling of Si-HA hydrogels was then evaluated by immersing the hydrogels in ultrapure H_2O and incubating at 37 °C. After calculating the swelling ratio of each hydrogel, it was found that the swelling ratio was lower the higher the degree of silanization, i.e., the hydrogel 4 presents the lowest swelling ratio and the hydrogel 1 presents the highest swelling ratio (Figure 13). Although hydrogel 4 has a higher amount of cross-linker, its degree of silanization is low since condensation of the APTES molecules occurred during its preparation. Thus, the low swelling ratio that this hydrogel presents is not due to a high degree of cross-linking, but to the fact that it may contain silicate aggregates that influence the swelling capacity. Furthermore, the hydrogel 1 swelled the fastest over the 7 h incubation period. After 7 h from the start of the test, it was found for all hydrogels that the swelling ratio did not increase as sharply as up to that timepoint. Thus, it is likely that after 120 h, the swelling ratio would eventually stabilise. In general, these results indicate that

the swelling profiles of Si-HA hydrogels are ruled by the crosslink density (Flegeau *et al.*, 2020; H.-Y. Lee *et al.*, 2019; Maiz-Fernández *et al.*, 2022). In fact, an additional siloxane linkage increases crosslinking density, thus reducing swelling. Furthermore, the grafted silane groups were less hydrophilic than HA, resulting in lower association with water (H.-Y. Lee *et al.*, 2019).

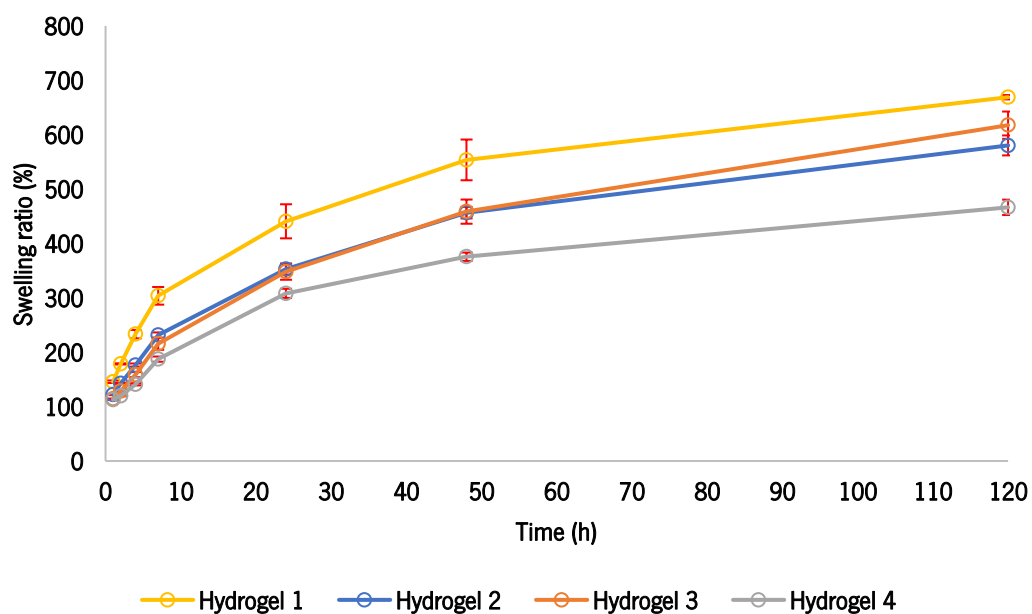


Figure 13 – Swelling behaviour of the APTES modified HA hydrogels 1, 2, 3 and 4 in ultrapure H₂O at 37 °C. The error bars represented in red correspond to the standard deviation.

Regarding rheology, all Si-HA hydrogels showed a gel-like behaviour since the values of G' are higher than the values of G'' (Figure 14). This behaviour reveals that elastic properties of the analysed hydrogels prevail over the viscous ones, which is the characteristic behaviour of hydrogels (Maiz-Fernández *et al.*, 2022).

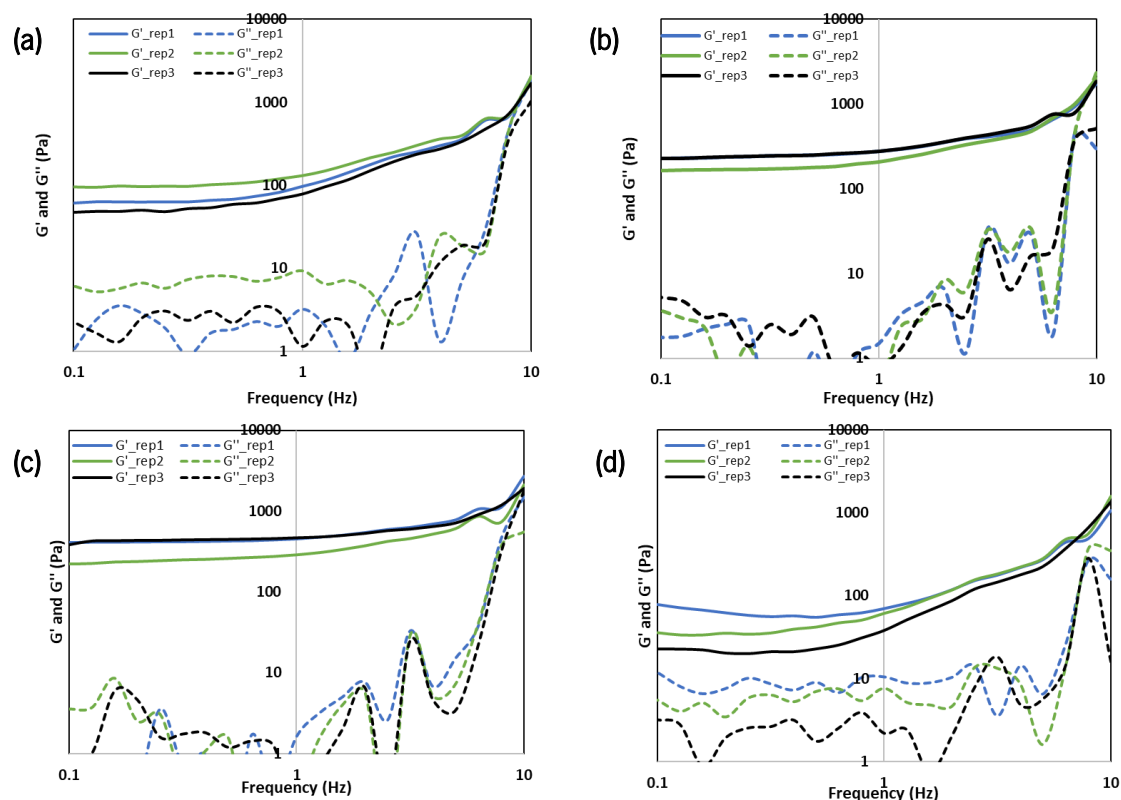


Figure 14 – Rheological behaviour of the APTES modified HA hydrogels (a) 1, (b) 2, (c) 3 and (d) 4 at 37 °C varying frequency (0.1 to 10 Hz at a fixed strain of 0.1 %). The filled lines represent the elastic modulus (G') and the dashed lines represent the viscous modulus (G'').

Comparing the G' values of the prepared hydrogels it can be noted that they differ, revealing a clear dependence of the rheological properties on the cross-linker ratio (Figure 15). In this way, as expected, an increase in cross-linker content in Si-HA hydrogel composition leads to an increase in the value of the G' , as can be seen in figure 15 for hydrogels 1,2 and 3. However, hydrogel 4 presents a different behaviour, since, despite being the one with the highest cross-linker ratio, it is the one with the lowest value of G' . This may be due to the fact that the amount of APTES added is too high, which can lead to a large part of the APTES molecules reacting with each other instead of reacting with the HA. In short, hydrogel 3 has the highest G' value, while hydrogel 4 has the weakest rheological properties.

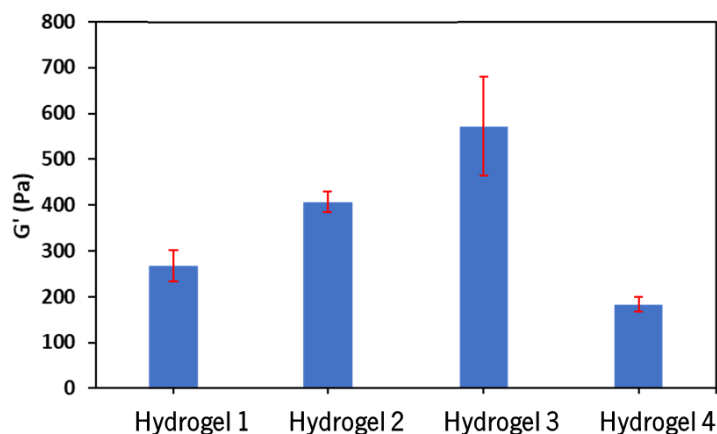


Figure 15 – Elastic modulus (G') of the APTES modified HA hydrogels 1, 2, 3 and 4 measured at 37 °C varying frequency (0.1 to 10 Hz at a fixed strain of 0.1 %). The error bars represented in red correspond to the standard deviation.

4. Conclusions and future perspectives

The need to look our best is of utmost importance in society. A well-known pronouncement is that “eyes are the windows to our soul”, but skin appearance can also tell a lot about a person health and state of mind. Therefore, advances in the cosmetics field are extremely important, since the development of new technologies, products and aesthetic procedures promotes the quality of the skin and, as a result, the general well-being of a person. In this context, the importance of developing personalised HA hydrogels that allow treatment tailored to the needs of each client should be highlighted.

This work allows the exploration of different methodologies for the development of hydrogels with different characteristics for dermocosmetic application. Moreover, the use of a silicon alkoxide as a cross-linker for the development of hydrogels may constitute an alternative to the cross-linkers commonly used (BDDE and DVS), since the silicon alkoxide has the advantage of having biologic properties and, therefore, does not present cytotoxicity.

In this work, it was developed HA-Tyr hydrogels through two methods (method I and method II). Initially, method I was performed, which consists of the carbodiimide coupling reaction between the carboxylic groups of HA and the amine groups of Tyr through EDC/NHS chemistry. The formulations obtained were purified and analysed by ATR-FTIR and NMR. The results obtained revealed the inefficiency of the purification process, even after its optimization, which led to a change in the purification method. Thus, purification was performed by centrifugation with Amicon

filters, which proved to be efficient. After successful purification, it was found that the reaction between Tyr and HA was not very efficient, since only a small part of Tyr could have reacted with HA. Consequently, the optimization of the method of preparation of the hydrogels was implemented, but without success because there were no changes in the results obtained. These results may be due to the possibility of occurrence of side reactions that generate adducts. Given the low efficiency of method I in the preparation of HA-Tyr hydrogels, they were prepared according to method II, which consists of using DMTMM as a coupling reagent. The results obtained through this method revealed the efficiency of the conjugation between HA and Tyr. As a result, it is possible to conclude that method II is more efficient than method I for the preparation of HA-Tyr hydrogels.

Moreover, it was developed four Si-HA hydrogels through method II, varying the ratio of APTES. The reactions consisted of using DMTMM as a coupling agent and APTES as a cross-linker. The resulting hydrogels were purified by centrifugation with Amicon filters and analysed by ATR-FTIR. The results obtained revealed the efficiency of the 4 reactions, however the hydrogel with the highest amount of APTES (hydrogel 4) showed turbidity, even after the fractional addition of the cross-linker. This may be a result of the reaction occurring between the APTES molecules, instead of reacting with the HA. The cross-linking of the different hydrogels was also successful, so their physical-chemical characterization was carried out. The swelling of the Si-HA hydrogels revealed that the swelling ratio was lower the higher the degree of silanization. Yet even though hydrogel 4 has a higher amount of cross-linker, its degree of silanization is low since condensation of the APTES molecules occurred during its preparation. Therefore, the low swelling ratio that this hydrogel presents is not due to a high degree of cross-linking, but to the fact that it may contain silicate aggregates that influence the swelling capacity. Moreover, the rheology performed on the prepared hydrogels showed a gel-like behaviour since the values of G' are higher than the values of G'' . It is also noteworthy that the rheological properties of the Si-HA hydrogels have a clear dependence of the on the cross-linker ratio. Indeed, an increase in cross-linker content in Si-HA hydrogel composition leads to an increase in the value of the G' . Nevertheless, the hydrogel 4 is the one with the lowest value of G' , since it contains a lower degree of cross-linking resulting from the condensation of the APTES molecules, as mentioned above. In conclusion, the possibility of modulating the cross-linking of hydrogels through a silicon alkoxide, and thus obtaining hydrogels with different properties (degree of cross-linking and rheological properties) was confirmed.

Regarding HA-Tyr hydrogels, as a future perspective, it might be important to perform the cross-linking reaction with the HRP enzyme, as well as the physical-chemical characterization, in order to compare with the Si-HA hydrogels. Furthermore, it is fundamental to perform a cytotoxicity study to all hydrogels developed.

Finally, it might be interesting to add PEG to all hydrogels (HA-Tyr and Si-HA), as it would allow the hydrogels to be stabilized, as well as increase their permanence at the application site, reducing their susceptibility to enzymatic degradation. Indeed, the commercial fillers do not have a very long effect duration as a result of enzymatic degradation, therefore PEG would solve this problem, which would be an asset for the cosmetic industry.

References

- Abou-Okeil, A., Fahmy, H. M., El-Bisi, M. K., & Ahmed-Farid, O. A. (2018). Hyaluronic acid/Na-alginate films as topical bioactive wound dressings. *European Polymer Journal*, *109*, 101–109. <https://doi.org/https://doi.org/10.1016/j.eurpolymj.2018.09.003>
- Amado, I. R., Vázquez, J. A., Pastrana, L., & Teixeira, J. A. (2017). Microbial production of hyaluronic acid from agro-industrial by-products: Molasses and corn steep liquor. *Biochemical Engineering Journal*, *117*, 181–187. <https://doi.org/https://doi.org/10.1016/j.bej.2016.09.017>
- Armstrong, S. E., & Bell, D. R. (2002). Relationship between lymph and tissue hyaluronan in skin and skeletal muscle. *American Journal of Physiology - Heart and Circulatory Physiology*, *283*(6 52-6), 2485–2494. <https://doi.org/10.1152/ajpheart.00385.2002>
- Aslam, M., & Dent, A. (1998). Bioconjugation : protein coupling techniques for the biomedical sciences. London : Macmillan reference books. <http://lib.ugent.be/catalog/rug01:000488488>
- Bae, J. W., Choi, J. H., Lee, Y., & Park, K. D. (2015). Horseradish peroxidase-catalysed in situ-forming hydrogels for tissue-engineering applications. *Journal of Tissue Engineering and Regenerative Medicine*, *9*(11), 1225–1232. <https://doi.org/10.1002/term.1917>
- Bai, K. J., Spicer, A. P., Mascarenhas, M. M., Yu, L., Ochoa, C. D., Garg, H. G., & Quinn, D. A. (2005). The role of hyaluronan synthase 3 in ventilator-induced lung injury. *American Journal of Respiratory and Critical Care Medicine*, *172*(1), 92–98. <https://doi.org/10.1164/rccm.200405-6520C>
- Ballin, A. C., Cazzaniga, A., & Brandt, F. S. (2013). Long-term efficacy, safety and durability of Juvéderm® XC. *Clinical, Cosmetic and Investigational Dermatology*, *6*, 183–189. <https://doi.org/10.2147/CCID.S33568>
- Banerji, S., Ni, J., Wang, S., Clasper, S., Su, J., Tammi, R., Jones, M., & Jackson, D. (1999). LYVE-1, a new homologue of the CD44 glycoprotein, is a lymph-specific receptor for hyaluronan. *Journal of Cell Biology*, *144*(4), 789–801.
- Barankin, B., & DeKoven, J. (2002). Psychosocial effect of common skin diseases. *Canadian Family Physician Medecin de Famille Canadien*, *48*, 712–716. <https://pubmed.ncbi.nlm.nih.gov/12046366>
- Bass, L. S., Smith, S., Busso, M., & McClaren, M. (2010). Calcium hydroxylapatite (Radiesse) for treatment of nasolabial folds: long-term safety and efficacy results. *Aesthetic Surgery Journal*, *30*(2), 235–238. <https://doi.org/10.1177/1090820X10366549>
- Baumann, L. (2004). Replacing dermal constituents lost through aging with dermal fillers. *Seminars in Cutaneous Medicine and Surgery*, *23*(3), 160–166. <https://doi.org/10.1016/j.sder.2004.06.006>
- Baumann, L. (2004). Dermal fillers. *Journal of Cosmetic Dermatology*, *3*(4), 249–250. <https://doi.org/https://doi.org/10.1111/j.1473-2130.2004.00143.x>

- Boeriu, C. G., Springer, J., Kooy, F. K., van den Broek, L. A. M., & Eggink, G. (2013). Production Methods for Hyaluronan. *International Journal of Carbohydrate Chemistry*, 2013, 624967. <https://doi.org/10.1155/2013/624967>
- Bogdan Allemann, I., & Baumann, L. (2008). Hyaluronic acid gel (Juvéderm) preparations in the treatment of facial wrinkles and folds. *Clinical Interventions in Aging*, 3(4), 629–634. <https://doi.org/10.2147/cia.s3118>
- Borrell, M., Leslie, D. B., & Tezel, A. (2011). Lift capabilities of hyaluronic acid fillers. *Journal of Cosmetic and Laser Therapy: Official Publication of the European Society for Laser Dermatology*, 13(1), 21–27. <https://doi.org/10.3109/14764172.2011.552609>
- Botelho, C. M., Brooks, R. A., Best, S. M., Lopes, M. A., Santos, J. D., Rushton, N., & Bonfield, W. (2006). Human osteoblast response to silicon-substituted hydroxyapatite. *Journal of Biomedical Materials Research. Part A*, 79(3), 723–730. <https://doi.org/10.1002/jbm.a.30806>
- Botelho, C. M., Brooks, R. A., Spence, G., McFarlane, I., Lopes, M. A., Best, S. M., Santos, J. D., Rushton, N., & Bonfield, W. (2006). Differentiation of mononuclear precursors into osteoclasts on the surface of Si-substituted hydroxyapatite. *Journal of Biomedical Materials Research Part A*, 78A(4), 709–720. <https://doi.org/https://doi.org/10.1002/jbm.a.30726>
- Botelho, C. M. da C. F. (2005). *Silicon-substituted hydroxyapatite for biomedical applications*.
- Bourges, X., Weiss, P., Daculsi, G., & Legeay, G. (2002). Synthesis and general properties of silylated-hydroxypropyl methylcellulose in prospect of biomedical use. *Advances in Colloid and Interface Science*, 99(3), 215–228. [https://doi.org/10.1016/S0001-8686\(02\)00035-0](https://doi.org/10.1016/S0001-8686(02)00035-0)
- Brandt, F. S., & Cazzaniga, A. (2008). Hyaluronic acid gel fillers in the management of facial aging. *Clinical Interventions in Aging*, 3(1), 153–159. <https://doi.org/10.2147/cia.s2135>
- Brincat, M. P. (2000). Hormone replacement therapy and the skin. *Maturitas*, 35(2), 107–117. [https://doi.org/10.1016/S0378-5122\(00\)00097-9](https://doi.org/10.1016/S0378-5122(00)00097-9)
- Brown, M. B., & Jones, S. A. (2005). Hyaluronic acid: a unique topical vehicle for the localized delivery of drugs to the skin. *Journal of the European Academy of Dermatology and Venereology*, 19(3), 308–318. <https://doi.org/https://doi.org/10.1111/j.1468-3083.2004.01180.x>
- Burdick, J. A., Chung, C., Jia, X., Randolph, M. A., & Langer, R. (2005). Controlled Degradation and Mechanical Behavior of Photopolymerized Hyaluronic Acid Networks. *Biomacromolecules*, 6(1), 386–391. <https://doi.org/10.1021/bm049508a>
- Burdick, J. A., & Prestwich, G. D. (2011). Hyaluronic Acid Hydrogels for Biomedical Applications. *Advanced Materials*, 23(12), H41–H56. <https://doi.org/https://doi.org/10.1002/adma.201003963>
- Campbell, K. L., & Lichtensteiger, C. A. (2003). Structure and Function of The Skin. In *Small Animal Dermatology Secrets* (pp. 1–9). <https://doi.org/10.1016/B978-1-56053-626-0.50005-7>

- Caton, T., Thibeault, S. L., Klemuk, S., & Smith, M. E. (2007). Viscoelasticity of hyaluronan and nonhyaluronan based vocal fold injectables: implications for mucosal versus muscle use. *The Laryngoscope*, *117*(3), 516–521. <https://doi.org/10.1097/MLG.0b013e31802e9291>
- Cavalcanti, A. D. D., Melo, B. A. G. de, Ferreira, B. A. M., & Santana, M. H. A. (2020). Performance of the main downstream operations on hyaluronic acid purification. *Process Biochemistry*, *99*, 160–170. <https://doi.org/https://doi.org/10.1016/j.procbio.2020.08.020>
- Chahuki, F. F., Aminzadeh, S., Jafarian, V., Tabandeh, F., & Khodabandeh, M. (2019). Hyaluronic acid production enhancement via genetically modification and culture medium optimization in *Lactobacillus acidophilus*. *International Journal of Biological Macromolecules*, *121*, 870–881. <https://doi.org/10.1016/j.ijbiomac.2018.10.112>
- Chang-S, C. (2020). *Revanesse® Lips+ – P160042/S010* / FDA. <https://www.fda.gov/medical-devices/recently-approved-devices/revanesser-lips-p160042s010>
- Chang-S, C. (2021). *Restylane Defyne – P140029/S027* / FDA. <https://www.fda.gov/medical-devices/recently-approved-devices/restylane-defyne-p140029s027>
- Cheng, F., Gong, Q., Yu, H., & Stephanopoulos, G. (2016). High-titer biosynthesis of hyaluronic acid by recombinant *Corynebacterium glutamicum*. *Biotechnology Journal*, *11*(4), 574–584. <https://doi.org/10.1002/biot.201500404>
- Cheung, R. C. F., Ng, T. B., Wong, J. H., & Chan, W. Y. (2015). Chitosan: An Update on Potential Biomedical and Pharmaceutical Applications. *Marine Drugs*, *13*(8), 5156–5186. <https://doi.org/10.3390/md13085156>
- Choi, K. Y., Saravanakumar, G., Park, J. H., & Park, K. (2012). Hyaluronic acid-based nanocarriers for intracellular targeting: Interfacial interactions with proteins in cancer. *Colloids and Surfaces B: Biointerfaces*, *99*, 82–94. <https://doi.org/https://doi.org/10.1016/j.colsurfb.2011.10.029>
- Choi, S., Choi, W., Kim, S., Lee, S.-Y., Noh, I., & Kim, C.-W. (2014). Purification and biocompatibility of fermented hyaluronic acid for its applications to biomaterials. *Biomaterials Research*, *18*, 6. <https://doi.org/10.1186/2055-7124-18-6>
- Choi, S. C., Yoo, M. A., Lee, S. Y., Lee, H. J., Son, D. H., Jung, J., Noh, I., & Kim, C.-W. (2015). Modulation of biomechanical properties of hyaluronic acid hydrogels by cross-linking agents. *Journal of Biomedical Materials Research. Part A*, *103*(9), 3072–3080. <https://doi.org/10.1002/jbm.a.35437>
- Chu, X., Han, J., Guo, D., Fu, Z., Liu, W., & Tao, Y. (2016). Characterization of UDP-glucose dehydrogenase from *Pasteurella multocida* CVCC 408 and its application in hyaluronic acid biosynthesis. *Enzyme and Microbial Technology*, *85*, 64–70. <https://doi.org/10.1016/j.enzmictec.2015.12.009>
- Clayton, K., Vallejo, A. F., Davies, J., Sirvent, S., & Polak, M. E. (2017). Langerhans cells-programmed by the epidermis. In *Frontiers in Immunology* (Vol. 8, Issue NOV, p. 1). Frontiers Media S.A. <https://doi.org/10.3389/fimmu.2017.01676>
- Darr, A., & Calabro, A. (2009). Synthesis and characterization of tyramine-based hyaluronan hydrogels. *Journal of Materials Science: Materials in Medicine*, *20*(1), 33–44. <https://doi.org/10.1007/s10856-008-3540-0>

- Dash, M., Chiellini, F., Ottenbrite, R. M., & Chiellini, E. (2011). Chitosan—A versatile semi-synthetic polymer in biomedical applications. *Progress in Polymer Science*, *36*(8), 981–1014. <https://doi.org/https://doi.org/10.1016/j.progpolymsci.2011.02.001>
- Delplace, V., Nickerson, P. E. B., Ortin-Martinez, A., Baker, A. E. G., Wallace, V. A., & Shoichet, M. S. (2020). Nonswelling, Ultralow Content Inverse Electron-Demand Diels–Alder Hyaluronan Hydrogels with Tunable Gelation Time: Synthesis and In Vitro Evaluation. *Advanced Functional Materials*, *30*(14), 1903978. <https://doi.org/https://doi.org/10.1002/adfm.201903978>
- Dovedytis, M., Liu, Z. J., & Bartlett, S. (2020). Hyaluronic acid and its biomedical applications: A review. *Engineered Regeneration*, *1*, 102–113. <https://doi.org/https://doi.org/10.1016/j.engreg.2020.10.001>
- Eslahi, N., Simchi, A., Mehrjoo, M., Shokrgozar, M. A., & Bonakdar, S. (2016). Hybrid cross-linked hydrogels based on fibrous protein/block copolymers and layered silicate nanoparticles: tunable thermosensitivity, biodegradability and mechanical durability. *RSC Advances*, *6*(67), 62944–62957. <https://doi.org/10.1039/C6RA08563F>
- Fallacara, A., Manfredini, S., Durini, E., & Vertuani, S. (2017). Hyaluronic Acid Fillers in Soft Tissue Regeneration. *Facial Plastic Surgery*, *33*(1), 87–96. <https://doi.org/10.1055/s-0036-1597685>
- Feifel, S., & Lisdat, F. (2011). Silica nanoparticles for the layer-by-layer assembly of fully electroactive cytochrome c multilayers. *Journal of Nanobiotechnology*, *9*, 59. <https://doi.org/10.1186/1477-3155-9-59>
- Fiorica, C., Pitarresi, G., Palumbo, F. S., Di Stefano, M., Calascibetta, F., & Giammona, G. (2013). A new hyaluronic acid pH sensitive derivative obtained by ATRP for potential oral administration of proteins. *International Journal of Pharmaceutics*, *457*(1), 150–157. <https://doi.org/https://doi.org/10.1016/j.ijpharm.2013.09.005>
- Flégeau, K., Pace, R., Gautier, H., Rethore, G., Guicheux, J., Le Visage, C., & Weiss, P. (2017). Toward the development of biomimetic injectable and macroporous biohydrogels for regenerative medicine. *Advances in Colloid and Interface Science*, *247*, 589–609. <https://doi.org/10.1016/j.cis.2017.07.012>
- Flegeau, K., Toquet, C., Rethore, G., d'Arros, C., Messenger, L., Halgand, B., Dupont, D., Autrusseau, F., Lesoeur, J., Veziers, J., Bordat, P., Bresin, A., Guicheux, J., Delplace, V., Gautier, H., & Weiss, P. (2020). In Situ Forming, Silanized Hyaluronic Acid Hydrogels with Fine Control Over Mechanical Properties and In Vivo Degradation for Tissue Engineering Applications. *Advanced Healthcare Materials*, *9*(19), 2000981. <https://doi.org/10.1002/adhm.202000981>
- Fong Chong, B., & Nielsen, L. K. (2003). Aerobic cultivation of *Streptococcus zooepidemicus* and the role of NADH oxidase. *Biochemical Engineering Journal*, *16*(2), 153–162. [https://doi.org/https://doi.org/10.1016/S1369-703X\(03\)00031-7](https://doi.org/https://doi.org/10.1016/S1369-703X(03)00031-7)
- Fraser, J. R. E. ;, Laurent, T. C. ;, & Laurent, U. B. G. (1997). The nature of hyaluronan. *Journal of Internal Medicine*, *242*, 27–33.

- Fraser, J R F; Laurent, T C; Pertoft, H; Baxter, E. (1981). Plasma clearance, tissue distribution and metabolism of hyaluronic acid injected intravenously in the rabbit. *Biochemical Journal*, *200*(2), 415–424. <https://doi.org/10.1042/bj2000415>
- Fu, Y., Zoetebier, B., Both, S., Dijkstra, P. J., & Karperien, M. (2021). Engineering of Optimized Hydrogel Formulations for Cartilage Repair. In *Polymers* (Vol. 13, Issue 9). <https://doi.org/10.3390/polym13091526>
- Funt, D., & Pavicic, T. (2013). Dermal fillers in aesthetics: An overview of adverse events and treatment approaches. In *Clinical, Cosmetic and Investigational Dermatology* (Vol. 6, pp. 295–316). Dove Press. <https://doi.org/10.2147/CCID.S50546>
- Garcia-Fuentes, M., & Alonso, M. J. (2012). Chitosan-based drug nanocarriers: Where do we stand? *Journal of Controlled Release*, *161*(2), 496–504. <https://doi.org/https://doi.org/10.1016/j.jconrel.2012.03.017>
- Gold, M. H. (2007). Use of hyaluronic acid fillers for the treatment of the aging face. *Clinical Interventions in Aging*, *2*(3), 369–376. <https://doi.org/10.2147/cia.s1244>
- Goulas A, Hatzichristou DG, K. G., & Mirtsou-Fidani V, Kalinderis A, P. E. (2000). Benign hyperplasia of the human prostate is associated with tissue enrichment in chondroitin sulphate of wide size distribution. *Prostate*, *44*, 104–110.
- Goulas, A., Papakonstantinou, E., Karakiulakis, G., Mirtsou-Fidani, V., Kalinderis, A., & Hatzichristou, D. G. (2000). Tissue structure-specific distribution of glycosaminoglycans in the human penis. *International Journal of Biochemistry and Cell Biology*, *32*(9), 975–982. [https://doi.org/10.1016/S1357-2725\(00\)00038-8](https://doi.org/10.1016/S1357-2725(00)00038-8)
- Greene, J. J., & Sidle, D. M. (2015). The Hyaluronic Acid Fillers. Current Understanding of the Tissue Device Interface. In *Facial Plastic Surgery Clinics of North America* (Vol. 23, Issue 4, pp. 423–432). W.B. Saunders. <https://doi.org/10.1016/j.fsc.2015.07.002>
- Gunasekaran, V., D., G., & V., P. (2020). Role of membrane proteins in bacterial synthesis of hyaluronic acid and their potential in industrial production. *International Journal of Biological Macromolecules*, *164*, 1916–1926. <https://doi.org/https://doi.org/10.1016/j.ijbiomac.2020.08.077>
- Hamerman, D., & Schuster, H. (1958). Hyaluronate in normal human synovial fluid. *The Journal of Clinical Investigation*, *37*(1), 57–64. [https://doi.org/10.1016/s0262-1762\(08\)70267-0](https://doi.org/10.1016/s0262-1762(08)70267-0)
- Haxaire, K., Maréchal, Y., Milas, M., & Rinaudo, M. (2003). Hydration of polysaccharide hyaluronan observed by IR spectrometry. I. Preliminary experiments and band assignments. *Biopolymers*, *72*(1), 10–20. <https://doi.org/10.1002/bip.10245>
- Heinemann, S., Coradin, T., & Desimone, M. F. (2013). Bio-inspired silica–collagen materials: applications and perspectives in the medical field. *Biomaterials Science*, *1*(7), 688–702. <https://doi.org/10.1039/C3BM00014A>
- Hirao, T. (2017). *Chapter 40 - Structure and Function of Skin From a Cosmetic Aspect* (K. Sakamoto, R. Y. Lochhead, H. I. Maibach, & Y. B. T.-C. S. and T. Yamashita, Eds.; pp. 673–683). Elsevier. <https://doi.org/https://doi.org/10.1016/B978-0-12-802005-0.00040-9>
- Hong, B. M., Kim, H. C., Jeong, J. E., Park, S. A., & Park, W. H. (2020). Visible-light-induced hyaluronate hydrogel for soft tissue fillers. *International Journal of Biological*

- Hong, B. M., Park, S. A., & Park, W. H. (2019). Effect of photoinitiator on chain degradation of hyaluronic acid. *Biomaterials Research*, 23(1), 21. <https://doi.org/10.1186/s40824-019-0170-1>
- Horton, M. R., McKee, C. M., Bao, C., Liao, F., Farber, J. M., Hodge-DuFour, J., Puré, E., Oliver, B. L., Wright, T. M., & Noble, P. W. (1998). Hyaluronan fragments synergize with interferon- γ to induce the C-X-C chemokines mig and interferon-inducible protein-10 in mouse macrophages. *Journal of Biological Chemistry*, 273(52), 35088–35094. <https://doi.org/10.1074/jbc.273.52.35088>
- Hu, X., Li, D., Zhou, F., & Gao, C. (2011). Biological hydrogel synthesized from hyaluronic acid, gelatin and chondroitin sulfate by click chemistry. *Acta Biomaterialia*, 7(4), 1618–1626. <https://doi.org/https://doi.org/10.1016/j.actbio.2010.12.005>
- Humphrey, S., Manson Brown, S., Cross, S. J., & Mehta, R. (2021). Defining Skin Quality: Clinical Relevance, Terminology, and Assessment. *Dermatologic Surgery: Official Publication for American Society for Dermatologic Surgery [et al.]*, 47(7), 974–981. <https://doi.org/10.1097/DSS.0000000000003079>
- Isacke CM, Y. H. (2002). The hyaluronan receptor, CD44. *J Biochem Cell Biol*, 34, 718–721. [https://doi.org/10.1016/s1357-2725\(01\)00166-2](https://doi.org/10.1016/s1357-2725(01)00166-2)
- Itano, N., Atsumi, F., Sawai, T., Yamada, Y., Miyaishi, O., Senga, T., Hamaguchi, M., & Kimata, K. (2002). Abnormal accumulation of hyaluronan matrix diminishes contact inhibition of cell growth and promotes cell migration. *Proceedings of the National Academy of Sciences of the United States of America*, 99(6), 3609–3614. <https://doi.org/10.1073/pnas.052026799>
- Jacovella, P. F. (2008). Use of calcium hydroxylapatite (Radiesse) for facial augmentation. *Clinical Interventions in Aging*, 3(1), 161–174. <https://doi.org/10.2147/cia.s2065>
- Jameson, J. M., Cauvi, G., Sharp, L. L., Witherden, D. A., & Havran, W. L. (2005). T cell-induced hyaluronan production by epithelial cells regulates inflammation. *Journal of Experimental Medicine*, 201(8), 1269–1279. <https://doi.org/10.1084/jem.20042057>
- Jeong, C. H., Kim, D. H., Yune, J. H., Kwon, H. C., Shin, D.-M., Sohn, H., Lee, K. H., Choi, B., Kim, E. S., Kang, J. H., Kim, E. K., & Han, S. G. (2021). In vitro toxicity assessment of cross-linking agents used in hyaluronic acid dermal filler. *Toxicology in Vitro*, 70, 105034. <https://doi.org/https://doi.org/10.1016/j.tiv.2020.105034>
- Jeong, E., Shim, W. Y., & Kim, J. H. (2014). Metabolic engineering of *Pichia pastoris* for production of hyaluronic acid with high molecular weight. *Journal of Biotechnology*, 185, 28–36. <https://doi.org/10.1016/j.jbiotec.2014.05.018>
- Jia, Y., Zhu, J., Chen, X., Tang, D., Su, D., Yao, W., & Gao, X. (2013). Metabolic engineering of *Bacillus subtilis* for the efficient biosynthesis of uniform hyaluronic acid with controlled molecular weights. *Bioresource Technology*, 132, 427–431. <https://doi.org/10.1016/j.biortech.2012.12.150>

- Jiang, D., Liang, J., Fan, J., Yu, S., Chen, S., Luo, Y., Prestwich, G. D., Mascarenhas, M. M., Garg, H. G., Quinn, D. A., Homer, R. J., Goldstein, D. R., Bucala, R., Lee, P. J., Medzhitov, R., & Noble, P. W. (2005). Regulation of lung injury and repair by Toll-like receptors and hyaluronan. *Nature Medicine*, *11*(11), 1173–1179. <https://doi.org/10.1038/nm1315>
- Jiang, D., Liang, J., Li, Y., & Noble, P. W. (2006). The role of Toll-like receptors in non-infectious lung injury. *Cell Research*, *16*(8), 693–701. <https://doi.org/10.1038/sj.cr.7310085>
- Johl, S. S., & Burgett, R. A. (2006). Dermal filler agents: A practical review. *Current Opinion in Ophthalmology*, *17*(5), 471–479. <https://doi.org/10.1097/01.icu.0000243021.20499.4b>
- Jones, D. H. (2009). Semipermanent and permanent injectable fillers. *Dermatologic Clinics*, *27*(4), 433–444, vi. <https://doi.org/10.1016/j.det.2009.08.003>
- Keen, M. (2017). Hyaluronic Acid in Dermatology. *Skinmed.*, *15*(6), 441–448.
- Khetan, S., Guvendiren, M., Legant, W. R., Cohen, D. M., Chen, C. S., & Burdick, J. A. (2013). Degradation-mediated cellular traction directs stem cell fate in covalently crosslinked three-dimensional hydrogels. *Nature Materials*, *12*(5), 458–465. <https://doi.org/10.1038/nmat3586>
- Khunmanee, S., Jeong, Y., & Park, H. (2017). Cross-linking method of hyaluronic-based hydrogel for biomedical applications. *Journal of Tissue Engineering*, *8*, 2041731417726464. <https://doi.org/10.1177/2041731417726464>
- Kim, K. S., Park, S. J., Yang, J.-A., Jeon, J.-H., Bhang, S. H., Kim, B.-S., & Hahn, S. K. (2011). Injectable hyaluronic acid–tyramine hydrogels for the treatment of rheumatoid arthritis. *Acta Biomaterialia*, *7*(2), 666–674. <https://doi.org/https://doi.org/10.1016/j.actbio.2010.09.030>
- Kim, Z.-H., Lee, Y., Kim, S.-M., Kim, H., & Yun, C.-K. (2015). A Composite Dermal Filler Comprising Cross-Linked Hyaluronic Acid and Human Collagen for Tissue Reconstruction. *Journal of Microbiology and Biotechnology*, *25*(3), 399–406. <https://doi.org/10.4014/jmb.1411.11029>
- Klagas, I., Goulet, S., Karakiulakis, G., Zhong, J., Baraket, M., Black, J. L., Papakonstantinou, E., & Roth, M. (2009). Decreased hyaluronan in airway smooth muscle cells from patients with asthma and COPD. *European Respiratory Journal*, *34*(3), 616–628. <https://doi.org/10.1183/09031936.00070808>
- Klein, A. W., & Fagien, S. (2007). Hyaluronic Acid Fillers and Botulinum Toxin Type A: Rationale for Their Individual and Combined Use for Injectable Facial Rejuvenation. *Plastic and Reconstructive Surgery*, *120*(6S). https://journals.lww.com/plasreconsurg/Fulltext/2007/11001/Hyaluronic_Acid_Fillers_and_Botulinum_Toxin_Type.12.aspx
- Knudson, W., Chow, G., & Knudson, C. B. (2002). CD44-mediated uptake and degradation of hyaluronan. *Matrix Biology*, *21*(1), 15–23. [https://doi.org/10.1016/S0945-053X\(01\)00186-X](https://doi.org/10.1016/S0945-053X(01)00186-X)
- Krause-S, D. (2020a). *JUVÉDERM® VOLUMA™ XC - P110033/S047 | FDA*. <https://www.fda.gov/medical-devices/recently-approved-devices/juvedermr-volumatm-xc>

p110033s047

- Krause-S, D. (2020b). *Restylane® Kysse - P140029/S021 | FDA*. <https://www.fda.gov/medical-devices/recently-approved-devices/restylaner-kysse-p140029s021>
- Kurisawa, M., Chung, J. E., Yang, Y. Y., Gao, S. J., & Uyama, H. (2005). Injectable biodegradable hydrogels composed of hyaluronic acid–tyramine conjugates for drug delivery and tissue engineering. *Chemical Communications*, 34, 4312–4314. <https://doi.org/10.1039/B506989K>
- Kwarta, C. P., Widiyanti, P., & Siswanto. (2017). Hyaluronic Acid (HA)-Polyethylene glycol (PEG) as injectable hydrogel for intervertebral disc degeneration patients therapy. *Journal of Physics: Conference Series*, 853(1), 012036. <https://doi.org/10.1088/1742-6596/853/1/012036>
- Lai-Cheong, J. E., & McGrath, J. A. (2009). Structure and function of skin, hair and nails. *Medicine*, 37(5), 223–226. <https://doi.org/https://doi.org/10.1016/j.mpmed.2009.03.002>
- Lai, J.-Y. (2014). Relationship between structure and cytocompatibility of divinyl sulfone cross-linked hyaluronic acid. *Carbohydrate Polymers*, 101, 203–212. <https://doi.org/https://doi.org/10.1016/j.carbpol.2013.09.060>
- Lapcik L Jr and, L., Lapcık, L., De Smedt, S., Demeester, J., & Chabrecek, P. (1998). Hyaluronan: Preparation, Structure, Properties, and Applications. *Chemical Reviews*, 98(8), 2663–2684. <https://doi.org/10.1021/cr941199z>
- Lapcık, L., Jr, Chabrecek, P., & Stasko, A. (1991). Photodegradation of Hyaluronic Acid: EPR and Size Exclusion Chromatography Study. *Biopolymers*, 31(12), 1429–1435.
- Laugier, J. P., Shuster, S., Rosdy, M., Csóka, A. B., Stern, R., & Maibach, H. I. (2000). Topical hyaluronidase decreases hyaluronic acid and CD44 in human skin and in reconstituted human epidermis: Evidence that hyaluronidase can permeate the stratum corneum. *British Journal of Dermatology*, 142(2), 226–233. <https://doi.org/10.1046/j.1365-2133.2000.03289.x>
- Laurent, T. C., & Fraser, J. R. E. (1992). Hyaluronan1. *The FASEB Journal*, 6(7), 2397–2404. <https://doi.org/https://doi.org/10.1096/fasebj.6.7.1563592>
- Laurent, U. B. G., Dahl, L. B., & Reed, R. K. (1991). Catabolism of hyaluronan in rabbit skin takes place locally, in lymph nodes and liver. *Experimental Physiology*, 76(5), 695–703. <https://doi.org/10.1113/expphysiol.1991.sp003536>
- Lee, F., Chung, J. E., & Kurisawa, M. (2008). An injectable enzymatically crosslinked hyaluronic acid–tyramine hydrogel system with independent tuning of mechanical strength and gelation rate. *Soft Matter*, 4(4), 880–887. <https://doi.org/10.1039/B719557E>
- Lee, H.-Y., Kim, H.-E., & Jeong, S.-H. (2019). One-pot synthesis of silane-modified hyaluronic acid hydrogels for effective antibacterial drug delivery via sol-gel stabilization. *Colloids and Surfaces. B, Biointerfaces*, 174, 308–315. <https://doi.org/10.1016/j.colsurfb.2018.11.034>
- Lemperle, G., Knapp, T. R., Sadick, N. S., & Lemperle, S. M. (2010). ArteFill permanent injectable for soft tissue augmentation: I. Mechanism of action and injection techniques. *Aesthetic Plastic Surgery*, 34(3), 264–272. <https://doi.org/10.1007/s00266-009-9413-1>

- Lemperle, G., Morhenn, V., & Charrier, U. (2003). Human histology and persistence of various injectable filler substances for soft tissue augmentation. *Aesthetic Plastic Surgery*, *27*(5), 354–366; discussion 367. <https://doi.org/10.1007/s00266-003-3022-1>
- Liang, H.-C., Chang, W.-H., Liang, H.-F., Lee, M.-H., & Sung, H.-W. (2004). Cross-linking structures of gelatin hydrogels crosslinked with genipin or a water-soluble carbodiimide. *Journal of Applied Polymer Science*, *91*(6), 4017–4026. <https://doi.org/https://doi.org/10.1002/app.13563>
- Liu, M. H., Beynet, D. P., & Gharavi, N. M. (2019). Overview of Deep Dermal Fillers. *Facial Plastic Surgery: FPS*, *35*(3), 224–229. <https://doi.org/10.1055/s-0039-1688843>
- Loebel, C., D'Este, M., Alini, M., Zenobi-Wong, M., & Eglin, D. (2015). Precise tailoring of tyramine-based hyaluronan hydrogel properties using DMTMM conjugation. *Carbohydrate Polymers*, *115*, 325–333. <https://doi.org/10.1016/j.carbpol.2014.08.097>
- Loebel, C., Szczesny, S. E., Cosgrove, B. D., Alini, M., Zenobi-Wong, M., Mauck, R. L., & Eglin, D. (2017). Cross-Linking Chemistry of Tyramine-Modified Hyaluronan Hydrogels Alters Mesenchymal Stem Cell Early Attachment and Behavior. *Biomacromolecules*, *18*(3), 855–864. <https://doi.org/10.1021/acs.biomac.6b01740>
- Lowther, D. A., & Rogers, H. J. (1955). Biosynthesis of Hyaluronate. *Nature*, *175*(4453), 435. <https://doi.org/10.1038/175435a0>
- MacLennan, A. P. (1956). The Production of Capsules, Hyaluronic Acid and Hyaluronidase by 25 Strains of Group C Streptococci. *Journal of General Microbiology*, *15*(3), 485–491. <https://doi.org/10.1099/00221287-15-3-485>
- Maiz-Fernández, S., Pérez-Álvarez, L., Silván, U., Vilas-Vilela, J. L., & Lanceros-Mendez, S. (2022). Photocrosslinkable and self-healable hydrogels of chitosan and hyaluronic acid. *International Journal of Biological Macromolecules*, *216*, 291–302. <https://doi.org/https://doi.org/10.1016/j.ijbiomac.2022.07.004>
- Makrantonaki, E., Adjaye, J., Herwig, R., Brink, T. C., Groth, D., Hultschig, C., Lehrach, H., & Zouboulis, C. C. (2006). Age-specific hormonal decline is accompanied by transcriptional changes in human sebocytes in vitro. *Aging Cell*, *5*(4), 331–344. <https://doi.org/10.1111/j.1474-9726.2006.00223.x>
- Makrantonakia, E., & Zouboulis, C. C. (2009). Androgens and ageing of the skin. *Current Opinion in Endocrinology, Diabetes and Obesity*, *16*(3), 240–245. <https://doi.org/10.1097/MED.0b013e32832b71dc>
- Manuskiatti, W., & Maibach, H. I. (1996). Hyaluronic acid and skin: Wound healing and aging. *International Journal of Dermatology*, *35*(8), 539–544. <https://doi.org/10.1111/j.1365-4362.1996.tb03650.x>
- Mao, Z., Shin, H.-D., & Chen, R. (2009). A recombinant E. coli bioprocess for hyaluronan synthesis. *Applied Microbiology and Biotechnology*, *84*(1), 63–69. <https://doi.org/10.1007/s00253-009-1963-2>
- Marklein, R. A., & Burdick, J. A. (2010). Spatially controlled hydrogel mechanics to modulate stem cell interactions. *Soft Matter*, *6*(1), 136–143. <https://doi.org/10.1039/B916933D>
- Marks, J. G., & Miller, J. J. (2019). *2 - Structure and Function of the Skin* (J. G. Marks & J. J. B. T.-

- L. and M. P. of D. (Sixth E. Miller, Eds.; pp. 2–10). Elsevier. <https://doi.org/https://doi.org/10.1016/B978-0-323-43040-1.00002-6>
- Martina, V., Gallo, A., Tarantino, E., Esposito, C., Zerbinati, U., Mocchi, R., Monticelli, D., Lotti, T., Tirant, M., Van Thuong, N., Rauso, R., & Zerbinati, N. (2019). Viscoelastic properties and thermodynamic balance improvement of a hyaluronic acid hydrogel enriched with proline and glycine. In *Journal of biological regulators and homeostatic agents* (Vol. 33, Issue 6, pp. 1955–1959). <https://doi.org/10.23812/19-252-L>
- Matarasso, S. L., Carruthers, J. D., & Jewell, M. L. (2006). Consensus recommendations for soft-tissue augmentation with nonanimal stabilized hyaluronic acid (Restylane). *Plastic and Reconstructive Surgery*, *117*(3 SUPPL.), 3–34. <https://doi.org/10.1097/01.prs.0000204759.76865.39>
- McCabe, M. C., Hill, R. C., Calderone, K., Cui, Y., Yan, Y., Quan, T., Fisher, G. J., & Hansen, K. C. (2020). Alterations in extracellular matrix composition during aging and photoaging of the skin. *Matrix Biology Plus*, *8*, 100041. <https://doi.org/https://doi.org/10.1016/j.mbplus.2020.100041>
- McKee, C. M., Lowenstein, C. J., Horton, M. R., Wu, J., Bao, C., Chin, B. Y., Choi, A. M. K., & Noble, P. W. (1997). Hyaluronan fragments induce nitric-oxide synthase in murine macrophages through a nuclear factor κ B-dependent mechanism. *Journal of Biological Chemistry*, *272*(12), 8013–8018. <https://doi.org/10.1074/jbc.272.12.8013>
- McKee, C. M., Penno, M. B., Cowman, M., Burdick, M. D., Strieter, R. M., Bao, C., & Noble, P. W. (1996). Hyaluronan (HA) fragments induce chemokine gene expression in alveolar macrophages: The role of HA size and CD44. *Journal of Clinical Investigation*, *98*(10), 2403–2413. <https://doi.org/10.1172/JCI119054>
- Meyer, K. & Palmer, J. W. (1934). The polysaccharide of the vitreous humor. *Journal of Biological Chemistry*, *107*, 629–634.
- Montheil, T., Echaliier, C., Martinez, J., Subra, G., & Mehdi, A. (2018). Inorganic polymerization: an attractive route to biocompatible hybrid hydrogels. *Journal of Materials Chemistry B*, *6*(21), 3434–3448. <https://doi.org/10.1039/C8TB00456K>
- Muzzarelli, R. A., Mattioli-Belmonte, M., Pugnali, A., & Biagini, G. (1999). Biochemistry, histology and clinical uses of chitins and chitosans in wound healing. *EXS*, *87*, 251–264. https://doi.org/10.1007/978-3-0348-8757-1_18
- Nehls, V., & Hayen, W. (2000). Are hyaluronan receptors involved in three-dimensional cell migration? *Histology and Histopathology*, *15*(2), 629–636. <https://doi.org/10.14670/HH-15.629>
- Okada, S., Hagan, J. B., Kato, M., Bankers-Fulbright, J. L., Hunt, L. W., Gleich, G. J., & Kita, H. (1998). Lidocaine and its analogues inhibit IL-5-mediated survival and activation of human eosinophils. *Journal of Immunology (Baltimore, Md. : 1950)*, *160*(8), 4010–4017.
- Pan, N. C., Baldo, C., Pereira, H. C. B., Vignoli, J. A., & Celligoi, M. A. P. C. (2021). 9 - Perspectives of microbial hyaluronic acid utilization in wound healing. In R. C. B. T.-M. B. in F. and H. Ray (Ed.), *Applied Biotechnology Reviews* (pp. 227–250). Academic Press. <https://doi.org/https://doi.org/10.1016/B978-0-12-819813-1.00009-8>

- Pan, N. C., Pereira, H. C. B., da Silva, M. de L. C., Vasconcelos, A. F. D., & Celligoi, M. A. P. C. (2017). Improvement Production of Hyaluronic Acid by *Streptococcus zoeepidemicus* in Sugarcane Molasses. *Applied Biochemistry and Biotechnology*, *182*(1), 276–293. <https://doi.org/10.1007/s12010-016-2326-y>
- Papakonstantinou, E., Karakiulakis, G., Eickelberg, O., Perruchoud, A. P., Block, L. H., & Roth, M. (1998). A 340 kDa hyaluronic acid secreted by human vascular smooth muscle cells regulates their proliferation and migration. *Glycobiology*, *8*(8), 821–830. <https://doi.org/10.1093/glycob/8.8.821>
- Papakonstantinou, E., Kouri, F. M., Karakiulakis, G., Klagas, I., & Eickelberg, O. (2008). Increased hyaluronic acid content in idiopathic pulmonary arterial hypertension. *European Respiratory Journal*, *32*(6), 1504–1512. <https://doi.org/10.1183/09031936.00159507>
- Papakonstantinou, Eleni, & Karakiulakis, G. (2009). The “sweet” and “bitter” involvement of glycosaminoglycans in lung diseases: Pharmacotherapeutic relevance. *British Journal of Pharmacology*, *157*(7), 1111–1127. <https://doi.org/10.1111/j.1476-5381.2009.00279.x>
- Papakonstantinou, Eleni, Karakiulakis, G., Roth, M., & Block, L. H. (1995). Platelet-derived growth factor stimulates the secretion of hyaluronic acid by proliferating human vascular smooth muscle cells. *Proceedings of the National Academy of Sciences of the United States of America*, *92*(21), 9881–9885. <https://doi.org/10.1073/pnas.92.21.9881>
- Papakonstantinou, Eleni, Roth, M., & Karakiulakis, G. (2012). Hyaluronic acid: A key molecule in skin aging. In *Dermato-Endocrinology* (Vol. 4, Issue 3, p. 253). Landes Bioscience. <https://doi.org/10.4161/derm.21923>
- Papakonstantinou, Eleni, Roth, M., Tamm, M., Eickelberg, O., Perruchoud, A. P., & Karakiulakis, G. (2002). Hypoxia differentially enhances the effects of transforming growth factor- β isoforms on the synthesis and secretion of glycosaminoglycans by human lung fibroblasts. *Journal of Pharmacology and Experimental Therapeutics*, *301*(3), 830–837. <https://doi.org/10.1124/jpet.301.3.830>
- Pavicic, T., Gauglitz, G. G., Lersch, P., Schwach-Abdellaoui, K., Malle, B., Korting, H. C., & Farwick, M. (2011). Efficacy of cream-based novel formulations of hyaluronic acid of different molecular weights in anti-wrinkle treatment. *Journal of Drugs in Dermatology : JDD*, *10*(9), 990–1000.
- Perret, S., Eble, J. A., Siljander, P. R.-M., Merle, C., Farndale, R. W., Theisen, M., & Ruggiero, F. (2003). Prolyl Hydroxylation of Collagen Type I Is Required for Efficient Binding to Integrin $\alpha 1\beta 1$ and Platelet Glycoprotein VI but Not to $\alpha 2\beta 2^*$. *Journal of Biological Chemistry*, *278*(32), 29873–29879. <https://doi.org/10.1074/jbc.M304073200>
- Pierre, S., Liew, S., & Bernardin, A. (2015). Basics of dermal filler rheology. *Dermatologic Surgery : Official Publication for American Society for Dermatologic Surgery [et al.]*, *41* Suppl 1, S120–6. <https://doi.org/10.1097/DSS.0000000000000334>
- Prehm, P. (1990). Release of hyaluronate from eukaryotic cells. *Biochemical Journal*, *267*(1), 185–189. <https://doi.org/10.1042/bj2670185>
- Presti, D., & Scott, J. E. (1994). Hyaluronan-mediated protective effect against cell damage caused by enzymatically produced hydroxyl (OH \cdot) radicals is dependent on hyaluronan molecular mass. *Cell Biochemistry and Function*, *12*(4), 281–288.

<https://doi.org/10.1002/cbf.290120409>

- Ragan, C., & Meyer, K. (1949). The hyaluronic acid of synovial fluid in rheumatoid arthritis. *The Journal of Clinical Investigation*, *28*(1), 56–59. <https://doi.org/10.1172/JC1102053>
- Ralf Paus, L., Berneburg, M., Trelles, M., Friguet, B., Ogden, S., Esrefoglu, M., Kaya, G., Goldberg, D. J., Mordon, S., Calderhead, R. G., Griffiths, C. E. M., Saurat, J. H., & Thappa, D. M. (2008). How best to halt and/or revert UV-induced skin ageing: strategies, facts and fiction. *Experimental Dermatology*, *17*(3), 228–240. <https://doi.org/10.1111/j.1600-0625.2007.00665.x>
- Ramamurthi, A., & Vesely, I. (2002). Smooth muscle cell adhesion on crosslinked hyaluronan gels. *Journal of Biomedical Materials Research*, *60*(1), 195–205. <https://doi.org/10.1002/jbm.10061>
- Rangaswamy, V., & Jain, D. (2008). An efficient process for production and purification of hyaluronic acid from *Streptococcus equi* subsp. *zooepidemicus*. *Biotechnology Letters*, *30*(3), 493–496. <https://doi.org/10.1007/s10529-007-9562-8>
- Reed, R. K., Lilja, K., & Laurent, T. C. (1988). Hyaluronan in the rat with special reference to the skin. *Acta Physiologica Scandinavica*, *134*(3), 405–411. <https://doi.org/10.1111/j.1748-1716.1988.tb08508.x>
- Reed, Rolf K, Laurent, B. G., Robert, J., Fraser, E., Laurent, C., Rolf, K., Laurent, U. B. G., Robert, J. E., & Laurent, T. C. (1990). Removal rate of [³H] hyaluronan injected subcutaneously in rabbits. *American Journal of Physiology - Heart and Circulatory Physiology*, *259*(2), 532–535. <https://doi.org/10.1152/ajpheart.1990.259.2.H532>
- Richter, A. W., Ryde, E. M., & Zetterström, E. O. (1979). Non-Immunogenicity of a Purified Sodium Hyaluronate Preparation in Man. *International Archives of Allergy and Immunology*, *59*(1), 45–48. <https://doi.org/10.1159/000232238>
- Roberts, M. J., Bentley, M. D., & Harris, J. M. (2002). Chemistry for peptide and protein PEGylation. *Advanced Drug Delivery Reviews*, *54*(4), 459–476. [https://doi.org/https://doi.org/10.1016/S0169-409X\(02\)00022-4](https://doi.org/https://doi.org/10.1016/S0169-409X(02)00022-4)
- Rohrich, R. J., & Potter, J. K. (2004). Liquid injectable silicone: is there a role as a cosmetic soft-tissue filler? *Plastic and Reconstructive Surgery*, *113*(4), 1239–1241. <https://doi.org/10.1097/01.prs.0000118022.71802.78>
- Sánchez-Téllez, D. A., Rodríguez-Lorenzo, L. M., & Téllez-Jurado, L. (2020). Siloxane-inorganic chemical cross-linking of hyaluronic acid – based hybrid hydrogels: Structural characterization. *Carbohydrate Polymers*, *230*, 115590. <https://doi.org/https://doi.org/10.1016/j.carbpol.2019.115590>
- Sapijaszko, M. J. A. (2007). Dermal fillers: ever-expanding options for esthetic use. *Skin Therapy Letter*, *12*(8), 4–7.
- Sauerová, P., Pilgrová, T., Pekař, M., & Hubálek Kalbáčová, M. (2017). Hyaluronic acid in complexes with surfactants: The efficient tool for reduction of the cytotoxic effect of surfactants on human cell types. *International Journal of Biological Macromolecules*, *103*, 1276–1284. <https://doi.org/https://doi.org/10.1016/j.ijbiomac.2017.05.173>
- Scott, J. E. (2007). Secondary Structures in Hyaluronan Solutions: Chemical and Biological

Implications. In *Ciba Foundation Symposium 143 - The Biology of Hyaluronan* (pp. 6–20). <https://doi.org/https://doi.org/10.1002/9780470513774.ch2>

- Scott, John E., & Heatley, F. (1999). Hyaluronan forms specific stable tertiary structures in aqueous solution: A ¹³C NMR study. *Proceedings of the National Academy of Sciences of the United States of America*, *96*(9), 4850–4855. <https://doi.org/10.1073/pnas.96.9.4850>
- Sehlinger, A., Kreye, O., & Meier, M. A. R. (2013). Tunable Polymers Obtained from Passerini Multicomponent Reaction Derived Acrylate Monomers. *Macromolecules*, *46*(15), 6031–6037. <https://doi.org/10.1021/ma401125j>
- Serban, M. A., & Prestwich, G. D. (2007). Synthesis of Hyaluronan Haloacetates and Biology of Novel Cross-Linker-Free Synthetic Extracellular Matrix Hydrogels. *Biomacromolecules*, *8*(9), 2821–2828. <https://doi.org/10.1021/bm700595s>
- Shukla, S. K., Mishra, A. K., Arotiba, O. A., & Mamba, B. B. (2013). Chitosan-based nanomaterials: a state-of-the-art review. *International Journal of Biological Macromolecules*, *59*, 46–58. <https://doi.org/10.1016/j.ijbiomac.2013.04.043>
- Slevin, M., Kumar, S., & Gaffney, J. (2002). Angiogenic oligosaccharides of hyaluronan induce multiple signaling pathways affecting vascular endothelial cell mitogenic and wound healing responses. *Journal of Biological Chemistry*, *277*(43), 41046–41059. <https://doi.org/10.1074/jbc.M109443200>
- Tammi, R., Ripellino, J. A., Margolis, R. U., & Tammi, M. (1988). Localization of epidermal hyaluronic acid using the hyaluronate binding region of cartilage proteoglycan as a specific probe. In *Journal of Investigative Dermatology* (Vol. 90, Issue 3, pp. 412–414). <https://doi.org/10.1111/1523-1747.ep12456530>
- Teriete, P., Banerji, S., Noble, M., Blundell, C. D., Wright, A. J., Pickford, A. R., Lowe, E., Mahoney, D. J., Tammi, M. I., Kahmann, J. D., Campbell, I. D., Day, A. J., & Jackson, D. G. (2004). Structure of the regulatory hyaluronan binding domain in the inflammatory leukocyte homing receptor CD44. *Molecular Cell*, *13*(4), 483–496. [https://doi.org/10.1016/S1097-2765\(04\)00080-2](https://doi.org/10.1016/S1097-2765(04)00080-2)
- Tezel, A., & Fredrickson, G. H. (2008a). The science of hyaluronic acid dermal fillers. In *Journal of Cosmetic and Laser Therapy* (Vol. 10, Issue 1, pp. 35–42). Taylor and Francis Ltd. <https://doi.org/10.1080/14764170701774901>
- Tezel, A., & Fredrickson, G. H. (2008b). The science of hyaluronic acid dermal fillers. In *Journal of Cosmetic and Laser Therapy* (Vol. 10, Issue 1, pp. 35–42). Taylor and Francis Ltd. <https://doi.org/10.1080/14764170701774901>
- Tezel, A., & Fredrickson, G. H. (2008c). The science of hyaluronic acid dermal fillers. In *Journal of Cosmetic and Laser Therapy* (Vol. 10, Issue 1, pp. 35–42). Taylor and Francis Ltd. <https://doi.org/10.1080/14764170701774901>
- Tomihata, K., & Ikada, Y. (1997). Preparation of cross-linked hyaluronic acid films of low water content. *Biomaterials*, *18*(3), 189–195. [https://doi.org/10.1016/S0142-9612\(96\)00116-0](https://doi.org/10.1016/S0142-9612(96)00116-0)
- Toole, B. P. (2004). Hyaluronan: from extracellular glue to pericellular cue. *Nature Reviews Cancer*, *4*(7), 528–539. <https://doi.org/10.1038/nrc1391>

- Trapani, A., Palazzo, C., Contino, M., Perrone, M. G., Cioffi, N., Ditaranto, N., Colabufo, N. A., Conese, M., Trapani, G., & Puglisi, G. (2014). Mucoadhesive Properties and Interaction with P-Glycoprotein (P-gp) of Thiolated-Chitosans and -Glycol Chitosans and Corresponding Parent Polymers: A Comparative Study. *Biomacromolecules*, *15*(3), 882–893. <https://doi.org/10.1021/bm401733p>
- Tripodo, G., Trapani, A., Torre, M. L., Giammona, G., Trapani, G., & Mandracchia, D. (2015). Hyaluronic acid and its derivatives in drug delivery and imaging: Recent advances and challenges. *European Journal of Pharmaceutics and Biopharmaceutics*, *97*, 400–416. <https://doi.org/https://doi.org/10.1016/j.ejpb.2015.03.032>
- Trojani, C., Boukhechba, F., Scimeca, J.-C., Vandenbos, F., Michiels, J.-F., Daculsi, G., Boileau, P., Weiss, P., Carle, G. F., & Rochet, N. (2006). Ectopic bone formation using an injectable biphasic calcium phosphate/Si-HPMC hydrogel composite loaded with undifferentiated bone marrow stromal cells. *Biomaterials*, *27*(17), 3256–3264. <https://doi.org/10.1016/j.biomaterials.2006.01.057>
- Turino, G. M., & Cantor, J. O. (2003). Hyaluronan in respiratory injury and repair. *American Journal of Respiratory and Critical Care Medicine*, *167*(9), 1169–1175. <https://doi.org/10.1164/rccm.200205-449PP>
- Tzellos, T. G., Klagas, I., Vahtsevanos, K., Triaridis, S., Printza, A., Kyrgidis, A., Karakiulakis, G., Zouboulis, C. C., & Papakonstantinou, E. (2009). Extrinsic ageing in the human skin is associated with alterations in the expression of hyaluronic acid and its metabolizing enzymes. *Experimental Dermatology*, *18*(12), 1028–1035. <https://doi.org/10.1111/j.1600-0625.2009.00889.x>
- Tzellos, T. G., Sinopidis, X., Kyrgidis, A., Vahtsevanos, K., Triaridis, S., Printza, A., Klagas, I., Karakiulakis, G., & Papakonstantinou, E. (2011). Differential hyaluronan homeostasis and expression of proteoglycans in juvenile and adult human skin. *Journal of Dermatological Science*, *61*(1), 69–72. <https://doi.org/10.1016/j.jdermsci.2010.11.007>
- Ueno, H., Mori, T., & Fujinaga, T. (2001). Topical formulations and wound healing applications of chitosan. *Advanced Drug Delivery Reviews*, *52*(2), 105–115. [https://doi.org/https://doi.org/10.1016/S0169-409X\(01\)00189-2](https://doi.org/https://doi.org/10.1016/S0169-409X(01)00189-2)
- Vanderhooff, J. L., Mann, B. K., & Prestwich, G. D. (2007). Synthesis and Characterization of Novel Thiol-Reactive Poly(ethylene glycol) Cross-Linkers for Extracellular-Matrix-Mimetic Biomaterials. *Biomacromolecules*, *8*(9), 2883–2889. <https://doi.org/10.1021/bm0703564>
- Vasvani, S., Kulkarni, P., & Rawtani, D. (2020). Hyaluronic acid: A review on its biology, aspects of drug delivery, route of administrations and a special emphasis on its approved marketed products and recent clinical studies. *International Journal of Biological Macromolecules*, *151*, 1012–1029. <https://doi.org/https://doi.org/10.1016/j.ijbiomac.2019.11.066>
- Vedamurthy, M. (2018). Beware What You Inject: Complications of Injectables-Dermal Fillers. *Journal of Cutaneous and Aesthetic Surgery*, *11*(2), 60–66. https://doi.org/10.4103/JCAS.JCAS_68_18
- Vleggaar, D., & Bauer, U. (2004). Facial enhancement and the European experience with Sculptra (poly-L-lactic acid). *Journal of Drugs in Dermatology: JDD*, *3*(5), 542–547.

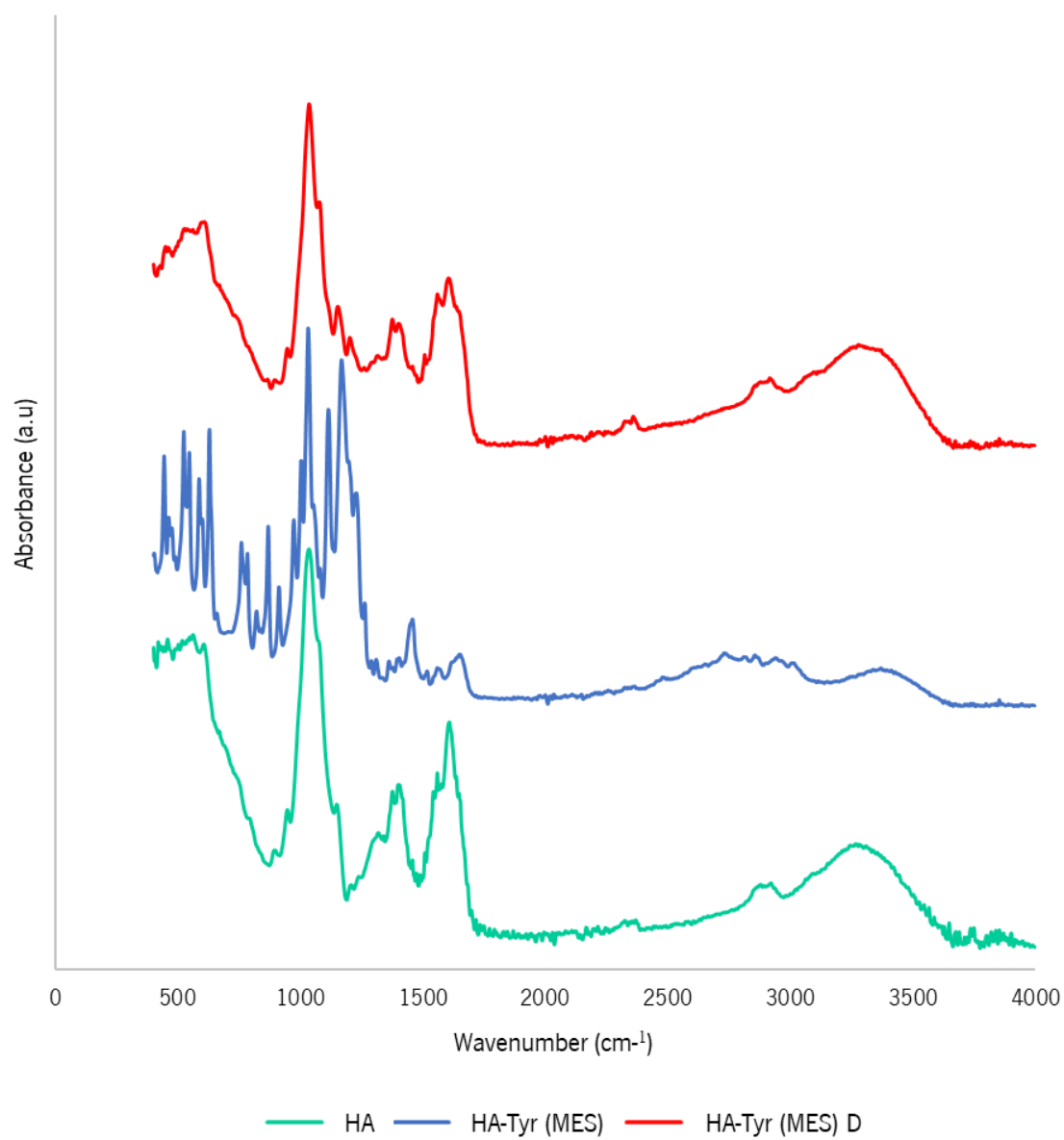
- Wang, Lin, Xu, B., Nong, Y., Wang, P., Yu, Y., Deng, C., Yuan, J., & Wang, Q. (2020). Laccase-mediated construction of flexible double-network hydrogels based on silk fibroin and tyramine-modified hyaluronic acid. *International Journal of Biological Macromolecules*, 160, 795–805. <https://doi.org/10.1016/j.ijbiomac.2020.05.258>
- Wang, L., Li, J., Zhang, D., Ma, S., Zhang, J., Gao, F., Guan, F., & Yao, M. (2020). Dual-enzymatically crosslinked and injectable hyaluronic acid hydrogels for potential application in tissue engineering. *RSC Advances*, 10(5), 2870–2876. <https://doi.org/10.1039/C9RA09531D>
- Wang, W. (2006). A novel hydrogel crosslinked hyaluronan with glycol chitosan. *Journal of Materials Science. Materials in Medicine*, 17(12), 1259–1265. <https://doi.org/10.1007/s10856-006-0600-1>
- Weigel, P. H., Fuller, G. M., & LeBoeuf, R. D. (1986). A model for the role of hyaluronic acid and fibrin in the early events during the inflammatory response and wound healing. *Journal of Theoretical Biology*, 119(2), 219–234. [https://doi.org/10.1016/S0022-5193\(86\)80076-5](https://doi.org/10.1016/S0022-5193(86)80076-5)
- Weissmann, B., Meyer, K., Sampson, P., & Linker, A. (1954). Isolation of oligosaccharides enzymatically produced from hyaluronic acid. *The Journal of Biological Chemistry*, 208(1), 417–429. [https://doi.org/10.1016/s0021-9258\(18\)65660-1](https://doi.org/10.1016/s0021-9258(18)65660-1)
- Weissmann, Bernard, & Meyer, K. (1954). The Structure of Hyalobiuronic Acid and of Hyaluronic Acid from Umbilical Cord. *Journal of the American Chemical Society*, 76(7), 1753–1757. <https://doi.org/10.1021/ja01636a010>
- Westbrook, A. W., Ren, X., Moo-Young, M., & Chou, C. P. (2018). Engineering of cell membrane to enhance heterologous production of hyaluronic acid in *Bacillus subtilis*. *Biotechnology and Bioengineering*, 115(1), 216–231. <https://doi.org/10.1002/bit.26459>
- Wu, Y., Yao, J., Zhou, J., & Dahmani, F. Z. (2013). Enhanced and sustained topical ocular delivery of cyclosporine A in thermosensitive hyaluronic acid-based in situ forming microgels. *International Journal of Nanomedicine*, 8, 3587–3601. <https://doi.org/10.2147/IJN.S47665>
- Xue, Y., Chen, H., Xu, C., Yu, D., Xu, H., & Hu, Y. (2020). Synthesis of hyaluronic acid hydrogels by cross-linking the mixture of high-molecular-weight hyaluronic acid and low-molecular-weight hyaluronic acid with 1,4-butanediol diglycidyl ether. *RSC Advances*, 10(12), 7206–7213. <https://doi.org/10.1039/C9RA09271D>
- Yang, J.-A., Yeom, J., Hwang, B. W., Hoffman, A. S., & Hahn, S. K. (2014). In situ-forming injectable hydrogels for regenerative medicine. *Progress in Polymer Science*, 39(12), 1973–1986. <https://doi.org/10.1016/j.progpolymsci.2014.07.006>
- Yu, H., & Stephanopoulos, G. (2008). Metabolic engineering of *Escherichia coli* for biosynthesis of hyaluronic acid. *Metabolic Engineering*, 10(1), 24–32. <https://doi.org/10.1016/j.ymben.2007.09.001>
- Zerbinati, N., Esposito, C., Cipolla, G., Calligaro, A., Monticelli, D., Martina, V., Golubovic, M., Binic, I., Sigova, J., Gallo, A. L., D'Este, E., Jafferany, M., Pratosoni, M., Tirant, M., Van Thuong, N., Sangalli, F., Rauso, R., & Lotti, T. (2020). Chemical and mechanical characterization of hyaluronic acid hydrogel cross-linked with polyethylen glycol and its use in dermatology. *Dermatologic Therapy*, 33(4). <https://doi.org/10.1111/dth.13747>

- Zhu, J., Tang, X., Jia, Y., Ho, C.-T., & Huang, Q. (2020). Applications and delivery mechanisms of hyaluronic acid used for topical/transdermal delivery – A review. *International Journal of Pharmaceutics*, 578, 119127. <https://doi.org/https://doi.org/10.1016/j.ijpharm.2020.119127>
- Ziادلou, R., Rotman, S., Teuschl, A., Salzer, E., Barbero, A., Martin, I., Alini, M., Eglin, D., & Grad, S. (2021). Optimization of hyaluronic acid-tyramine/silk-fibroin composite hydrogels for cartilage tissue engineering and delivery of anti-inflammatory and anabolic drugs. *Materials Science and Engineering: C*, 120, 111701. <https://doi.org/https://doi.org/10.1016/j.msec.2020.111701>
- Zoltan-Jones, A., Huang, L., Ghatak, S., & Toole, B. P. (2003). Elevated Hyaluronan Production Induces Mesenchymal and Transformed Properties in Epithelial Cells. *Journal of Biological Chemistry*, 278(46), 45801–45810. <https://doi.org/10.1074/jbc.M308168200>

Appendix I - Characterization of the HA-Tyr hydrogel

Purification method – Dialysis

(a)



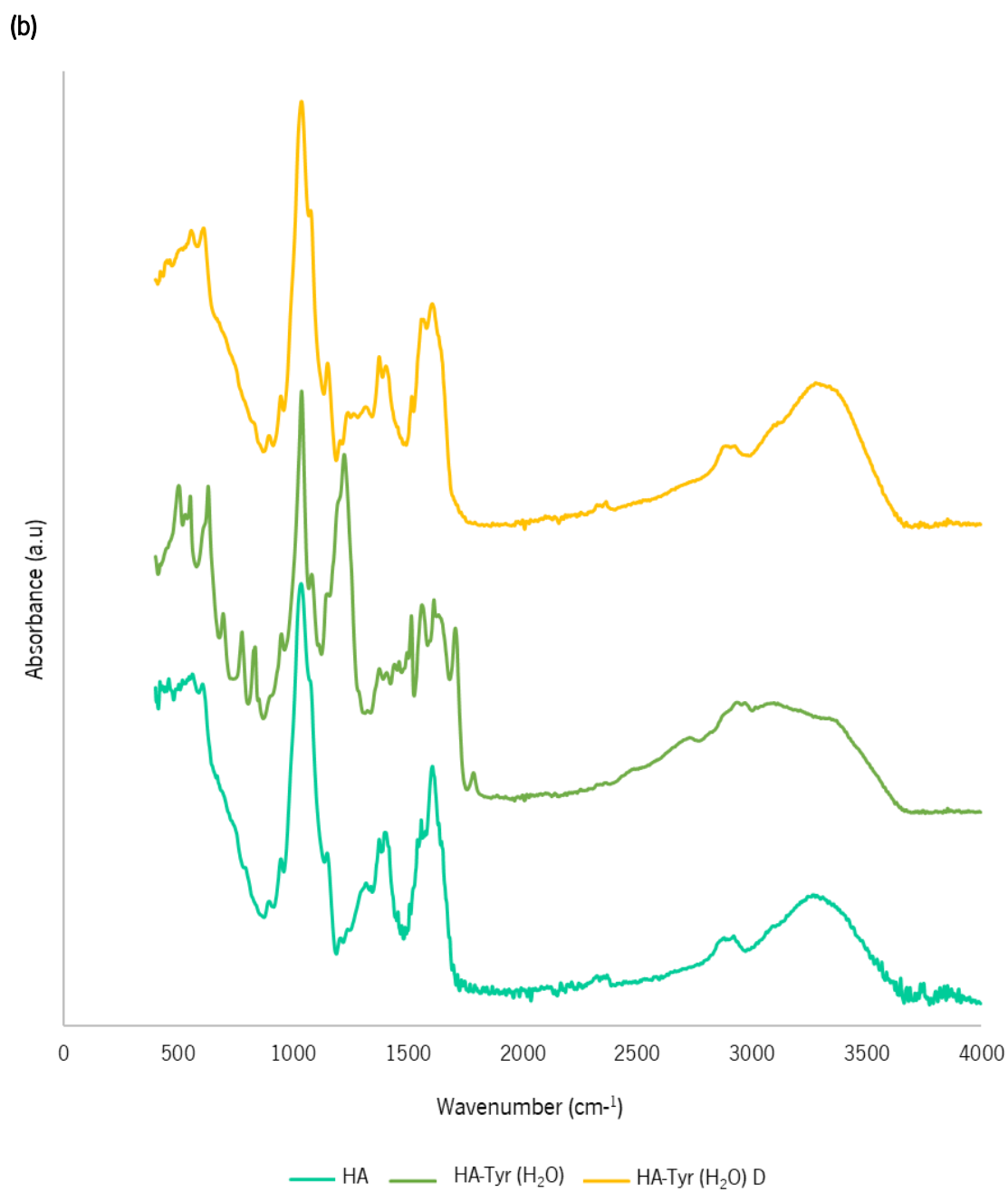
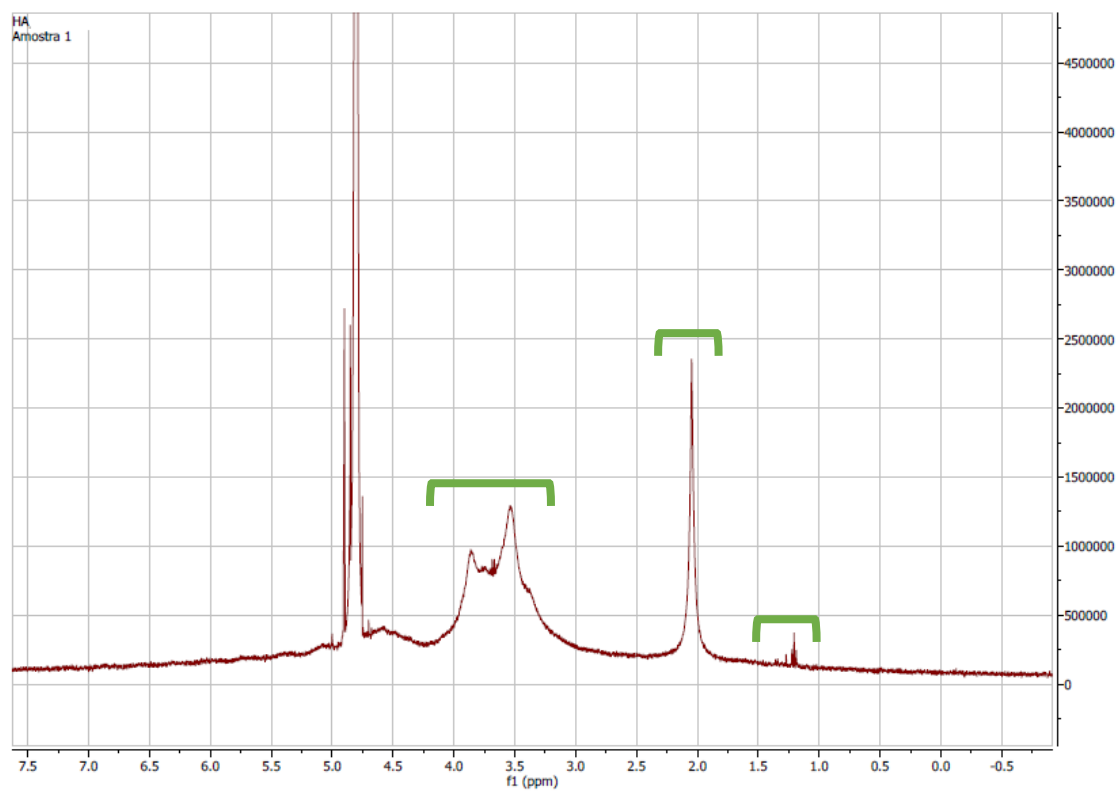
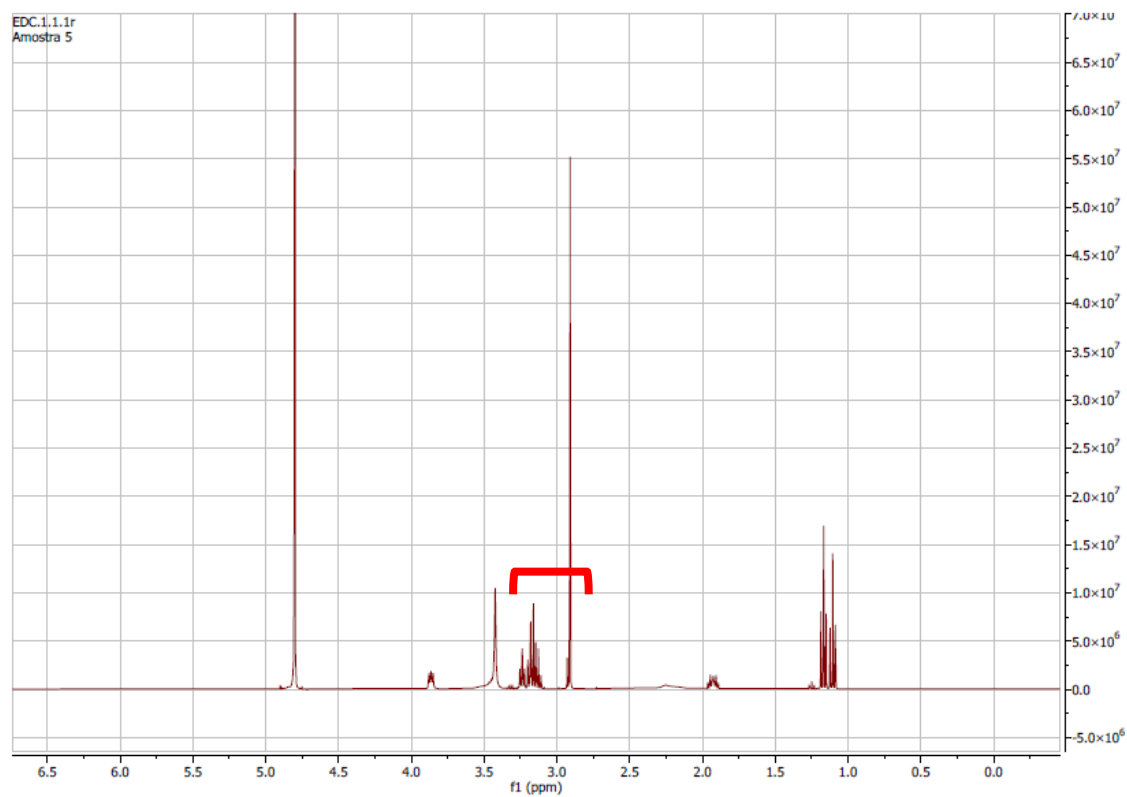


Figure A1 – Spectra obtained by ATR-FTIR analysis of the control consisting of HA alone and of the reactions of HA with Tyr in **(a)** MES buffer (0.1 M, pH 6.0) - HA-Tyr (MES) - and **(b)** in ultrapure H_2O - HA-Tyr (H_2O) - before and after dialysis (D).

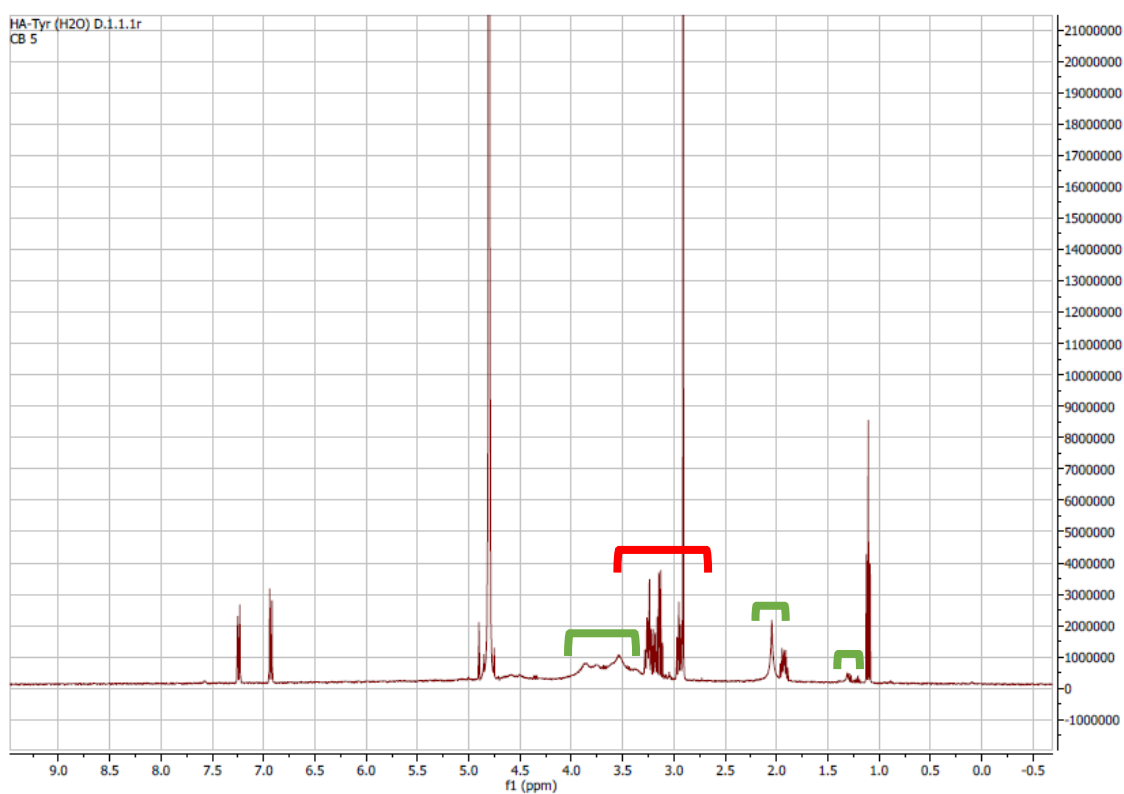
(a)



(b)



(c)



(d)

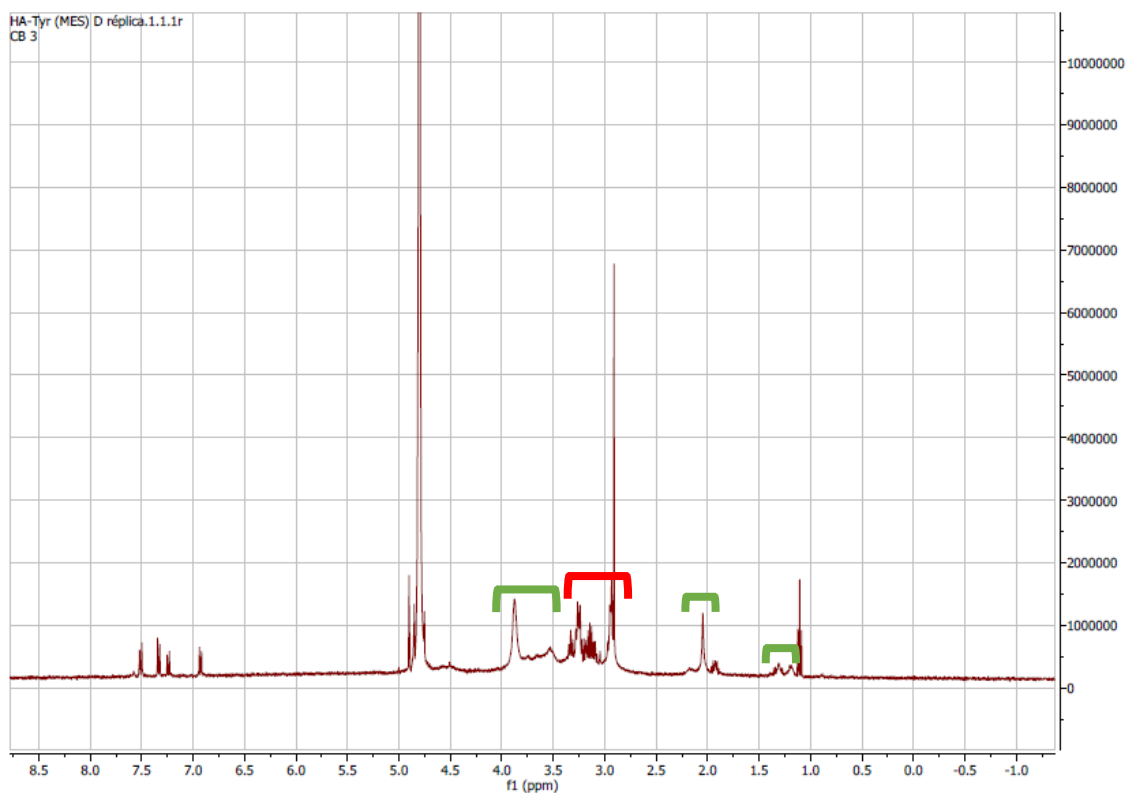


Figure A2 – NMR spectra obtained for (a) HA, (b) EDC, HA-Tyr reactions in (c) ultrapure H₂O and in (d) MES buffer (0.1 M, pH 6.0) after dialysis (D). The peaks marked in green correspond to the peaks of the HA spectrum and the peaks marked in red correspond to the peaks of the EDC spectrum.

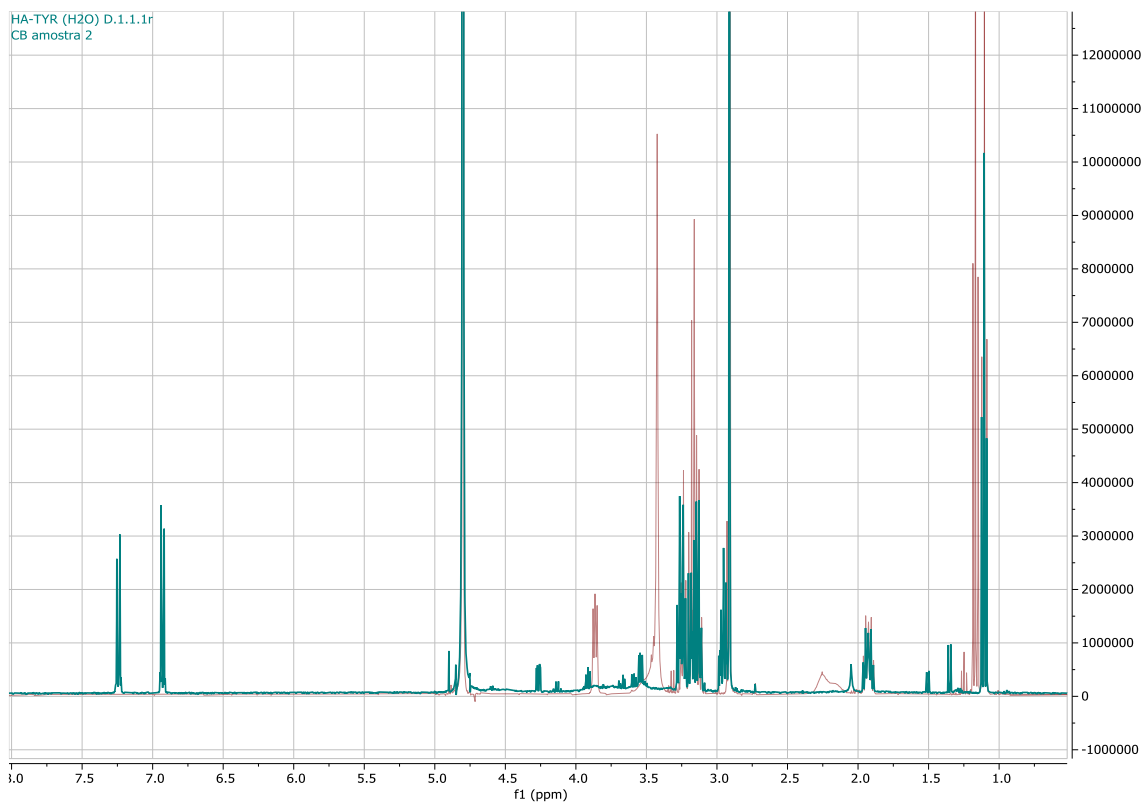


Figure A3 – NMR spectra obtained by NMR analysis for EDC shown in red and HA-Tyr reaction in ultrapure H₂O after dialysis (D) shown in blue.

Purification method – Centrifugation with Amicon filters

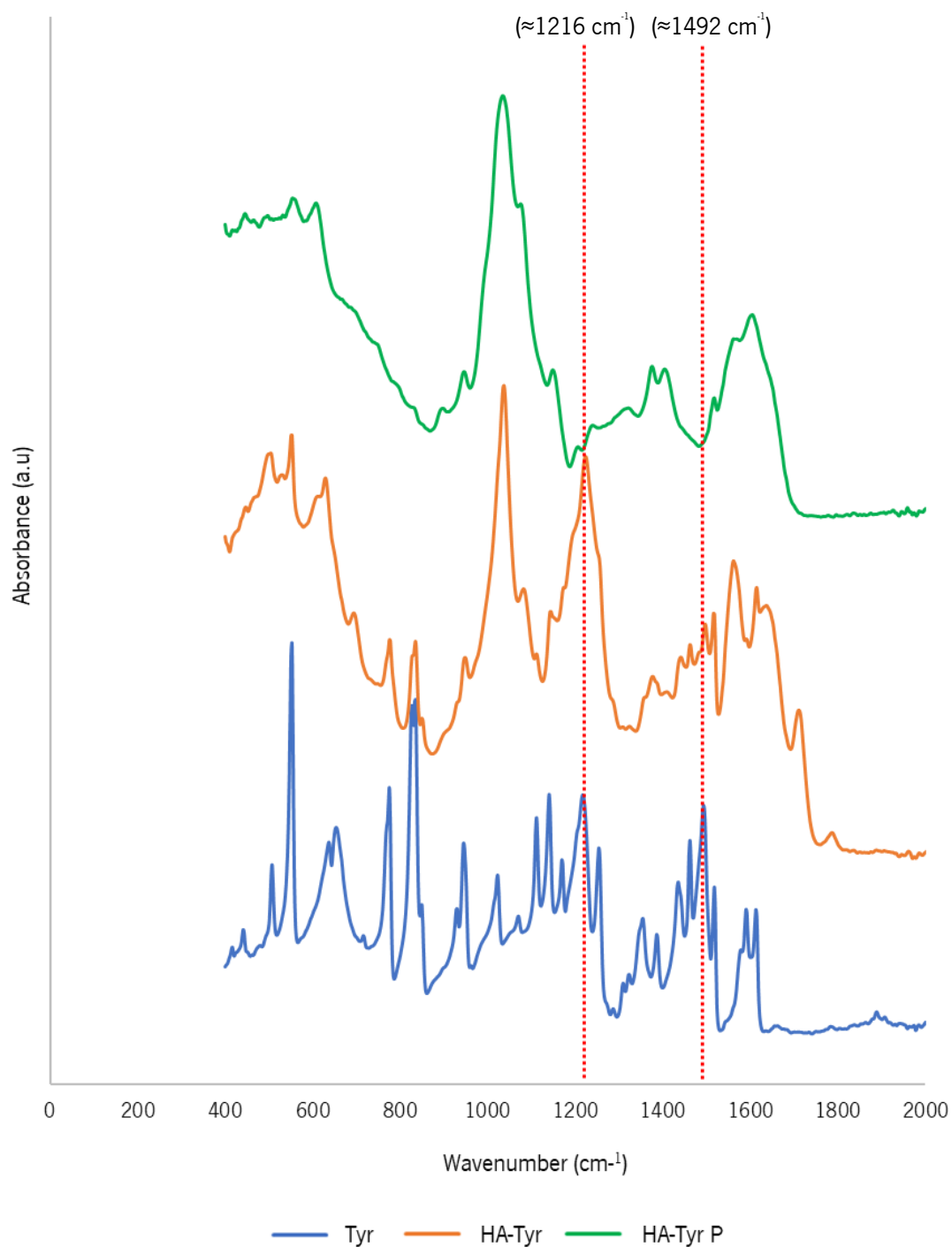


Figure A4 – Extended area between 0 cm⁻¹ and 2000 cm⁻¹ of the spectra obtained by ATR-FTIR analysis of the Tyr control and of the reaction of HA with Tyr in ultrapure H₂O before - HA-Tyr - and after purification with Amicon filters - HA-Tyr P. The red-highlighted peaks correspond to the characteristic peaks of the Tyr spectrum (1216 cm⁻¹ and 1492 cm⁻¹) that are not present in the spectrum of the pure sample, contrary to the impure sample.

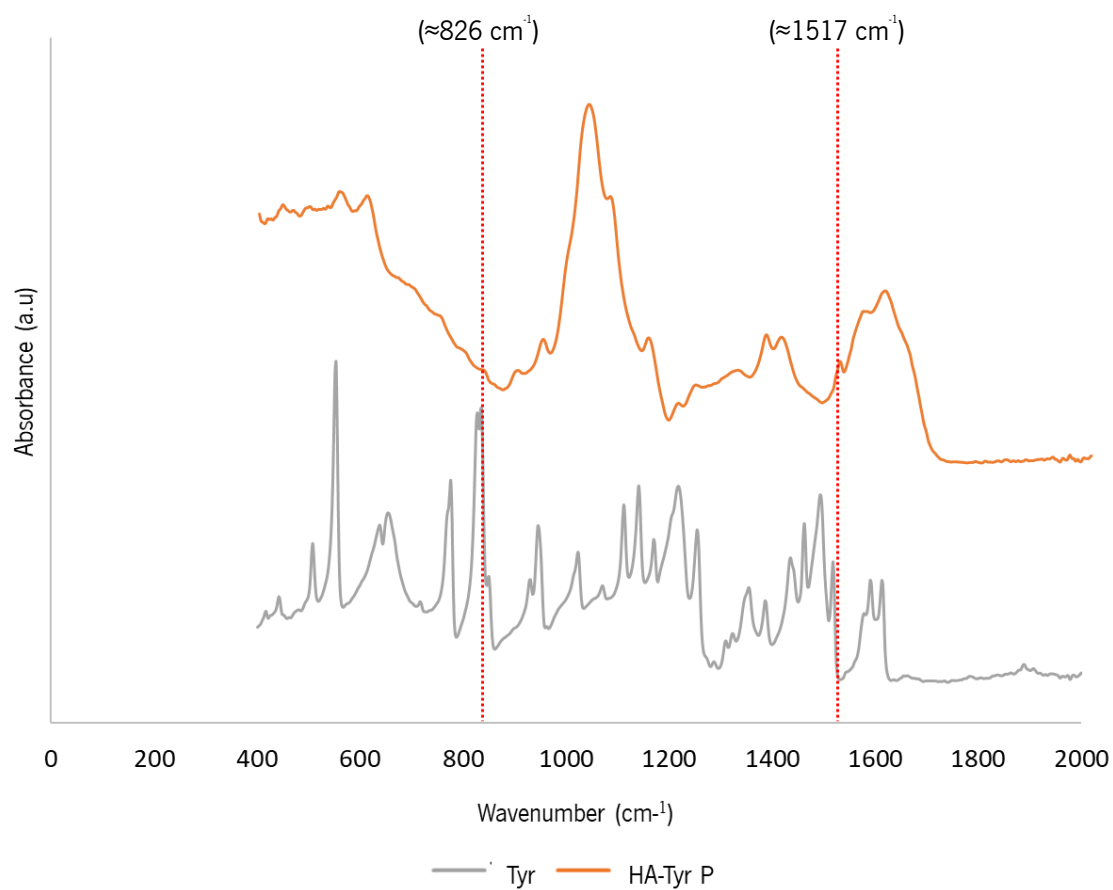
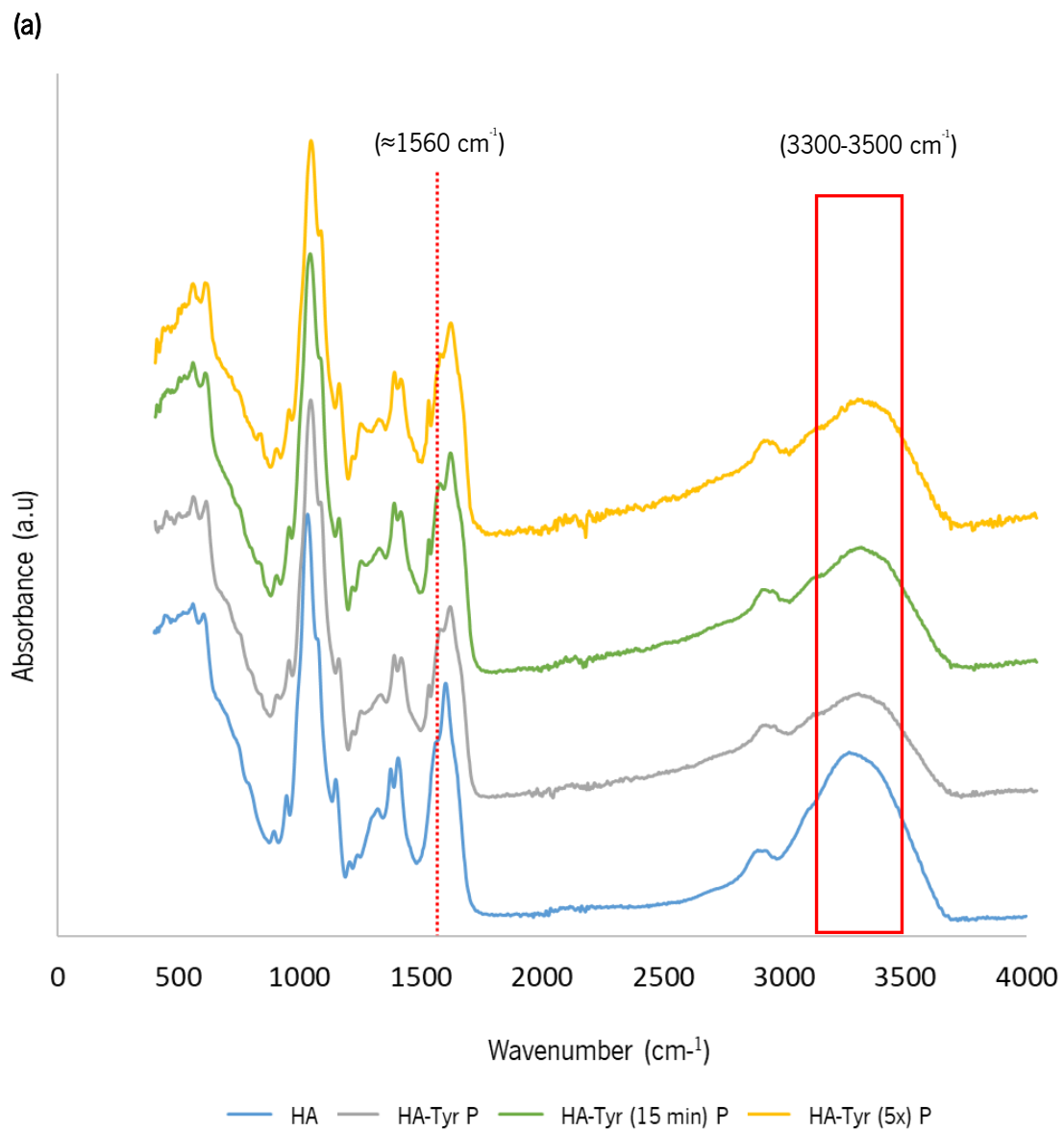


Figure A5 – Extended area between 0 cm^{-1} and 2000 cm^{-1} of the spectra obtained by ATR-FTIR analysis of the Tyr control and of the reaction of HA with Tyr in ultrapure H₂O after purification with Amicon filters - HA-Tyr P. The red-highlighted peaks of the HA-Tyr P spectrum correspond to the characteristic peaks of the Tyr spectrum (826 cm^{-1} and 1517 cm^{-1}).



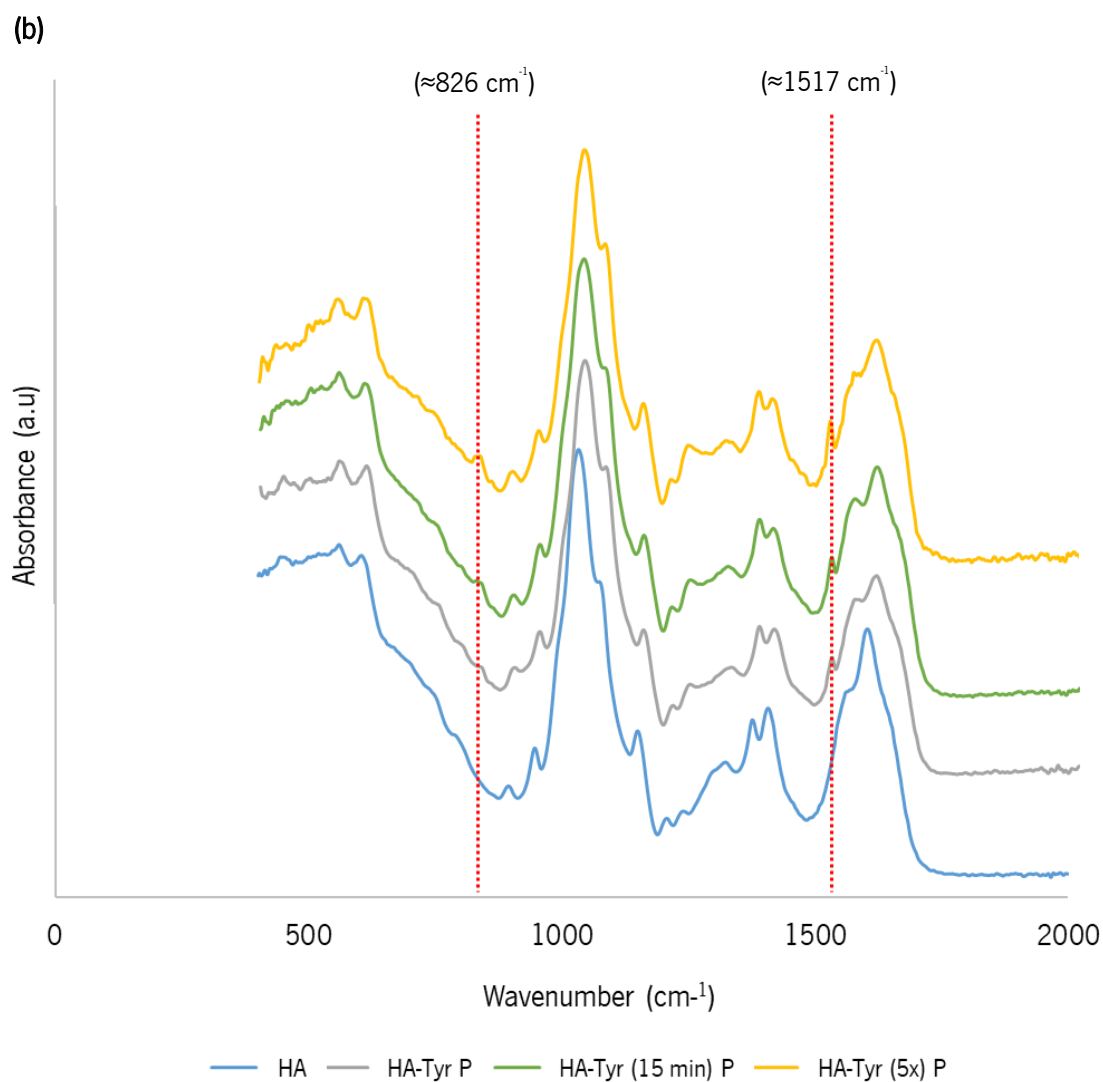


Figure A6 – (a) Spectra obtained by ATR-FTIR analysis and (b) extended area between 0 cm^{-1} and 2000 cm^{-1} of the spectra of the HA control and of the reactions of HA with Tyr in ultrapure H₂O after purification with Amicon filters with a time interval of 60 min between the addition of NHS and Tyr and a Tyr ratio of 3x - HA-Tyr P; with a time interval of 15 min between the addition of NHS and Tyr and a Tyr ratio of 3x - HA-Tyr (15 min) P; and with a time interval of 60 min between the addition of NHS and Tyr and a Tyr ratio of 5x - HA-Tyr (5x) P. (a) The peaks represented at 1560 cm^{-1} and $3300\text{-}3500 \text{ cm}^{-1}$ in the spectra of HA and HA-Tyr reactions corresponds to the amide bond bends and to the stretching vibration of -OH and -NH- groups, respectively. (b) The red-highlighted peaks of the HA-Tyr reactions spectra correspond to the characteristic peaks of the Tyr spectrum (826 cm^{-1} and 1517 cm^{-1}).

Appendix II - Characterization of the Si-HA hydrogel

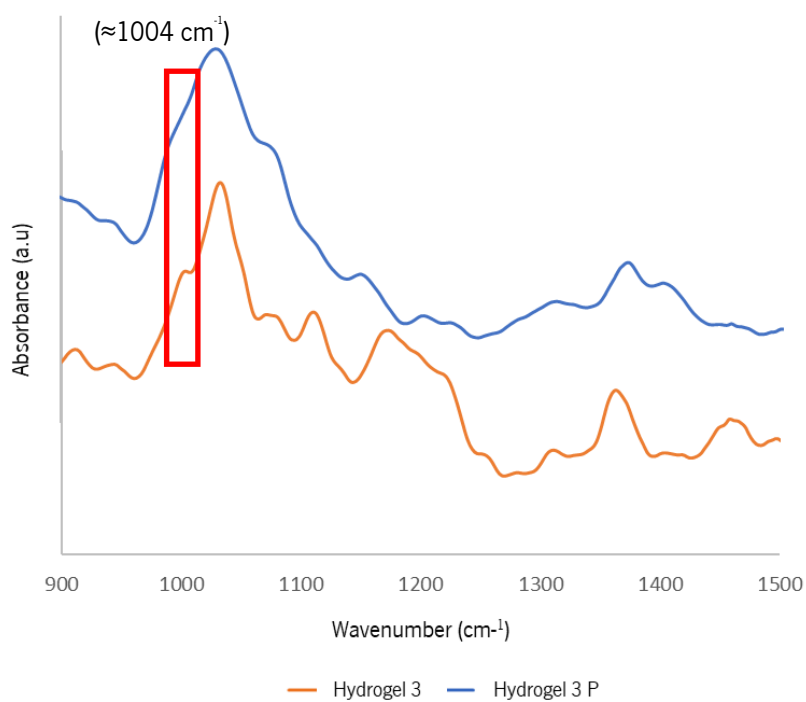
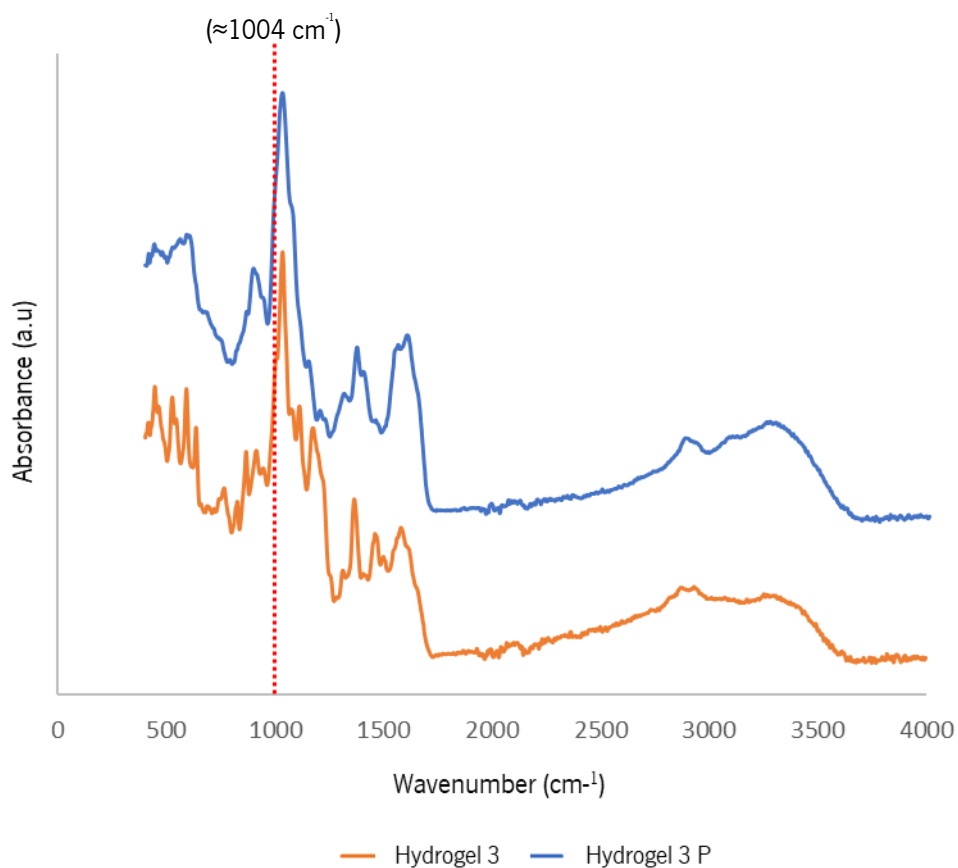


Figure A1 – (a) Spectra obtained by ATR-FTIR analysis and (b) extended area between 900 cm⁻¹ and 1500 cm⁻¹ of the spectra of the APTES modified HA hydrogels 3 in MES buffer (0.1 M, pH 6.0) before – Hydrogel 3 and after purification with Amicon filters – Hydrogel 3 P. The peak represented at 1004 cm⁻¹ in the spectra of Hydrogel 3 correspond to the stretching vibration of Si-O-Si.